AD-A234 343

VOLUME 8 • NUMBER 4 • 1989

(1)

MARINE GEOTECHNOLOGY

DTIC
ELECTE
APR 26 1991
C D

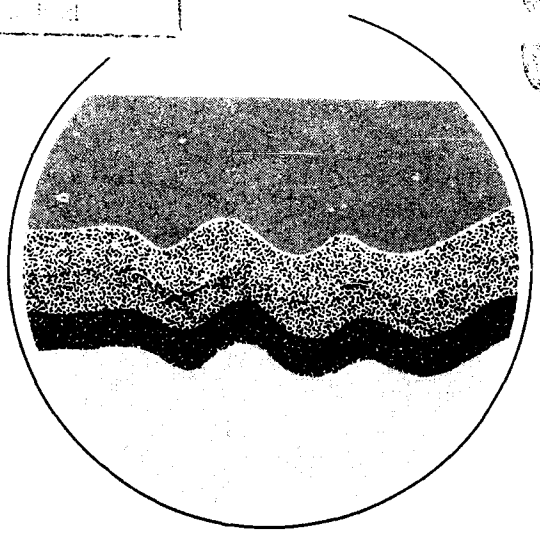

AN INTERNATIONAL
JOURNAL OF SEA-FLOOR SCIENCE
AND ENGINEERING

APPLICATIONS TO SEABED DISPOSAL: ISHTE—A MODEL EXPERIMENT

RICHARD H. BENNETT
GUEST EDITOR

DTIC FILE COPY

91 1 29 061

TAYLOR & FRANCIS
NEW YORK • BRISTOL, PA • WASHINGTON, DC • LONDON

MARINE GEOTECHNOLOGY

EDITOR-IN-CHIEF
Ronald C. Chaney,
Telonicher Marine Laboratory, Humboldt State University

ASSOCIATE EDITOR FOR EUROPE
Adrian F. Richards, Consultant, The Netherlands

ASSOCIATE EDITOR FOR THE FAR EAST
Shigeyasu Okusa, (deceased), Niigata University, Japan

EDITORIAL BOARD

Gideon Almagor, Geological Survey of Israel; **Richard H. Bennett,** NORDA, NSTL Station, Mississippi; **James S. Booth,** U.S. Geological Survey, Massachusetts; **Bengt B. Broms,** Nanyang Technological Institute, Singapore; **William R. Bryant,** Texas A & M University; **R. G. Campanella,** The University of British Columbia, Vancouver, Canada; **Kenneth R. Demars,** University of Connecticut; **Jaap De Ruiter,** Fugro Consultants International, Holland; **Earl Doyle,** Shell Development Company, Texas; **Ben C. Gerwick, Jr.,** University of California; **S. K. Gulhati,** Indian Institute of Technology, New Delhi, India; **Terence J. Hirst,** Vancouver, Canada; **Kaare Hoeg,** Norwegian Geotechnical Institute; **George H. Keller,** Oregon University; **Homa Lee,** U.S. Geological Survey, California; **Bramlette McClelland,** McClelland Engineers, Inc., Texas; **Iraj Noorany,** San Diego State University; **Shigeyasu Okusa,** Tokai University; **Harold W. Olsen,** U.S. Dept. of Interior; **Sibel Pamukcu,** Fritz Laboratory, Pennsylvania; **H. G. Poulos,** The University of Sydney; **V. Savelyev,** VNII Okeangeologia, U.S.S.R.; **Armand J. Silva,** University of Rhode Island; **Tokuo Yaminoto,** University of Miami; **Liang Yuanbo,** South China Sea Institute of Oceanology, Academia Sinica, P.R.C.

Abstracted and/or Indexed in: Aquatic Sciences and Fisheries Abstracts; Articles in Civil Engineering; Bibliography and Index of Geology; Bibliography and Index of Micropaleontology; Biological Abstracts; Cambridge Abstracting Services; Current Contents/Engineering, Technology and Applied Sciences; Engineering Index; Engineering Information, Geo Abstracts; Geotechnical Abstracts; IMM Abstracts; Marine Science Contents Tables; Oceanic Abstracts; Offshore Abstracts; Petroleum Abstracts.

Editorial Office: Ronald C. Chaney, Telonicher Marine Lab., Humboldt State University, P.O. Box AE, Trinidad, CA 95570.

Publishing, Advertising, and Subscription Offices: Taylor & Francis Inc., 1900 Frost Road, Suite 101, Bristol, PA 19007, USA; or Taylor & Francis Ltd., Rankine Road, Basingstoke, Hampshire RG24 0PR, England.

Marine Geotechnology (ISSN 0360-8867) is published quarterly by Taylor & Francis Ltd., 4 John Street, London, WC1N 2ET. Annual 1989 institutional subscription £50, US $90. Personal subscription rate available to home address only US £29, U.S. $50.

Application to mail at second-class postage rates is pending at New York, NY, and additional mailing offices. **POSTMASTER:** Send address changes to MARINE GEOTECHNOLOGY, Publications Expediting, Inc., 200 Meacham Avenue, Elmont, New York 11003, U.S.A.

Dollar rates apply to subscribers in all countries except the UK and the Republic of Ireland, where the sterling price applies. All subscriptions are payable in advance and all rates include postage. Subscriptions are entered on an annual basis, i.e., January to December. Payment may be made by sterling check, dollar check, international money order, National Giro, or credit card (AMEX, VISA, Mastercard/Access).

Orders originating in the following territories should be sent directly to: **Australia**—R. Hill & Son, Ltd., 117 Wellington Street, Windsor, Victoria 3181. **India**—Universal Subscription Agency Pvt. Ltd., 101-102 Community Centre, Malviya Nagar Extn., Post Bag No. 8, Saket, New Delhi. **Japan**—Kinokuniya Company Ltd., Journal Department, P.O. Box 55, Chitose, Tokyo 156. **New Zealand**—R. Hill & Son, Ltd., Private Bag, Newmarket, Auckland 1. **USA, Canada, and Mexico**—Taylor & Francis, Inc., 1900 Frost Road, Suite 101, Bristol, PA 19007, USA. **UK and all other territories**—Taylor & Francis Ltd., Rankine Road, Basingstoke, Hampshire RG24 0PR, England.

Copyright:
The appearance of the code at the top of the first page of each article in this journal indicates the copyright owner's consent that a single copy of the article may be made for personal use. This consent is given on the condition that for multiple copies of the article the copier pay a fee of $3.00 per copy through the Copyright Clearance Center, Inc., 27 Congress Street, Salem, MA 01970. This consent does not extend to other kinds of copying, such as copying for general distribution, for advertising or promotional purposes, for creating new collective works or for resale. No part of this publication may be stored on an electronic retrieval system or transmitted electronically without the prior written permission of the publisher.
Copyright © 1989 Taylor & Francis. Printed by Burgess Science Press, Basingstoke, England.

The publisher assumes no responsibility for any statements of fact or opinion expressed in the published papers or in the advertisements. **Marine Geotechnology** is owned by Taylor & Francis Inc.

REPORT DOCUMENTATION PAGE

Form Approved
OMB No. 0704-0188

Public reporting burden for this collection of information is estimated to average 1 hour per response, including the time for reviewing instructions, searching existing data sources, gathering and maintaining the data needed, and completing and reviewing the collection of information. Send comments regarding this burden estimate or any other aspect of this collection of information, including suggestions for reducing this burden, to Washington Headquarters Services, Directorate for Information Operations and Reports, 1215 Jefferson Davis Highway, Suite 1204, Arlington, VA 22202-4302, and to the Office of Management and Budget, Paperwork Reduction Project (0704-0188), Washington, DC 20503

1. Agency Use Only *(Leave blank)*	2. Report Date.	3. Report Type and Dates Covered.
	1989	Journal Article

4. Title and Subtitle.
Application to Subseabed Disposal: (ISHTE)-A Model Experiment

5. Funding Numbers.
Program Element No 61153N
Project No 03205
Task No 330
Accession No DN257003

6. Author(s).
C. Mark Percival, Leroy O. Olson, Richard H. Bennett, Frederick L. Sayles, and Armand J. Silva

7. Performing Organization Name(s) and Address(es).
Naval Oceanographic and Atmospheric Research Laboratory
Stennis Space Center, MS 39529-5004

8. Performing Organization Report Number.
JA 360:049:88

9. Sponsoring/Monitoring Agency Name(s) and Address(es).
Naval Oceanographic and Atmospheric Research Laboratory
Stennis Space Center, MS 39529-5004

10. Sponsoring/Monitoring Agency Report Number.
JA 360:049:88

11. Supplementary Notes.
Marine Geotechnology

12a. Distribution/Availability Statement.
Approved for public release; distribution is unlimited.

12b. Distribution Code

13. Abstract *(Maximum 200 words).*

This article provides the scientific and engineering community with a summary of the technical status and experimental accomplishments of the In Situ Heat Transfer Experiment (ISHTE) as of the project's termination. Vast amounts of technical effort and monetary resources were expended to achieve the objects defined in the ISHTE. Exciting new scientific and engineering successes were realized during the life of the ISHTE, and the technology has direct application to various present and future deep-sea studies. This study provides an excellent review of (1) the deep-ocean technology systems and subsystems developed for the ISHTE; (2) system performance and evaluation; (3) limited but important laboratory and in situ deep-ocean test results; (4) initial, but significant, scientific analyses of data; and (5) a good cross-section of literature and source materials for the reader desiring additional detailed information about the ISHTE.

14. Subject Terms.
(U) Sediment Transport; (U) Sediments; (U) Pore Pressure; (U) Clay

15. Number of Pages.
87

16. Price Code.

17. Security Classification of Report.	18. Security Classification of This Page.	19. Security Classification of Abstract.	20. Limitation of Abstract.
Unclassified	Unclassified	Unclassified	SAR

MARINE GEOTECHNOLOGY

Volume 8, Number 4
1989

Contents

Abstracted and/or indexed in: Aquatic Sciences and Fisheries Abstracts; Articles in Civil Engineering; Bibliography and Index of Geology; Bibliography and Index of Micropaleontology; Biological Abstracts; Current Contents/Engineering, Technology and Applied Sciences; Engineering Index; Geo Abstracts; Geotechnical Abstracts; IMM Abstract; Marine Science Contents Tables, Oceanic Abstracts; Offshore Abstracts; Petroleum Abstracts.

Taylor & Francis
New York • Bristol, PA • Washington, DC • London

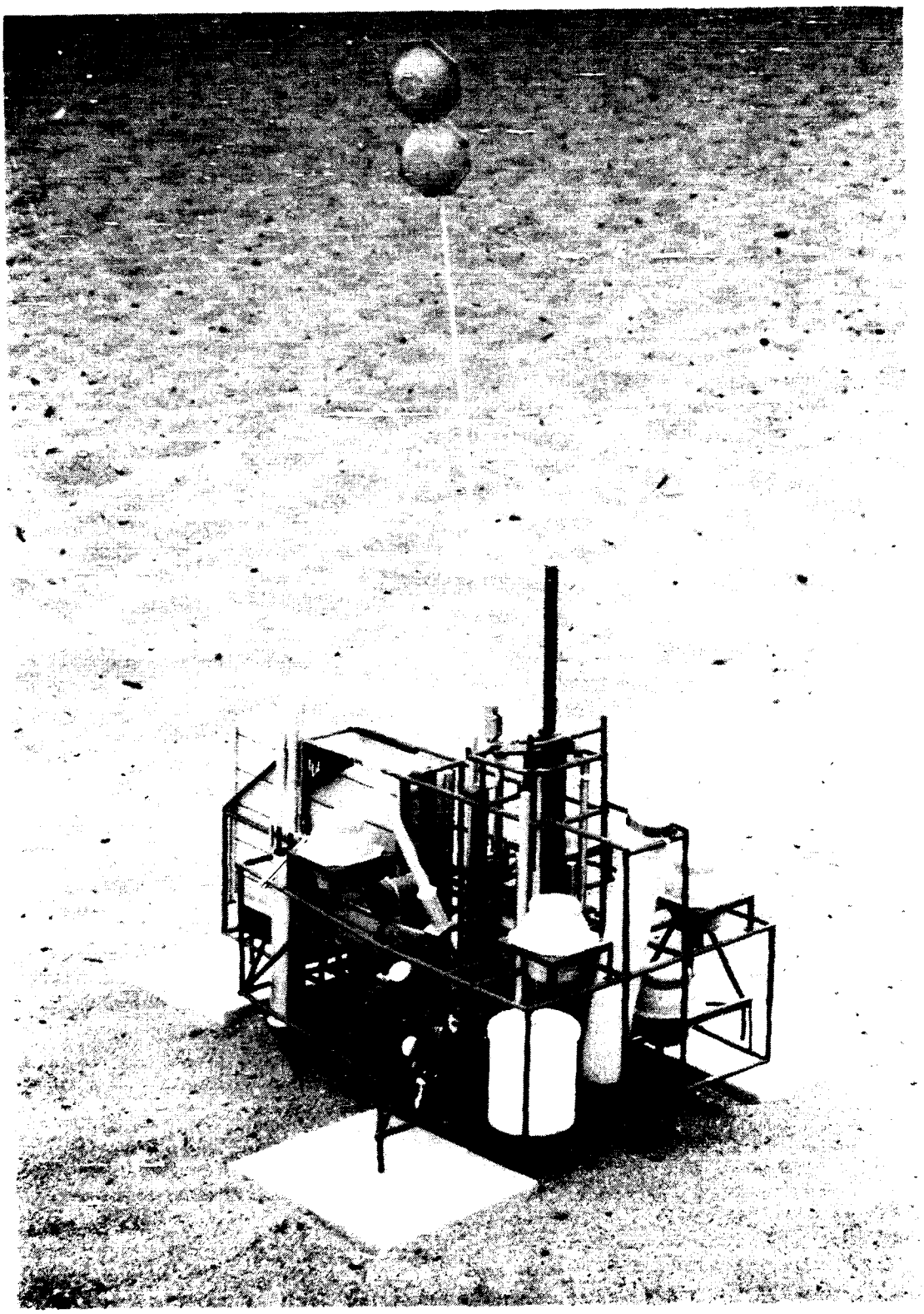

Marine Geotechnology, Volume 8, pp. 285-371
Printed in the UK. All rights reserved.

0360-8867/89 $3.00 + .00
Copyright © 1989 Taylor & Francis

Applications to Subseabed Disposal: (ISHTE)—A Model Experiment

AVAILABLE FOR $25.00 FROM
TAYLOR & FRANCIS INC.
1900 FROST RD., SUITE #101
BRISTOL, PA 19007
PER PHONECON 4-12-91
JK

C. MARK PERCIVAL

Sandia National Laboratories
Albuquerque, NM 87185

LEROY O. OLSON

University of Washington
Seattle, WA 98105

RICHARD H. BENNETT

Naval Oceanographic and Atmospheric Research Laboratory
Stennis Space Center, MS 39529-5004

FREDERICK L. SAYLES

Woods Hole Oceanographic Institution
Woods Hole, MA 02543

ARMAND J. SILVA

University of Rhode Island
Kingston, RI 02881

By
Distribution /
Availability Codes
Dist | Special
A-1 21

Preface

This article provides the scientific and engineering community with a summary of the technical status and experimental accomplishments of the In Situ Heat Transfer Experiment (ISHTE) as of the time of the project's termination. Vast amounts of technical effort and monetary resources were expended to achieve the objects defined in the ISHTE. Exciting new scientific and engineering successes were realized during the life of the ISHTE, and the technology has direct application to various present and future deep-sea studies. This study provides an excellent review of (1) the deep-ocean technology systems and subsystems developed for the ISHTE; (2) system performance and evaluation; (3) limited but important laboratory and in situ deep-ocean test results; (4) initial, but significant, scientific analyses of data; and (5) a good cross-section of literature and source materials for the reader desiring additional detailed information about the ISHTE.

The ISHTE was originally limited to the validation of laboratory measurements and analytical computer models of waste-sediment thermomechanical interactions and the development of capabilities to perform long-term scientific experiments in the deep-ocean environment. Later, the project developed into an interdisciplinary experiment

with multi-institution participation that provided a unique opportunity for enhanced and expanded scientific and engineering returns and cost effectiveness. Much of the motivation for this project originated from the perceived need to evaluate the potential use of deep-sea deposits for radioactive waste disposal, especially in terms of long-term containment (Hollister 1977).

In addition to the rigorous state-of-the-art engineering required for a planned 1-year deployment in a hostile deep-sea environment, the ISHTE developed into a major project that included the following experiments:

- In situ thermal conductivity
- Temperature
- Pore water pressure
- Ion migration
- Pore water chemistry
- Shear strength
- Posttest cores

Data acquisition and the integration of all experiments and subsystems into a workable and durable deep-sea system was a major task. The design of the ISHTE platform, including remote data collection, was ". . . a technological achievement comparable to designing the original lunar lander" (Briefing Book 1985, p. 18).

This article not only reviews the technical aspects of the ISHTE but also describes the relevance of the project to the Subseabed Disposal Program. Because of the importance of the ISHTE and its relationship to subseabed disposal in the deep ocean, the scientific and engineering achievements undoubtedly will be the springboard for future related thrusts and applications during the decade of the 1990s and into the 21st century. Any scientific or engineering research situation concerned with the deep-sea floor will benefit enormously from the knowledge gained during the ISHTE. Communications with the principal investigators are encouraged.

Richard H. Bennett
Seafloor Geosciences Division
Naval Oceanographic and Atmospheric Research Laboratory
Stennis Space Center, Mississippi

Nomenclature

ADM	action description memorandum
APL	Applied Physics Laboratory of the University of Washington
BCH	Bose-Chaudhuri-Hocqueghem (code)
CRT	cathode-ray tube
DPSK	differential phase shift keyed
EA	environmental assessment
FSA	fuel sphere assembly
GISSP	geotechnical in situ strength probe
GPC	giant piston core
HLC	hydrostatic core
IHS	isotopic heat source
ISHTE	in situ heat transfer experiment
ISIMU	ISHTE simulation
ISV	in situ vane
MANOP	Manganese Nodule Program
MPG	midplate, midgyre
NORDA*	Naval Ocean Research and Development Activity
NSRDC	Naval Ship Research and Development Center
PSK	phase-shift-keyed
RAM	random access memory
RTG	radioisotopic thermoelectric generator
SARP	Safety Analysis Report for Packaging
SDP	Subseabed Disposal Program
SNLA	Sandia National Laboratories, Albuquerque
URI	University of Rhode Island, Kingston
WHOI	Woods Hole Oceanographic Institution

a	radius of thermal conductivity probe
C_h	coefficient of horizontal consolidation
c_p	specific heat at constant pressure
C_v	coefficient of vertical consolidation
g	acceleration of gravity
k	permeability
K_D	distribution coefficient
σ'_e	effective vertical stress
Q	thermal power
Ra	Rayleigh number
S_u	Undrained shear strength
ΔT	Temperature rise of thermal conductivity, probe
t	Time
U_e	Ambient excess pressure
U_i	Excess pore water pressure (mechanically induced)
α	Effective thermal diffusivity of sediment
β	Thermal expansion coefficient for seawater
κ	Effective thermal conductivity
κ_s	Thermal conductivity of solid
κ_w	Thermal conductivity of water
μ	Viscosity of seawater
ρ_0	Density of seawater
ρ_s	Density of sediment
τ	Fourier number (nondimensional time)
ϕ	Porosity of sediment

*Renamed NOARL (Naval Oceanographic and Atmospheric Research Laboratory)

Introduction

The Subseabed Disposal Program (SDP) is concerned with assessing the technologic and environmental feasibility of using geologic formations in the deep ocean as possible disposal sites for nuclear waste (Bishop and Hollister 1974; Hollister 1977; Anderson 1979). The oceans cover about 70% of the surface of the earth and contain a wide variety of geologic formations. The formation of the SDP in 1975 was prompted by the premise that such a large portion of the earth should not be excluded as a possible repository for nuclear waste. The studies to date (Heath et al. 1980; Silva 1980; Hollister, Anderson, and Heath 1981) indicate that red clay sediments at ocean depths greater than 5000 m, near the central portions of tectonic plates and in regions of low bottom currents, appear to have the necessary characteristics for long-term isolation of nuclear waste. Of particular interest are illite and smectite clays at several sites in the central North Pacific and eastern North Atlantic. The sites being evaluated were selected on the basis of the following criteria:

(1) *Tectonic stability.* The area should have low earthquake and volcanic activity, with minimum evidence of recent faulting and no evidence of erosion processes.
(2) *Predictability.* Because the lifetime of some radionuclides in the waste is on the order of millions of years, geological changes in the area should be predictable (within the same time scale) from historical data and extrapolation of known physical processes (plate tectonics and sedimentation).The area should also have vertical and lateral uniformity on a scale suitable for use as a nuclear waste repository.
(3) *Minimum resources.* The area should be a marine "desert," where the biologic activity, present and past, is restricted to a low level by the absence of nutrients and light and where there are few or no mineral resources.

These criteria appear to be met by the ocean abyssal hill provinces in the central regions of tectonic plates.

In the disposal concept that was envisaged by the SDP, emplaced nuclear waste is to be contained in the ocean environment by a series of barriers: (1) the waste form, (2) the waste canister, (3) the sediment within which the waste is placed, (4) the benthic boundary layer, and (5) the water column. Because the benthic boundary layer and the water column act to dilute and disperse any radionuclides that might escape from the seabed, their behavior must be characterized and included in environmental impact assessments. The primary barriers are assumed to be the waste form, canister, and sediment layer, however.

The canister isolates the waste from the corrosive environment produced by the seawater-sediment chemical reactions that occur when the sediment temperature is elevated during the fission product–dominated heat-generation period. Development of the waste form, which will be designed to resist leaching of the radionuclides awaits more detailed information about the environment in which it must survive.

The sediment layers are intended to be the major long-term (10^4 to 10^5 years) containment barrier. The areas of interaction between the heat and radiation from the waste and the sediment must be thoroughly understood. Specific study areas in the near field included:

- capacity of the sediment to transport thermal energy away from the canister to prevent overheating
- capability of the sediment securely to restrain the canister from moving
- chemical and mineralogical changes induced by thermally activated reactions
- pressure build-up caused by thermal expansion of pore water
- permeability change of the sediment induced by pore water expansion and chemical alteration
- radionuclide sorption characteristics of the sediments in both the heated region and the cooler regions remote from the canister

These interactions were investigated by analytic methods, computer models, and supporting laboratory experiments. The overall objectives of the model and laboratory studies were to develop means of predicting the long-term response of the waste-sediment system to define problem areas, to propose solutions, to develop an optimum system design, and to ensure that the design is safe.

The approach to the model development was to form a physical-mathematic-computer description of a process; to measure, as well as possible, associated phenomena and properties in the laboratory; to make predictions and to run confirming in situ

experiments; and, finally, to modify or improve the fundamental knowledge of the process and the predictive tools if required. Models to describe the heat transfer, fluid-flow, geochemical, and radionuclide migration processes in the seabed sediment that were under development showed significant promise.

Thermal Studies

Thermal and fluid transport processes have been investigated analytically by Hickox and Watts (1980a, b) for an ideal situation. Their analysis shows that, for the small Rayleigh number anticipated for proposed emplacement schemes, the fluid velocity induced by the heating was so small that the energy transport could be assumed to occur solely by thermal conduction. The total fluid particle displacement that occurs as a result of heating also was shown to be insignificant. A more detailed analysis (Hickox et al. 1980) that used a computer model (Gartling and Hickox 1982a, b) resulted in the same conclusion.

In both the approaches described, the porous matrix was assumed to be rigid; the Boussinesq approximation was used (fluid density changes are accounted for only in the buoyancy term in the equations of motion), and Darcy's law was taken as an adequate model for fluid flow in the porous matrix. Analysis of the problem with another approach (Pruess and Schroeder 1980) that does not incorporate the Boussinesq approximation gave similar results for the thermal field but resulted in significantly higher pore fluid pressures (Hickox and Eaton 1980), which for a rigid matrix could indicate rupture of the sediment. A more complete model of the response that allows for sediment deformation is being developed, but actual predictions are some time away because of the lack of appropriate physical property data. It should be noted that a model incorporating sediment deformations was developed by Cambridge University (Savvidon 1988).

Thermal, physical, and chemical properties of sediments were measured in the laboratory (Hadley, McVey, and Morin 1980; Silva and Calnan 1981; McVey et al. 1983; Miller, Miller, and Olson 1982) to support the development of analytic models. The measurements were made on sediment samples cored or dredged from the seabed area of interest. For measurements, the sediments were processed and reconsolidated. The extent to which structural and chemical changes are produced in the sediment by coring or dredging, pore water expansion, and temperature change during recovery, processing, and reconsolidation is undefined. Although these changes are thought to be small, confirmation is required. This confirmation is being sought as part of the ongoing experimental effort. Investigations of the sediment microfabric of undisturbed and remolded ISHTE simulation samples reveal common microstructural features (Bennett et al. 1985a). The illite sediment appears to be a reasonably good material for reconstituting to in situ porosities for ISHTE-type experimental work (Bennett et al. 1986a, b; Burkett et al. 1987).

Thermal conductivity and thermal diffusivity of illite and smectite were measured at 600 bar over the temperature range of 20° to 350°C (Hadley, McVey, and Morin 1980). The results were correlated analytically by a model that assumes parallel thermal resistances of the water component and sediment matrix.

The effects of decay heat on the geochemistry of the seawater-sediment mixture have been studied in the laboratory (McVey, Erikson, and Seyfried 1983; Thornton 1983). Experiments in which a mixture of seawater and sediment are heated to temperatures of 200° and 300°C at pressures of 500 bar have shown a sharp decrease in pH from 8.3 to 3.5 (300°C) or 5.0 (200°C). It was also noted that water samples from the heated seawater-sediment mixture contained greater concentrations of trace elements such as Fe, Zn, Sr, Ca, and Ba in solution than are found in seawater-sediment mixtures

at room temperature. The increased concentration in solution of these elements may influence the radionuclide sorption process in the high-temperature region. In situ data are required to confirm the trends observed in the laboratory.

Experiments have been run to measure distribution coefficients in sediments for several of the more important radionuclides (Heath, Epstein, and Prince 1977; Erickson 1979; Fried, Friedman, and Sullivan 1980; Fried et al. 1980). The distribution coefficient, K_D, is defined as the equilibrium concentration of a particular radionuclide per unit mass of the sediment matrix divided by the concentration per unit volume of the sediment. These data have been used in theoretical studies of radionuclide transport in sedimentary layers (Hickox and Watts 1980a; Fried et al. 1980; Russo 1980; Nuttall, Ray, and Davis 1981). The studies were based on the worst-case assumption that the entire inventory of a waste canister was released instantaneously at the midplane of a 60-m thick sedimentary layer. The results indicate that, for the radionuclides considered, those that migrate as cations have relatively large distribution coefficients (K_D on the order of 10) and are contained within the sediment. The anionic species, for which low distribution coefficients were predicted, t ached the sediment-water interface in approximately 5000 years. Nevertheless, the predicted peak rates at which the radionuclides were released into the water column were less than the natural radioactive radon flux. The predictive methods may be modified in the future as data are obtained on in situ behavior of the sediment.

All conclusions concerning the thermal, fluid, chemical, and radionuclide sorption response of the sediment are based either on analyses that involve assumptions about in situ sediment behavior or on laboratory data that are derived from tests of processed sediment samples removed from the seabed. Because program decisions are based on the results of analyses and experiments, the applicability of the assumptions and the experimental data to the in situ problem must be verified. In addition, in situ data will be valuable in determining whether any heretofore unanticipated phenomena occur. On the basis of these considerations, an in situ experiment was planned. This article describes the experiment and its relevance to SDP, and documents the science and engineering contributions made.

ISHTE

ISHTE was designed and implemented by teams from several organizations.

- Sandia National Laboratories, Albuquerque (SNLA) provided program direction, thermal and fluid analysis, and heat transport experiment design.
- The University of Washington Applied Physics Laboratory (APL) provided the design and development of the experiment platform with the associated mechanical, electrical, and data-recording systems as well as ocean engineering for the launch and recovery system. APL also provided the thermal sensor array and coring systems.
- The University of Rhode Island, Marine Geomechanics Laboratory (URI) provided geotechnical analysis and sediment strength properties.
- Woods Hole Oceanographic Institution (WHOI) developed hardware for the geochemical experiments.
- Naval Ocean Research and Development Activity, now known as the Naval Oceanographic and Atmospheric Research Laboratory (NOARL), developed hardware for the pore pressure experiment and conducted microfabric investigations.

- Monsanto Research Corporation, Mound Laboratories, provided the isotopic heat source.

The experiment had undergone design and evaluation for 8 years. During that period, design tradeoffs and alternatives were explored extensively with the design group. The details of the experiment subsystem are discussed later, but here it is appropriate to present the overall configuration of ISHTE (Percival et al. 1980). A sketch of the platform is shown in Figure 1. Salient features include the experiment heater, with 500 W of thermal power being provided by five PuO_2 fuel spheres; vertical insertion of the heater into the sediment; electrical power supplied by batteries; drive forces supplied by ambient sea pressure; redundant data electronics; and redundant recovery systems. An experiment duration of 1 year was planned, with an anticipated maximum sediment temperature reaching 300 °C. The maximum temperature occurs adjacent to the heater near the horizontal midplane. The ambient temperature was ~2 °C. The experiments included in situ thermal conductivity, temperature field, pore pressure, ion migration, pore water chemistry, shear strength, and posttest cores.

Objectives of the Experiment

The primary objectives of ISHTE were:

(1) to provide data on the effects of heating on the response (temperature excursions, pore pressure variations, pore fluid motion, tracer particle transport, thermochemical reactions, etc.) of in situ sediment for use in verifying laboratory experiment approaches and computer models
(2) to observe any unanticipated phenomena that may occur in situ
(3) to develop and demonstrate the technology necessary to perform waste isolation-oriented experiments on and in the seabed at depths of 6000 m for an extended period of time, to obtain large quantities of reliable data, and to recover the experiment and postexperiment calibrations

Two points are emphasized. First, ISHTE was *not* a simulation of a waste emplacement. No effort was made to scale canister sizes, power, or emplacement depths. The experiment was designed only to provide a body of data to test and verify the accuracy and applicability of laboratory experimental approaches and computer models. Second, ISHTE was not *solely* a heat transfer experiment. In addition to the energy transport data, information to be obtained included pore fluid response, sediment-seawater-heater thermochemical reactions, sediment thermal stability, time-dependent sediment physical properties, and the transport and sorption of injected tracer species.

Site Selection

Because of the anticipated high temperatures to be generated during ISHTE and the need for fine-grained, low-permeability sediments, considerable effort was devoted to selecting a suitable site. One aspect was that the water pressure must be high enough to prevent boiling and possible abnormal, thermally induced volume increases. The ISHTE site criteria were:

- water depth of at least 4000 m
- known sedimentology, with a sediment type required for waste disposal
- low-relief bottom topography

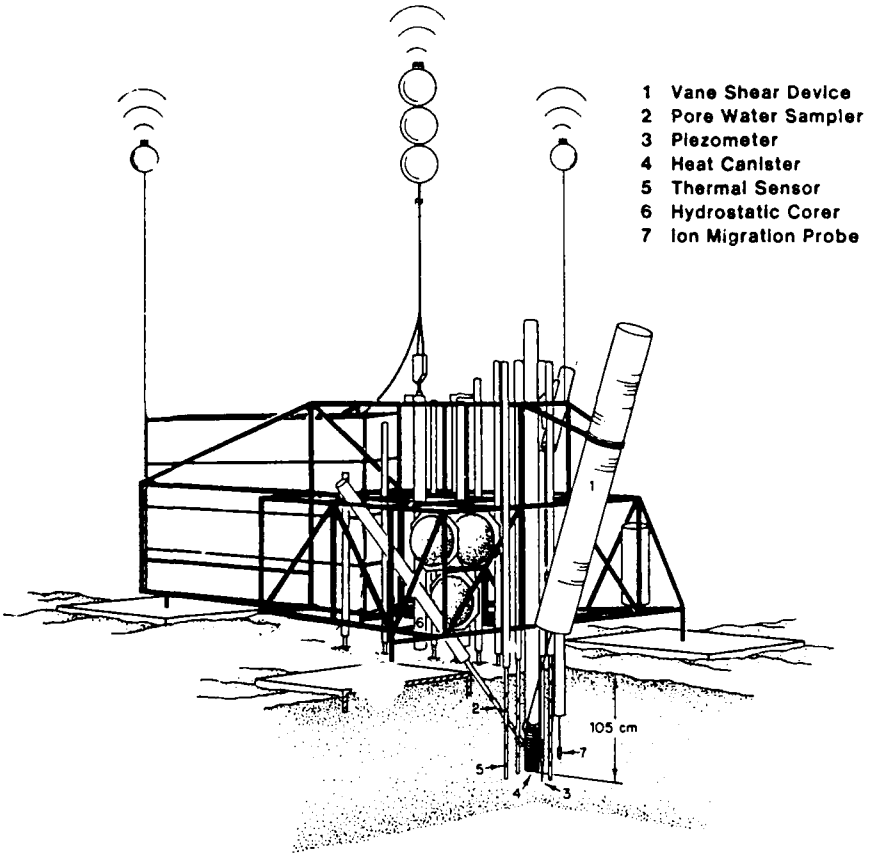

Figure 1. Artist's conception of ISHTE platform.

Several oceanographic research cruises were concentrated in a region ~1800 km north of Hawaii in an area designated MPG-I (MPG, midplate, midgyre); this area lies between latitudes 30° and 31°30′N and longitudes 157° and 159°W. A great deal of data has been collected on the geologic aspects of the region as well as on the geotechnical and geochemical characteristics of the sediments to depths of more than 24 m into the sediment layer. ISHTE could have been performed at other sites, but the MPG-I site had the best characterization. Sufficient material and site characterizations were required to provide the necessary thermal and mechanical properties for the model calculations.

On the basis of collected data, the most likely site for the ISHTE was determined to be near the location of a giant piston core (GPC-3) obtained during C/S *Long Lines* cruise LL44 (Heath et al. 1980). A detailed site survey with sampling was made in this area in cooperation with the Manganese Nodule Program (MANOP) in spring 1980 (cruise RAMA-I). As part of this cruise, the Deep Tow instrument of Scripps Institution of Oceanography Marine Physical Laboratory was used to conduct a near-bottom, sea floor survey to document details of a specific site for ISHTE. The Deep Tow package provides a precision echo sounder, side-scan sonar, photographic coverage, and high-resolution sub-bottom profiling in addition to depth, water temperature, and conductivity measurements. The data were tied together by precise near-bottom acoustic transponder navigation.

Special long-life transponders were emplaced near the surveyed site so that the site can be relocated. Data from Deep Tow, box core samples, and gravity core samples have been analyzed. Results of these studies indicate that a suitable site 3 by 5 km exists at 30°23′N, 157°43′W. The sediment in the area of the planned test site is quite uniform both laterally and vertically. The sediment consists of illite or mixed-layer illite-smectite quartz, Fe-chlorite to a depth of ~5 m, and smectite, clinofilolite, and amorphous material associated with minor quartz and mixed-layer illite-smectite at greater depths. Because of limits in both cost and instrumentation design, ISHTE was limited to a depth of about 1.5 m in the sediment, placing it within the illite layer.

Several ISHTE cruises have verified portions of the data obtained from the MANOP cruise and located more precisely a desirable ISHTE site (Miller, Miller, and Olson 1982; Olson and Roberts-Backes 1980). A detailed map of the proposed lander site area was produced, and the nature of the manganese nodule layer that the lander's instrumentation system must penetrate was documented. The data were referenced to a precise ISHTE acoustic transponder navigation system (Roberts-Backes et al. 1980) and referenced to latitude and longitude by satellite navigation. Special acoustically secure transponders were developed by APL (Backes, Bell, and Olson 1981) for precise navigation during ISHTE.

Platform Mechanical Systems

Platform Structure

The ISHTE instrumentation was supported by a mild steel spaceframe as shown in Figure 2. Most of the structural members were welded circular tubing with a few rectangular sections in the highly stressed area of the lift point. The platform, without the support pads, was 3.12 m wide, 3.4 m high, and 4.24 m long. The instrumented platform, when ready for ISHTE deployment, weighed 5923 kg in air and 3213 kg in seawater. After removal of the bolted components, the platform fit into a standard shipping van for transport by truck or container ship. This frame served as a protective package for shipping many ISHTE instruments. Figure 3 shows the ISHTE platform loaded in a truck.

From a corrosion standpoint the platform was a large steel anode, which galvanically protected the more noble materials of the instrumentation. The few items less noble than mild steel were electrically isolated from the frame and were protected by individual anodes. To prevent hydrogen generation around the heater caused by galvanic action, the Inconel heater case and drive arm were isolated electrically from the platform. All external parts of the heater were constructed from materials of nearly the same galvanic potential. A Zn-rich paint on the outside surface of the mild steel structure provided a clean surface during instrumentation and testing of the platform but was not expected to protect the frame during the year on the seafloor. A thin, uniform coating of rust was expected to form on the mild steel.

The ISHTE platform was supported on the seafloor by three large fiberglass pads. The average sediment pressure for the pads, assuming a flat sediment surface, was 5.89 kPa. These pads provided a stable base for the structure and prevented lateral motion resulting from drag forces from the mooring lines. The pads were 0.99 m wide by 1.83 m long. Each pad had 66 25.4-m diameter holes that allowed venting of water during deployment and recovery. Lateral support was provided by 150-mm deep skirts of fiberglass around the perimeter of each pad.

The pads were designed to limit settlement of the platform to tolerable and predictable values for the duration of the experiment, to control the effects of erosion, and to minimize the stress levels induced into the instrumented portion of the testbed beneath the platform. The pads were sized according to the allowable bearing capacity of the MPG-I sediment. Total settlement predictions for the pads included elastic deformation, primary consolidation, and secondary compression (plastic deformation) of the sediment.

Heater Implantment System

The most important item to be driven into the sediment for ISHTE was the isotope heater. All experiments on the ISHTE platform were based on an increased temperature field in the sediment. The heater drive arm with the electric test heater is shown in Figure 4. It consisted of a 45-cm long heater at the lower end, an implantment tube that would span the distance from the heater up into the seawater, a pressure case for the thermocouple electronics, and a drive tube at the top. The hydraulic implantment system shown in Figure 5 pushed the bottom end of the heater vertically downward 105 cm into the clay sediment with a rack-and-pinion drive. The rack, which was attached to the outside of the drive tube, was electrically isolated from it by a flame-sprayed coating of Al_2O_3 and TiO_2. The pinion gear was driven by a standard Gerotor-type hydraulic motor mounted on the platform. The high-ambient pressure seawater in the deep ocean was channeled through a pressure intensifier to supply oil at above-ambient pressure to the hydraulic motor (Olson and Harrison 1982). A pressure case served as the low-pressure reservoir to accept the hydraulic fluid from the system. Hydraulic locks were used to secure the arm in both the stored and the implanted positions.

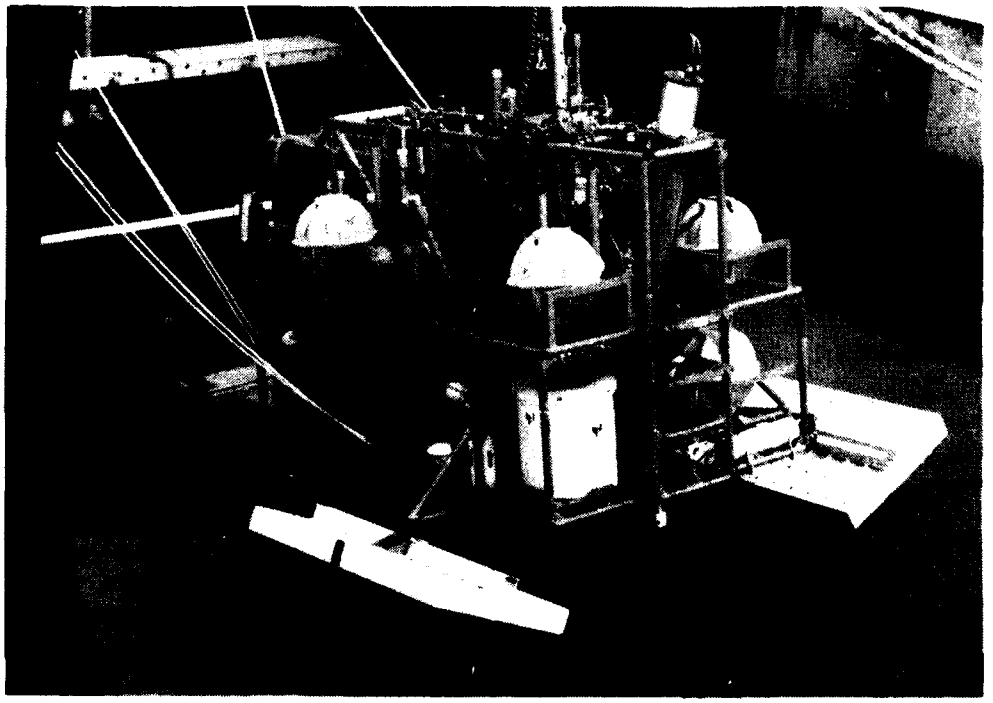

Figure 2. Instrumented ISHTE platform.

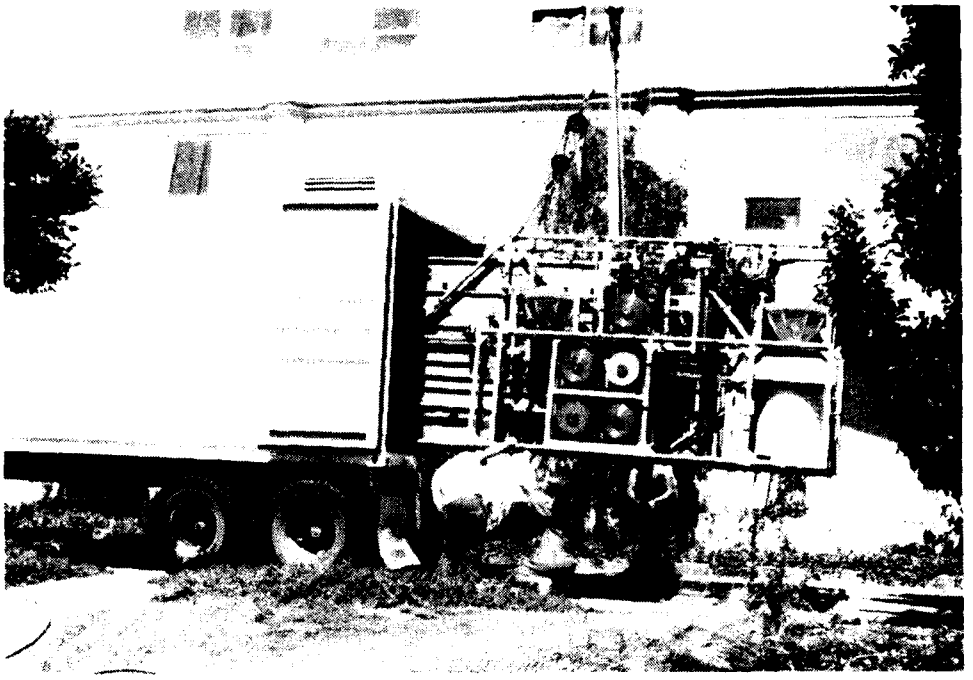

Figure 3. Loading ISHTE platform into shipping container.

Two implantment arms, one with the electric heater for use on the ocean test cruise and one with the isotope heater, were to be used during the actual experiment. These two arms were designed to be interchangeable. The isotope heater and arm assembly were designed to be slipped into the platform in place of the test arm. This was not to be done until the ship was ready to leave port for the final deployment of ISHTE.

At the end of the ISHTE deployment another hydraulic system was to use the high-ambient pressure seawater to extend two cylinders that would retract the heater from the sediment. This was accomplished by opening a valve between an evacuated reservoir and the rod end of the retracted hydraulic cylinders. Sea pressure acting on the other side of the pistons caused the cylinders to extend their rods. This action lifted the heater and adjacent equipment out of the sediment (the adjacent equipment was the 140-cm long corer and the attached small-diameter corer).

Sensor Implantment Systems

There were many systems on the ISHTE platform to drive samplers and probes into the sediment for the individual experiments and to retract them before recovery. Some of the drive systems are discussed in the sections dealing with specific experiments. Central to the platform was one system to drive and retract the temperature, the thermal conductivity, and the pore pressure probes. This system, which handled 89 of the 128 sensors and samplers to be driven into the sediment, encompassed most of the platform and had a network of electrical and hydraulic conductors semipermanently attached to the frame.

The sensor probe implantment and retraction system was a low-differential pressure

electrohydraulic system that operates fully flooded in high-ambient pressure fluid (Miller, Miller, and Olson 1986). The electric motor, running immersed in a pressurized fluid, drove a hydraulic pump that could generate a 345-kPa oil pressure above the ambient 58.8-MPa sea pressure. This pressurized oil operated a bank of hydraulic cylinders, one cylinder for each probe to be driven. The electronics case of each probe acted as the piston in a hydraulic cylinder. The sensors for each probe were housed at various distances down the center of an 8-mm diameter metal tube that was connected to the electronics case and served as the piston rod in the hydraulic cylinder.

Figure 4. Heater implantment arm.

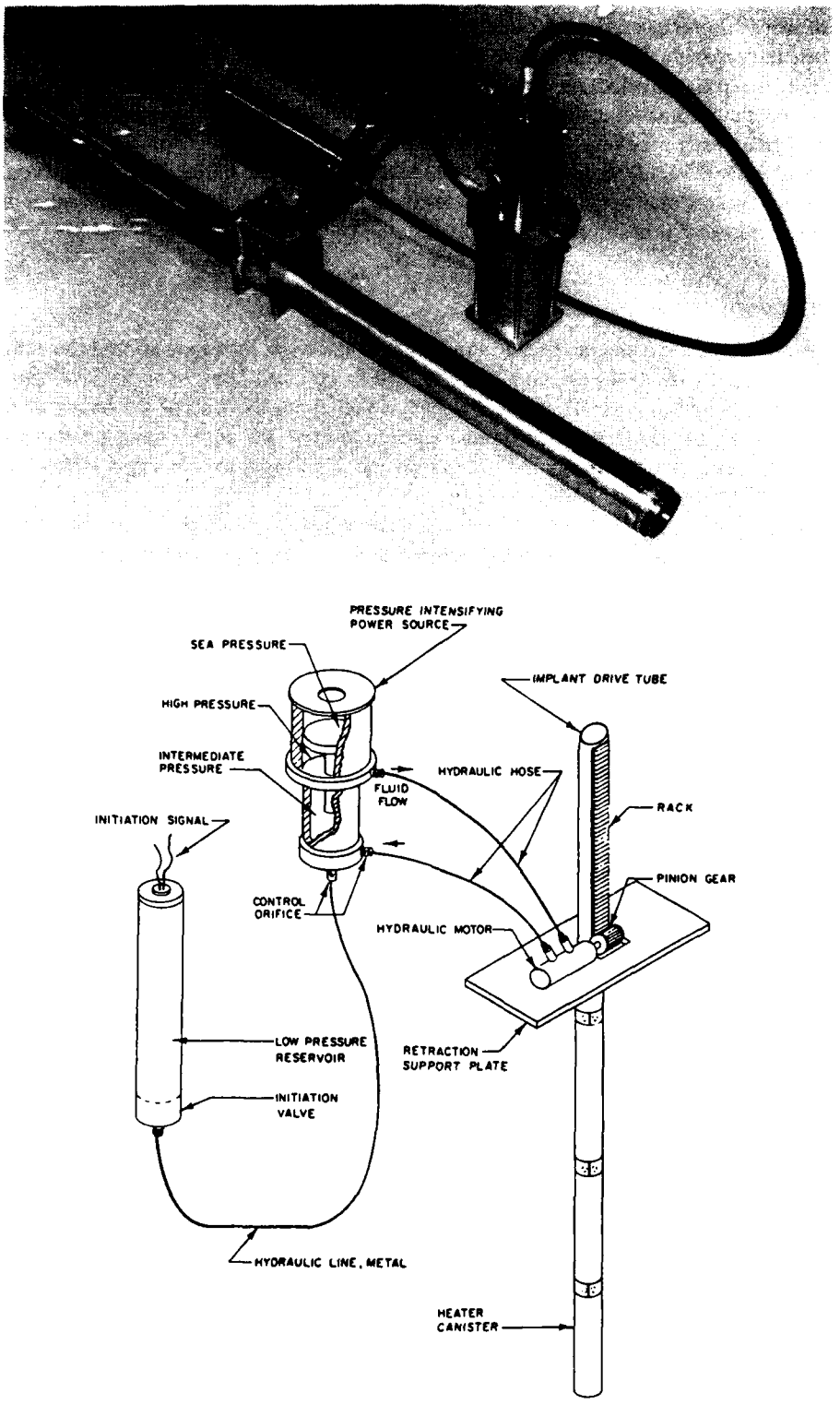

Figure 5. Hydraulic heater drive.

There were 20 probe-implanting cylinders. Each was secured to the platform in a vertical orientation with the sensor tube down. When fluid was pumped to the top of a cylinder, the rod extended and this implanted the sheathed sensors into the sediment. When the pump was operated in the reverse direction the pressure in the cylinder dropped below sea pressure, and the sea pressure pushed the rod with the sensors back into the cylinder. Valves were used to sequence the drive of the probe. This system could be turned on and off, which allowed individual groups of probes to be driven or retracted at different times during ISHTE.

Corer Systems

At the end of the experiment, five 10-cm diameter corers at locations around the heater (Fig. 6) were driven to depths ranging from 120 to 160 cm. One 5-cm diameter piston corer was attached to corer II and was driven down along the side of the heater as the corer actuated. The hundreds of newtons required to drive the corers were generated by hydrostatic actuators that used the energy in the high-pressure seawater (Olson and Harrison 1979; Olson and Miller 1986*).

Figure 7 shows a cross-sectional view of a corer incorporating the hydrostatic actuator. The corer used standard hydraulic design practices to generate and control the forces to slowly drive the core barrel. The difference is that these units used the high-pressure fluid on the outside of the hydraulic cylinder to generate the force. The fluid on the inside was used to control the rate of actuation.

The hydraulic cylinder (corer) was mounted vertically with the open end toward the sediment. The piston rod was secured to the platform. With the initiation valve closed, the working fluid was trapped between the piston and the upper end of the cylinder (core barrel). The working fluid was pressure balanced to the sea pressure by slight motion of the core barrel.

When actuated by an electrical signal, the initiation valve opened explosively by rupturing a disc. The working fluid was then free to flow into the low-pressure reservoir located in the piston rod. Frictional resistance to flow through the small-diameter control tube created a back pressure that limited the rate of actuation. The differential pressure across the top of the core barrel generated a force that drove the barrel into the sediment.

Both the 5-cm diameter corer and the number II corer were extracted from the sediment as a unit with the heater. The remaining corers were extracted from the sediment when the platform was lifted from the seafloor at recovery. Various lengths of recovery lines connected them to the platform after drive, so that the pull-out forces of the corers acted sequentially on the platform during recovery (Olson and Miller 1986a).

Photographic Equipment

Two Benthos 35-mm deep-sea cameras were part of the platform. One was the model 371 camera and strobe system, which had a capacity of about 60 pictures and was triggered by a bottom contact switch, that took a series of photographs of the ISHTE test area as the platform was set onto the seafloor. The second was a model 377 camera, which used two strobe lights to illuminate the area around the ISHTE heater and provided the view shown in Figure 8. This camera system could take 3200 pictures, providing a minimum of 4 pictures a day for the duration of ISHTE. The pictures would show signs of increased macrobiologic activity around the heated zone or any changes in the surface of the sediment adjacent to the heater's implantment arm.

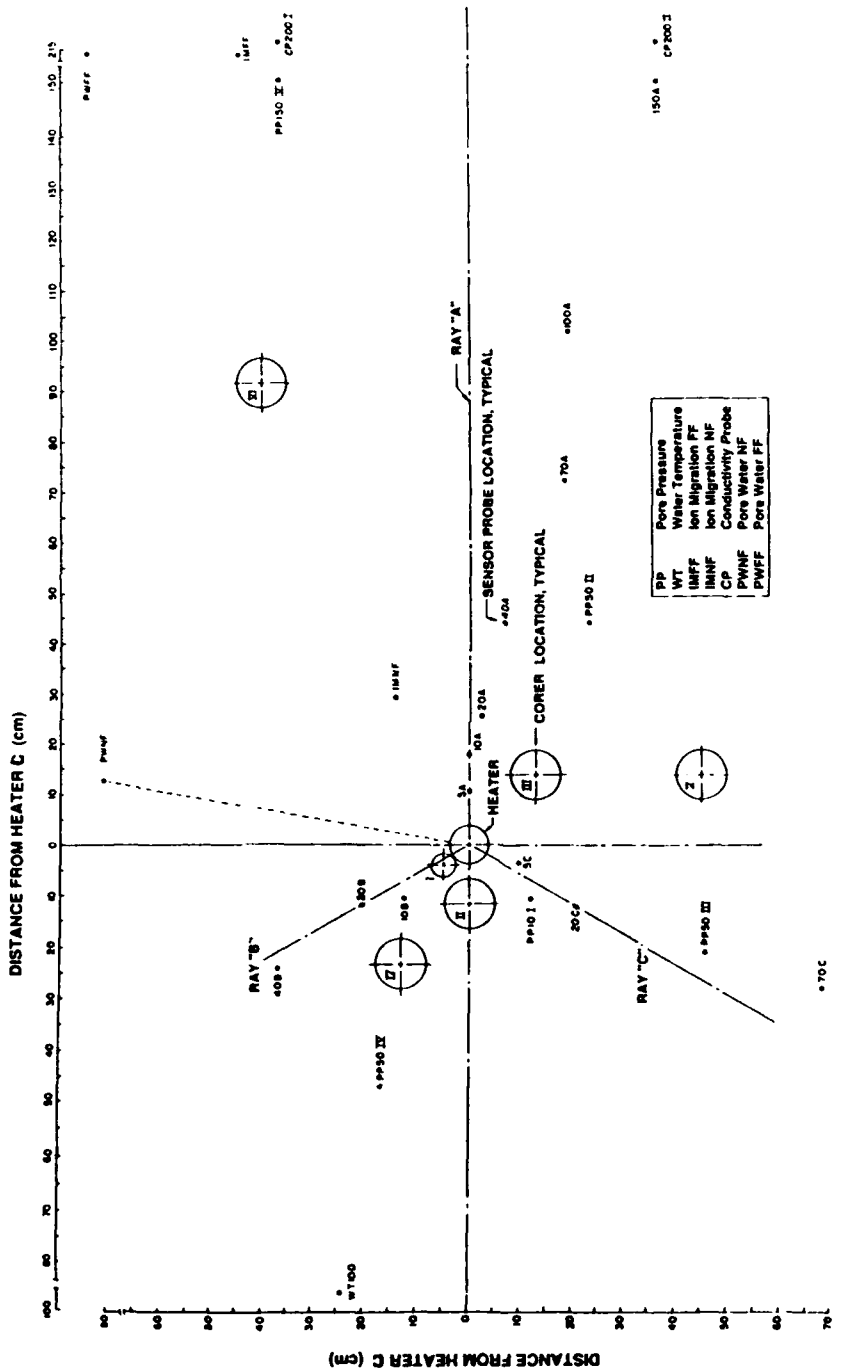

Figure 6. Schematic of radial core distances.

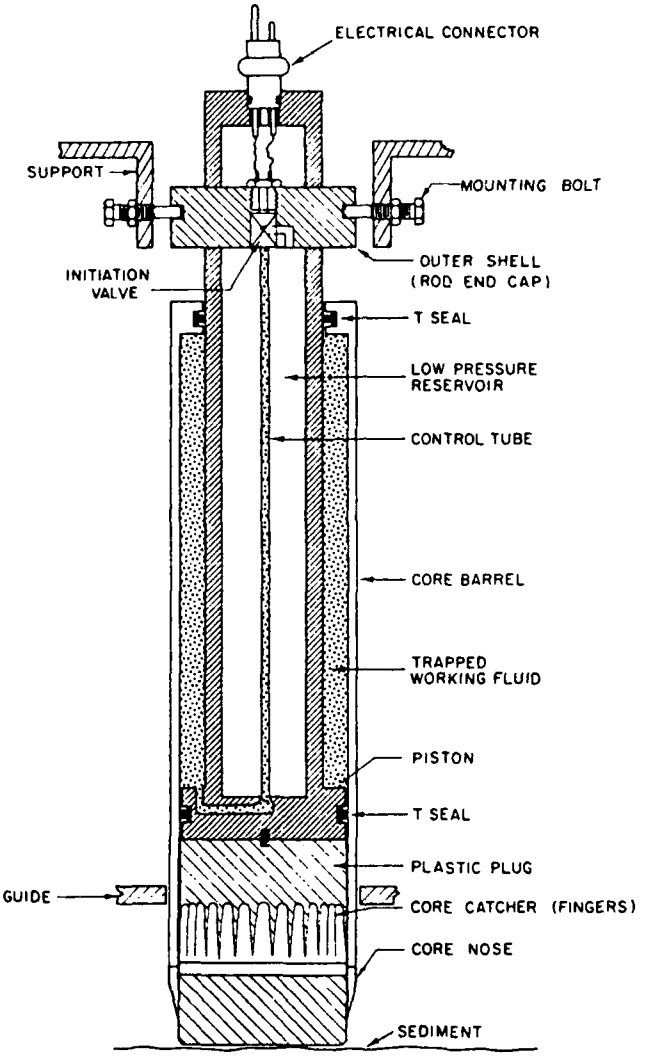

Figure 7. Cross-section of corer.

Platform Electrical and Acoustic Systems

Tracking and Telemetry

The deployment and recovery of the ISHTE platform required an underwater tracking system to display the location of the launch ship and the platform and to provide information about platform status. A tracking system was also needed to position the ship over the platform for acoustic communication and data transmission. If the primary and back-up platform recovery systems malfunctioned, a tracking system would be needed to guide a grapnel to the backup recovery lines. Also, a means of telemetering experimental data from the platform to a surface ship was needed.

Many underwater tracking ranges have acoustic transducers located close to land so that electrical cables connect them directly to a computer facility. In deep-water areas,

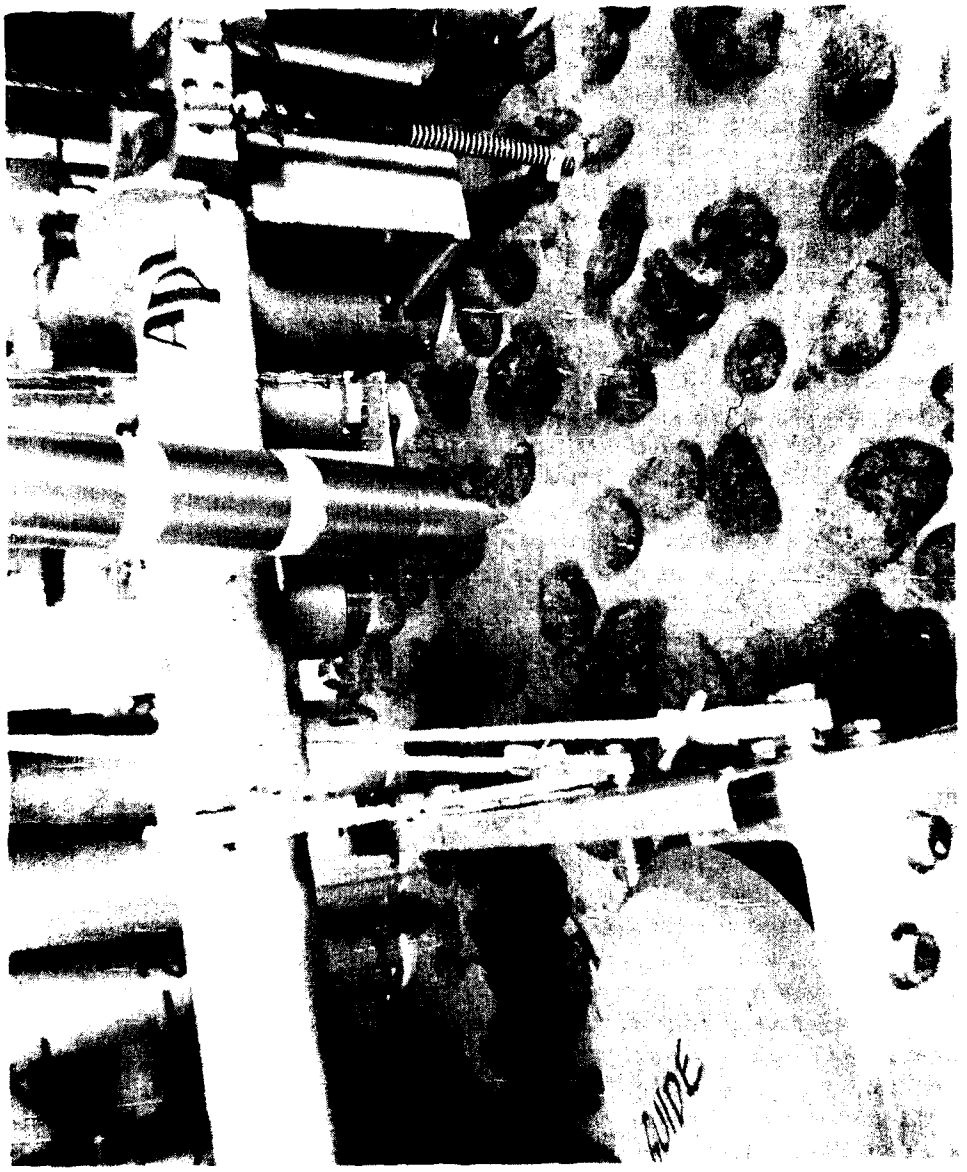

Figure 8. Photograph of heater area.

such as the MPG-I area, this is not possible. Several ship-mounted, short-baseline array systems are available for open-ocean tracking at shallow depths, but they lose their accuracy at greater depths because of the short distance between transducers. Also, the range is usually limited because of the frequencies required to optimize the timing differences between arrivals of the signals at the closely spaced transducers. A few acoustic tracking systems are available that will track at long ranges (10 km), but they have little or no data capacity in their signals. Most of these systems use bottom-mounted transponders that merely respond with a short pulse to obtain round-trip travel times.

The acoustic tracking and telemetry system developed for ISHTE (Roberts-Backes et al. 1980) differs from most other deep-ocean tracking systems because it uses differential phase shift-keyed (DPSK) modulation to superimpose digital data on the acoustic tracking and telemetry pulses. This technique allowed real-time acquisition of data from several sensors on the submerged platform while the surface ship and the platform were simultaneously tracked with respect to a fixed coordinate reference. In addition, large amounts of data (>2 Mbits) could be obtained from the platform by temporarily suspending tracking and by commanding the platform to telemeter to the ship a series of closely spaced acoustic pulses.

The ISHTE long-baseline tracking system consisted of four low-power, bottom-mounted transponders and one or more tracked objects together with a shipboard tracking computer, CRT display, and acoustic transmitter-receiver. An object, such as the ISHTE platform, is tracked by attaching a special transponder that can be interrogated by the tracking system. The position of the ship and one object can be tracked simultaneously. The bottom-mounted transponders could be commanded to perform a number of tasks: to measure distances with time pulses, to vary their internal delays to prevent pulse overlaps, to check internal status, to recognize coded identification numbers, and to release themselves from their anchors.

Figure 9 illustrates the ISHTE platform on the seafloor and the long-baseline tracking array. The transponders typically were located ~2 km apart and 200 m off the bottom in 5.8 km of water, the depth of MPG-I. The tracking system was designed for an acoustic communication range of 10 km from the farthest transponder. This means that a ship could track itself in an area of ~150 km^2 with a three-transponder array.

Four transponders were planted in roughly a square pattern on the ocean floor. Any three at a time were used for tracking. The fourth was a spare in case one transponder malfunctioned or was located in terrain that hindered acoustic communication. All tracking in the x,y plane (horizontal plane) was referenced to one designated transponder at location (0,0). After the initial transponder survey, the displayed depth was referenced from the surface of the ocean.

The surface ship's computer simultaneously displayed the x,y positions of both the ISHTE platform and the ship on a CRT screen. An update was made every 15 or 20 seconds (limited by the speed of sound in water, 1500 m/sec, which requires a 9-second round trip to the bottom). The last 10 to 50 positions of each track were retained on the screen to give a short history of the track. The depth of the platform was written on the screen along with the grid scale. A sample tracking display is shown in Figure 10.

All communication between the surface and the sea-floor platform was over an acoustic telemetry system that used the same format as the tracking system but could send longer data words. Information was transmitted on a 10-kHz carrier frequency with DPSK modulation and a binary data rate of 2 kbaud.

All tracking and telemetry signals consisted of a correlation code (a particular binary sequence selected to have a single sharp binary correlation function) that was followed by a data block. A correlation code allows the system to operate at low signal-to-noise ratios with low false-alarm and false-rest rates. In addition, the correlation peak generates precise timing that is used to process the data.

Commands, platform status, and experimental data were transmitted and received over the acoustic telemetry system. To ensure data integrity, the data block of all acoustic signals was encoded with error detection and correction codes (Backes, Bell, and Miller 1983). Commands were sent to the platform to initiate experiments and to retrieve data. Commands to the platform were encoded with a Bose-Chaudhuri-Hocqueghem (BCH) code, which allows the detection of up to 5-bit errors. This reduced the chance of a garbled command being received by the platform as a valid but unintended command.

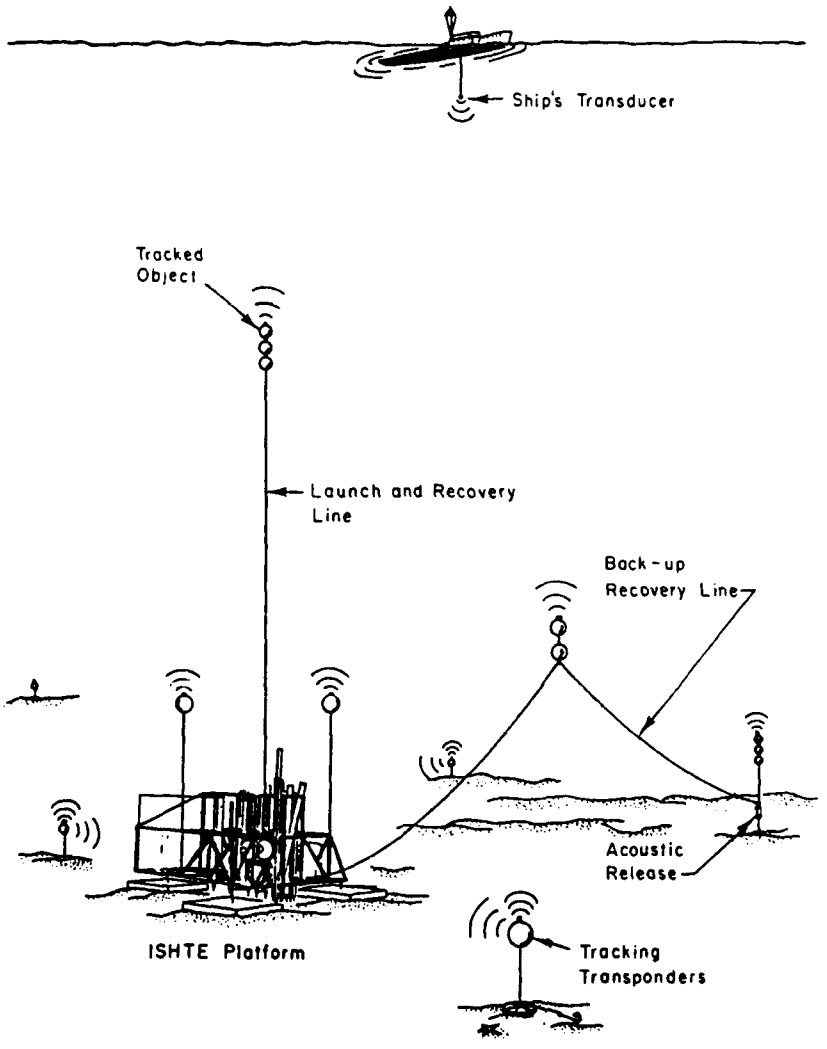

Figure 9. ISHTE platform deployed.

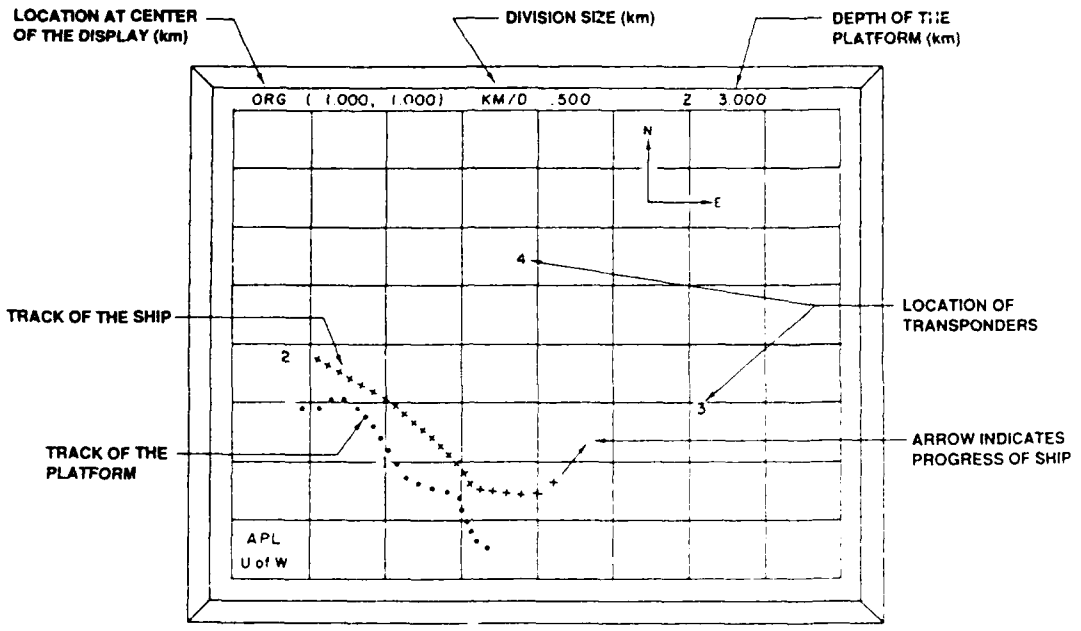

Figure 10. Sample of tracking display.

For increased security, redundancy was added to all commands, each command to the platform had to be received twice without error before it was accepted.

While the platform was being lowered to or raised from the seafloor, its x,y and z coordinates were tracked with respect to a fixed, bottom-mounted transponder array. Deployment and recovery status from the platform were received while tracking. This status was displayed in real time in addition to the position of the platform. Each status reply was encoded with a BCH code. This code, by allowing the detection of up to 5-bit errors, permitted the surface computer to use the arrival time of a garbled status reply to compute the location of the platform for tracking and, at the same time, to ignore the garbled data for display.

During the year-long experiment, data stored in the platform electronics were telemetered on command to a surface ship at 6-month intervals. Experimental data transmitted from the platform to a surface ship were encoded with a Reed-Solomon code, with each character in the code consisting of 8 bits. This enabled detection of up to three character errors and correction of up to two character errors as well as detection of burst errors of up to 17 bits. Use of error correction for up to two characters reduced the amount of transmission required when experimental data were transmitted from the ISHTE platform to the surface ship in a noisy environment.

Platform Control and Data Logging

The electronics for the ISHTE platform were designed as a dual-redundant system (Olson, Backes, and Miller 1985). There were two platform transponders, two master controllers, two slave controllers, and parallel sets of stepper switches. Any combination of platform transponder, master controller, and slave controller could be independently addressed, powered up, and used for platform command and control. Each platform

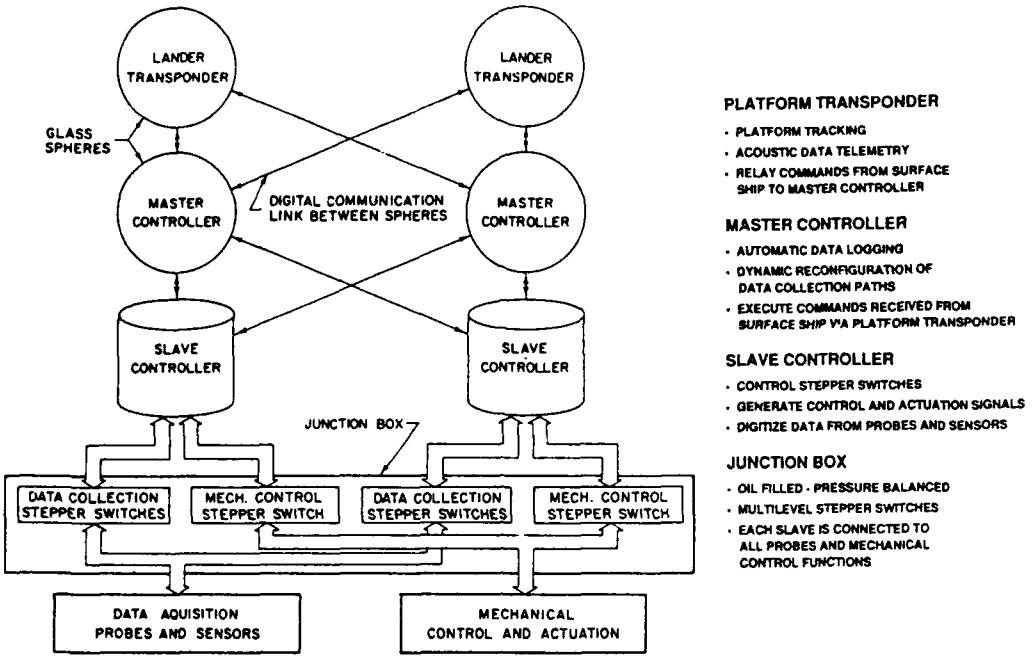

Figure 11. Block diagram, ISHTE platform control data logging.

transponder, master controller, and slave controller was packaged in a separate instrument housing. This partitioning scheme was designed to limit catastrophic failures (such as the flooding of an electronic housing) to the affected package. Also, the distribution of the electronics allowed the design to consist of a few simpler packages, each with distinct functions, rather than one complicated package that performed all the functions. The interconnection electronics were designed so the failure of one electronics package would not cause a malfunction in the packages connected to it. A simplified block diagram of the ISHTE platform electronics system is shown in Figure 11.

Platform control and data logging operated under the direction of a master controller that operated in two modes: the normal mode, in which commands were executed as they were received, and the autonomous mode, in which the surface ship initiated an experiment that the master controller then controlled. The surface ship could obtain platform status information, request the platform to telemeter data, and stop an experiment while the platform was in autonomous mode. Autonomous mode experiments could involve actuating any of the mechanical systems and sampling of single probes or groups of probes at various rates.

To help make the control system flexible, the experiments were defined in an Englishlike language. The experiment definitions were translated automatically into tables that the master controller interpreted. A short example of an experiment definition is shown in Table 1. Experiments could be added, deleted, or changed by modifying the definitions. The control program was not affected by the modification.

The control program in the master controller was run by an NSC800 CMOS microprocessor with 56k of EPROM/RAM and two timer-counters. In autonomous mode, a

real-time clock "awakened" the microprocessor when it was time to scan the probes. Two Intel magnetic bubble memories, each nonvolatile and capable of holding up to 1 Mbit of information, were used to store data taken during the first 10 days of the experiment (high data rate) and subsequently to store data collected over 6-month intervals. The bubble memories also stored the current status of the platform. A Sea Data cassette recorder, which can hold 10 Mbit of data, was used to store all the data collected for the duration of the experiment. The master controller communicated with the platform transponder and the slave controller through a 4800-baud serial data link. Because the master controller was designed for low-power consumption, it could operate from a self-contained battery pack. Each master controller with its self-contained battery supply was packaged in a glass instrument housing. Each housing had 20 single-pin electrical penetrators and two vacuum ports. The master controller specifications are summarized in Table 2.

The platform transponders were acoustic communication transponders used to track the platform, to receive commands from the surface ship, and to telemeter status or data

Table 1
Sample Experiment Definition

Experiment Definition	Comments
nameexp ("exp5");	This is experiment #5.
beginstep (0,1,0);	Do this step once.
lockout ();	Prevent surface ship from accessing slave controller during experiment.
sample (GROUP5);	Sample group 5 (ambient water temperature and pressure).
endstep ();	
beginstep (10 sec,1,0);	Wait 10 sec then do this step once.
arm (DEVICE8);	Arm device 8 (heater implant).
wait (2 sec);	Wait 2 seconds.
actuate (DEVICE8);	Implant heater.
endstep ();	
beginstep (5 sec,24,10 min);	Wait 5 sec, do this step 24 times, waiting 10 min between repetitions.
sample (GROUP3 | GROUP4);	Sample group 3 (pore water pressure) and group 4 (sediment temperature).
endstep ();	
beginstep (10 min,1,0);	Wait 10 min then do this step once.
sample (GROUP5);	Sample water temperature and pressure.
nolockout ();	Allow access to slave controller.
endstep ();	
endexp ();	End of experiment #5.

Table 2
Master Controller Specifications

Functions	Execute commands from a surface ship (relayed through a platform transponder) Execute commands from a platform transponder Collect and store data from the slave controller Run autonomous experiments Retrieve data for acoustic telemetry to a surface ship Keep track of time
Components	Data processor: 2.5-MHz NSC800 CPU, 40K EPROM, 16K RAM, two IM6402 UARTs Data storage: Two INTEL BPK-72 1-Mbit bubble memories, one Sea Data model 633 10-Mbit cassette recorder Platform transponder and slave controller interface: Two independent 4,800-baud low-power current loops (data are in ASCII with an escape character to mark the start of message) Real-time clock: 1-year calendar with resolution of 1 ms Batteries: Nominal 24-V, rechargeable lead-acid batteries for short use, lithium thionyl chloride for long use Power consumption: 90 μA standby (2.2 mW), 35 mA operating (840 mW), 325 mA (7.8 W) read/write bubble records
Commands from surface ship relayed through a platform transponder	Begin experiment Stop experiment Sample data Send data stored in bubble memory Arm a device Actuate a device Send current platform status Send status of last command accepted from surface ship Set primary slave Initialize bubble memory Erase data records from bubble memory Reset slave
Commands from platform transponder	Set real-time clock Begin experiment Get current deployment and recovery status Send status of last command accepted from platform transponder

to the surface. A platform transponder checked that all commands were received twice without error before executing them or relaying them to a master controller. A platform transponder also encoded all telemetry pings transmitted to the surface with error detection and correction codes. Each platform transponder with its self-contained battery supply was packaged in an instrument housing like that of the master controller. The platform transponder specifications are summarized in Table 3.

The slave controllers actuated mechanical controls and digitized data from the probes and sensors as directed by the master controllers. Selection of a particular probe or activation of a specific mechanical function was accomplished by using stepper switches. A slave controller was powered up by and responded to commands sent by a master controller. Data commands caused the slave controller to power up various sensor, collect, and buffer data from the sensors and to transmit the data to the master controller. Control commands actuated various devices by firing squibs, closing relays, and powering probes on and off.

Each slave controller was connected to all the sensors and control functions through separate sets of stepper switches housed in an oil-filled, pressure-balanced junction box. This allowed each controller to have complete access to the sensors and to control functions through its set of switches, even if the other slave controller or set of switches was inoperable. This interconnection scheme also reduced the number of penetrators on the slave controller and permitted electrical isolation of the sensors. All components for each slave controller, including batteries, were designed to fit into one cylindrical pressure housing. A metal housing was selected so that one connector could be used to connect electrical leads instead of multiple single penetrators, which are normally used with glass spheres.

Several different types of sensor interfaces were provided in the slave controller. Digital, frequency, and analog sensor outputs could be accommodated. Digital communication occurred through a serial link, typically at 2400 baud. A precise period-counting scheme was used to digitize the output of sensors that provided an FM signal related to the measured variable. Whenever possible, frequency-modulated or digital data were transmitted between each sensor and a slave controller instead of analog voltages because voltages are sensitive to reductions in the insulation resistance between cable wires and seawater. This problem can cause data errors that are impossible to detect. Table 4 details the specifications of the slave controller.

Sensors

Many types of sensors were developed for ISHTE. Table 5 lists some of the sensors and their pertinent specifications.

Thermocouples were attached to the surface of the ISHTE heater to monitor the temperature. Two were positioned at the top of the heater, three around the middle, one at the bottom, and two at different elevations in the implantment tube. The total was limited to eight because of space constraints where the thermocouple sheaths were brought through the 69-MPa pressure interface to the electronics package. The digitizing electronics for the thermocouples consisted of two independent 13-bit A/D converters, each digitizing the outputs from four thermocouples and one platinum resistance sensor (for measuring the reference junction temperature of the thermocouples). Thus a single electronic failure could cause a loss of no more than half the heater temperature data.

The encoded thermocouple data were sent serially from the implant arm to the

Table 3
Platform Transponder Specifications

Functions	Respond to tracking pings from surface ship Execute commands from surface ship Execute commands from master controller Relay commands from surface ship to a master controller Append error detection and correction codes to pings
Components	Transmitter: Transformer-coupled push-pull class B transistor amplifier followed by transducer-matching network Transmit power: 183 dB at 1 μPa at 1 m (data telemetry), 193 dB at 1 μPa at 1 m (tracking) Transducer pattern: Hemispherical Acoustic data: 10-kHz carrier with DPSK modulation at 2-kbaud data rate (pings consist of 20-bit correlation code followed by data block of length 25 for received pings and length 25, 63, or 256 for transmitted pings) Receiver: Low-noise preamp followed by bandpass filter followed by amplifier with AGC, overall gain 90 dB Phase demodulator: Partially coherent detection Correlator: 20 bits with timing resolution of ± 15 μsec Data processor: 2.5-MHz NSC800 CPU, 16K EPROM, 8K RAM, IM6402 UART Master controller interface: 4,800-baud low-power current loop (data are in ASCII with an escape character to mark the start of message) Batteries: Nominal 24-V, rechargeable lead-acid batteries for short use, lithium sulfuryl chloride for long use Power consumption: 300 μA standby (7.2 mW), 21 mA operating (500 mW)
Commands from surface ship	Power on/off Enable/disable reply to tracking pings (to permit tracking of multiple objects) Set status to indicate leak/low battery voltage Set transmit power for tracking/telemetry pings Start experiment (transponder starts experiments in both master controllers to synchronize start times) Set master controller real-time clocks Set tracking ping response time Send test telemetry ping data Arm and fire back-up release Set deployment and recovery status parameters Send status of last command accepted from surface ship Relay command to specified master controller
Commands from master controller	Send telemetry ping to surface ship Send 25-bit pings (8 data bits/ping) to surface ship Store this deployment and recovery status information Send status of last command accepted from master controller

Table 4
Slave Controller Specifications

Functions	Execute commands from master controller Digitize data from probes and sensors Actuate mechanical controls
Components	Data processor: 2.5-MHz NSC800 CPU, 16K EPROM, 24K RAM, two IM6402 UARTs Power to probes and sensors: ±12 V at 240 mA Squib firing circuits: 10 A into 0.25-Ω load for > 7 ms A/D conversion: 0 to 7 V with 0.85-mV resolution (13 bits) Master controller interface: 4,800-baud low-power current loop (data are in ASCII with an escape character to mark the start of message) Digital data interface: UART-compatible low-power current loop, 1,200, 2,400, 4,800, or 9,600 baud (data are in binary with 8 data bits and 1 parity bit) F/D converter: Sine wave or square wave 155 Hz to 330 kHz with 0.0001% resolution, 10-Hz sampling rate Batteries: Nominal 24-V, rechargeable lead-acid batteries for short use, lithium thionyl chloride for long use Power consumption: 70 μA (1.7 mW) standby, 60 to 80 mA (1.4 to 1.9 W) operating
Commands from master controller	Send status of last command accepted from master controller Arm device Actuate device Move stepper switch Sample sensors (power probe on, sample specified groups of sensors, power off probe and send data to master) Rapid sample sensors (leave probe powered on, send data from previous sample to master while sampling specific groups of sensors) Multiple sample sensors (leave probe powered on, send data from previous sample to master while multiplexing samples of specified groups of sensors at specified rate) Send data from last rapid sample or multiple sample Give me more data Power off Reset

Table 5
ISHTE Platform Sensors

Measured Variable	Sensor Type	Number of Sensors	Range	Resolution	Maximum (sample/min)	Conditioned output	Power Source
Sediment temperature	Thermistor	24	0° to 30°C	0.001°C	120	Sine wave	Slave controller
Sediment temperature	Pt-resistance	54	0° to 260°C	0.002°C	120	Sine wave	Slave controller
Canister temperature	Thermocouple	8	0° to 600°C	0.09°C	10	Digital	Slave controller
Thermocouple cold junction temperature	Pt-resistance	2	0° to 30°C	0.015°C	10	Digital	Slave controller
Water temperature	Thermistor	6	0° to 30°C	0.0001°C	120	Sine wave	Slave controller
Sediment thermal conductivity[a]	Thermistor	6	0° to 30°C	0.0001°C	120	Sine wave	Slave controller
Water pressure	Quartz-crystal	1	0 to 10,000 psi[c]	0.1 psi	120	Square wave	Slave controller
Sediment pore water pressure	Variable-reluctance	5	±20 psid	0.01 psid	240	Digital	Self-powered
Lander tilt (two-axis)	Force-balance	2	±30°C	0.007°C	20	Digital	Self-powered
Line tension	Strain-gauge	2	0 to 20,000 lb	2.5 lb	20	Digital	Self-powered
Probe position[b]	Potentiometer	20	0 to 208 cm	0.025 cm	240	Digital	Slave controller

[a]This sensor uses a 12-cm long heater to heat the sediment locally and thermistors to sense the temperature. The thermal conductivity can be calculated from knowledge of the heating rate per unit length of the heater and measurement of the rate of temperature rise of the surrounding sediment.

[b]A voltage proportional to probe travel is generated (for digitization by a slave controller) by using a precision current source together with a potentiometer whose resistance varies as the probe is extended.

[c]1 psi = 6.89 kPa.

ISHTE slave controller. The resolution of the encoded thermocouple outputs was 0.09 °C/bit. The absolute accuracy and stability of the electronics were much better than the inherent long-term stability of the thermocouples, which was 3 °C or less.

Thirteen probes, each containing six thermal sensors, were to be driven vertically into the sediments around the heat source at selected locations. These thermal probes had sensing elements located at various elevations in an 8-mm diameter Hastelloy-C276 tube. The upper end of the tube remained above the sediment and were sealed into a pressure chamber containing the electronics. Resistant elements made of platinum were used as sensors in the near-field, high-temperature probes ($T_{max} > 50$ °C); thermistors were used in the far-field, low-temperature probes ($T_{max} < 50$ °C). Both types of thermal probes had mercury-wetted reed relays that sequentially switched the probes's resistance temperature-sensing elements into a bridge network of a single precision RC oscillator. The FM output signal was sent to the ISHTE slave controller.

The resolution of the low-temperature probes (thermistor sensors) was 0.001 °/bit after period counting at the recording station, and the absolute accuracy was 0.02 °/year. For the high-temperature probes (platinum resistance sensors), the resolution was 0.002 °/bit. Long-term stability was better than 0.2 °/year at 0 °C and 0.3 °/year at 200 °C. Because of limitations in the calibration facility, the probes were not calibrated above 200 °C. If the sediment in the area of these probes had become warmer than anticipated, the high-temperature accuracy would have been somewhat degraded because of extrapolation of the calibration curves.

Two line-source conductivity probes were to be driven vertically into the far-field sediment. The line-source probes measured the thermal conductivity of the sediment at the ISHTE site before the heater was implanted. During the data-logging phase of the experiment, each line source was used as a thermal probe. These probes were first used to make in situ measurements of the sediment thermal conductivity at MPG-I during the ISHTE component test cruise in 1984 (Olson and Miller 1985).

Five pore water pressure probes were to be driven vertically into the sediment at various radial distances from the heater. Sampling of the probes occurred under the direction of the master controller.

A Paroscientific Digiquartz pressure sensor measured ambient pressure. The temperature of the water near the sediment interface was measured with five Sea-Bird Electronics oceanographic thermometers. One Sea-Bird thermometer was mounted near the top of the ISHTE platform to measure background water temperature.

An in situ vane shear probe measured the shear strength of the sediment in the vicinity of the heater at the end of the year-long experiment. This probe was actuated by a master controller on command from the surface. Operation of the vane shear probe is described later.

Control Sequence

Before the platform was deployed, the real-time clocks for each master controller were synchronized. Once deployment began, a platform transponder, master controller, and slave controller were used to track the platform and to relay status information to the shipboard computer. This status information included platform tilt on two axes, tension in the lowering line and the ground line (a back-up recovery line), and heater temperature. After platform touch-down, a transponder, a master controller, and a slave controller were used to initiate the implant of the line-source conductivity probes and far-field thermal probes. Then two independent thermal conductivity measurements of the sedi-

ment were made. Next, on command from the surface ship, the pore pressure probes were implanted and the transient pore water pressures associated with probe insertion monitored. The implantment of the heater and near-field temperature probes then began.

Status information concerning heater and probe deployment was stored in the master controller. Once heater implantment was initiated, the master controllers began automatic data logging. Each master controller independently powered up and sequentially took data from the probes. The two controllers operated alternately; that is, each collected data at the same rate but operated out of phase with the other by half the sample interval. If either master controller malfunctioned, information would still be recorded by the other. If the slave controller or stepper switch malfunctioned, the affected master controller would attempt to detect the failure and to reconfigure so as to use the other slave controller to allow data logging to proceed (Miller, Miller, and Olson 1986). Data recovery from the platform during the first few days of the experiment and at 6-month intervals was initiated under command from the surface ship.

Ninety days after beginning the experiment, a master controller autonomously activated the ion diffusion probe control system. This system drove two ion diffusion probes into the sediment and released tracers.

Just before recovery, the master controllers were commanded by the shipboard computer to stop the automatic data logging. A platform transponder, master controller, and slave controller were then used to initiate sediment shear strength measurements, pore water sampling, and ion diffusion probe overcoring. Next, the retraction of the thermal and pore pressure probes and deployment of the sediment corers began. Once the corers had been deployed, the heater was retracted and the recovery line released. A platform transponder, master controller, and slave controller were then used to provide tracking and status information to the surface ship during recovery.

Deployment and Recovery

Deployment

The ISHTE platform was relatively heavy for its size, which made handling it on a moving ship difficult except in calm seas. After the platform was in the water its weight dropped because of buoyancy, and it could easily be set gently on the ocean floor. The complication with the ISHTE platform was that its weight in water made a buoyant recovery from the deep ocean impractical. Lines had to be used to lift the unit at recovery. Because of storms and fishing activity in the MPG-I area, however, no lines could be left on or near the surface of the ocean.

The plan was to deploy the ISHTE platform as shown by the configuration in Figure 9. Because of the value of the equipment, recovery was important. Every effort was made to add back-up recovery systems to guarantee retrieval. For the back-up systems to add reliability to the recovery plan, all components (the platform, anchors, and flotation) had to be accurately deployed. Information about the relative location of these major components was required during all stages of fielding ISHTE. The recovery team would be able to estimate the condition of the various recovery systems independent of the platform systems by checking for changes in location of the various components.

The acoustic tracking and telemetry system described in this report provided accurate location of the key components as well as of the status of the platform. The locations were obtained by attaching a tracked object at each key point in the system. The tracking system could track simultaneously any one of many objects or the ship with respect to

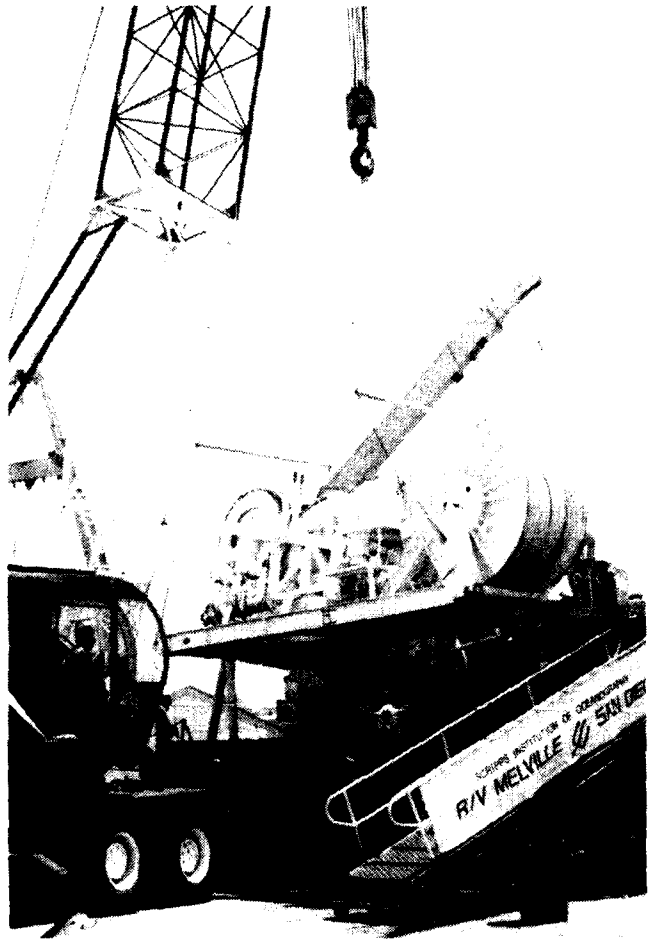

Figure 12. Loading Pengo traction winch.

the ocean bottom. The tracking data from the platform also could include the status of sensor systems, the tilt of the platform, and the tension in the lines attached to the platform. Rough values were provided in the tracking pulses. More accurate values of platform status could be obtained at any time by terminating tracking and lengthening the acoustic pulses to the telemetry mode of operation.

The R. V. *Melville*, an oceanographic research vessel operated by Scripps Institution of Oceanography, was modified to allow deployment by means of nylon lines and a traction winch. The stern of the ship has a 3.7-m wide by 7-m long ramp from the main deck to below the waterline. Normally this ramp is decked over with wooden planks and the stern end closed. For handling the ISHTE at sea, however, the stern planks were removed completely and the deck planks removed for ~4 m from the stern to the pivot point of the U frame. This allowed the ISHTE platform to be positioned with one end on the wooden planks and the other end supported by cantilevered steel beams out over the ramp at deck level. A removable catwalk in the ramp allowed access beneath the platform to check the instrumentation at sea before launch.

The traction winch shown in Figure 12 for handling the nylon line was built by Pengo Equipment Company. A unit was borrowed from the Navy for ISHTE test opera-

tions at sea. The winch delicately handles long lengths of synthetic line. The line is tensioned with two large-diameter, v-grooved wheels that are lined with rubber. After the line passes around the two traction wheels, it is normally stored on the drum at low tension. Because the line is stored at low tension, it can be pulled by hand over the top of the drum into any number of storage bins. For ISHTE the main lowering line was stored on the drum, and the back-up recovery line was stored in a bin.

The R. V. *Melville* was an ideal ship to handle the ISHTE platform except for the inadequate size of the original U frame. This frame, which is mounted over the stern ramp, was extended 2.74 m in height by cutting and welding sections into the side legs. The combination of this extra reach and the open ramp allowed the ISHTE platform to be handled over the stern of the ship for deployment and recovery. The Pengo traction winch, which is self-contained with diesel power, was bolted down on the starboard side of the main deck ~15 m forward of the stern ramp. The nylon lift line for the platform came from the winch, passed over a special sheave supported by the U frame, and fastened to the tension-monitored attachment point on the top of the platform.

The ISHTE deployment was accomplished by launching the back-up recovery line (anchor first) and the platform on the main line and then acoustically releasing the main line 1200 m below the ocean surface (Olson and Miller, 1986*). Deployment was begun by positioning the ship over the target area for the back-up recovery line anchor and lowering the anchor from the stern of the vessel. Two parallel acoustic releases connected the anchor clump to the 2.54-cm diameter nylon line. Enough floats to carry the line to the surface for recovery and a tracked object were attached to the end of the lowering line by an auxiliary line 100 m long. The assembly and the anchor were lowered 3050 m until the midpoint of the back-up line was at deck level. At this point, additional glass floats and another tracked object were attached to the line. The anchor system was lowered the rest of the way to the seafloor. When the anchor hits the bottom, the ship was 3.9 km from the targeted location for ISHTE.

As the ship slowly progressed toward the ISHTE site, an additional 600 m of back-up recovery line was released under light tension until the end was reached. A line stopper fastened to an attachment point on the end of the ISHTE platform was secured to the line several meters from the end. The short length of remaining line was laced along structural members of the platform to the tensioned lift point on top of the platform, where the end eye terminated. The attachment point at the end of the platform had a system to monitor the tension force in the back-up recovery line during deployment. This back-up line tension, along with the main lowering line tension from the lift point, was telemetered acoustically to the surface ship in each tracking signal from the platform.

With a 3.8-cm diameter nylon line from the traction winch and steadying lines, the platform was raised off the deck and shifted aft to the position shown in Figure 13. In this position, the outboard support pads for the platform were clear of the U-frame supports. The pads were pivoted from the vertical to the horizontal orientation and secured.

With slight headway on the ship and with the back-up recovery line trailing astern, the ISHTE platform was swung aft with the U frame while being lowered with the traction winch. As the platform submerged, the steadying lines, which were doubled through swivel blocks on the platform, were slipped free. The ship slowly moved toward the target area as the platform was lowered toward the seafloor. The acoustic tracking system displayed on a video screen the locations of the ship and the platform in plain view. The screen had a grid that also showed the fixed location of the back-up line, the recovery line anchor, the tracking transponder array, and the target area for ISHTE. Acoustic tracking updated the positions, the platform depth, and the maximum values of line tensions approximately every 40 seconds during the operation. By dropping the

Figure 13. ISHTE platform during launch.

platform status information that included the line tensions, the positional update could be made every 20 seconds.

To synchronize the rate of the ship's progression with the lowering rate of the platform, a plot of desired platform location against platform depth was used in conjunction with the tracking display. The platform and ship were continuously tracked so that bridge personnel could see what the platform was doing with respect to ship heading and velocity changes. Drag forces on the platform and lines, plus line tension caused by the buoyancy at the midpoint of the back-up recovery line, required the ship to pass over the platform target on the sea floor by ~ 100 m before the platform was in position to be set down. When the platform was within 100 m of the seafloor, the lowering was interrupted to allow a final acoustic test of the platform's sensor and control systems. The platform was then lowered to the seafloor at ~ 6 m/min. A test deployment located the platform within 133 m of the target in 5880 m of water. If desired, better accuracy could have been obtained.

The floats on the lowering line 1200 m below the surface allowed some slack line to be played out from the ship without fear of tangling after the platform rested on the bottom. This extra line allowed the ship to maintain a watch circle around the platform without disturbing it. After testing the platform for satisfactory operation, the lowering line was separated 1200 m below the surface by an acoustic release. Attached floats on the release carried the release and line away from the taut moor as soon as actuation occurred.

Recovery of this line and release completed the deployment of ISHTE as shown in Figure 9. The system was completely free of surface storms and fishing activity. After this point in the experiment, all communication with the platform was performed over the two-way acoustic link.

Recovery

ISHTE recovery was planned as a single-ship operation with the R. V. *Melville*. Acoustic commands from the shipboard computer terminated the experiment and prepared the equipment for recovery. A final acoustic command to the platform commanded the release of the main recovery line. Part of the recovery line was the taut moor above the platform. The additional line that allowed the taut moor to surface on release was packed in a bin on the platform. When the hydraulic release at the platform actuated, the buoyancy of the taut moor would float the end of the line to the surface.

The upper end of the recovery line had an acoustically tracked object attached so that it could be monitored during release and located on the surface. In case the large-diameter recovery line could not reach the surface because of excessive drag from the current, one glass float with a radio transmitter and flashing light was connected to it by 460 m of 6.4-mm diameter line. The reduced drag on this line would at least allow the float to surface in almost any anticipated surface current. This smaller-diameter line was stored in a bucket beneath the float at launch and retained by a special pressure release. At a predetermined depth during deployment the release would trip, but hydrostatic pressure on a piston would hold it together. As the release approached the surface during recovery, the hydrostatic pressure would be reduced. Then the unit would separate under the buoyancy force of the float. Most of the recovery line was 2.54 cm in diameter. The diameter increased in a smooth taper to 3.2 cm for the last 125 m at the platform end. The stronger line was provided for the final lift aboard ship (Fig. 14).

Should the ISHTE platform not respond acoustically at the end of the 1-year experiment, the platform would be recovered with the back-up line. Either one of the two commercial acoustic releases holding this line to the anchor could disconnect the anchor on command. The glass floats would carry the end of the line to the surface. A float with a radio transmitter and light was connected to the end of the line with a bucket of releasable line, like the unit on the main recovery line.

After the line surfaced, it would be pulled aboard under light tension while the R. V. *Melville* maneuvered over the platform. When the winch aboard the recovery ship took tension on the heavy line, a weak link securing the line to the end of the platform would release. The line termination would then transfer to the main lift point at the top of the platform. Increased tension would lift the platform from the seafloor for recovery.

If the commercial releases on the anchor were not to actuate, the next approach would be to grapple the line. An acoustic object marked the elevated midpoint of the back-up line as a target. Another tracked object would be attached to the grapnel so that its location could be monitored during the grappling operation. The last resort would be to grapple the vertical line above the platform. Although this method has been used, it is difficult, and there is a high risk of cutting the line.

Thermal Response

The major objectives of the experiment involved the investigation of thermally driven phenomena. To reach the goals of the experiment, particular attention was paid to heat transfer aspects. Numeric studies of the heat and fluid transport associated with the experiment were made. Studies of sediment properties were performed to give the best model for sediment thermal conductivity, and a parameter estimation study was initiated to determine more accurately the sediment thermal properties from the planned ISHTE. This section briefly reviews the most important results of these investigations.

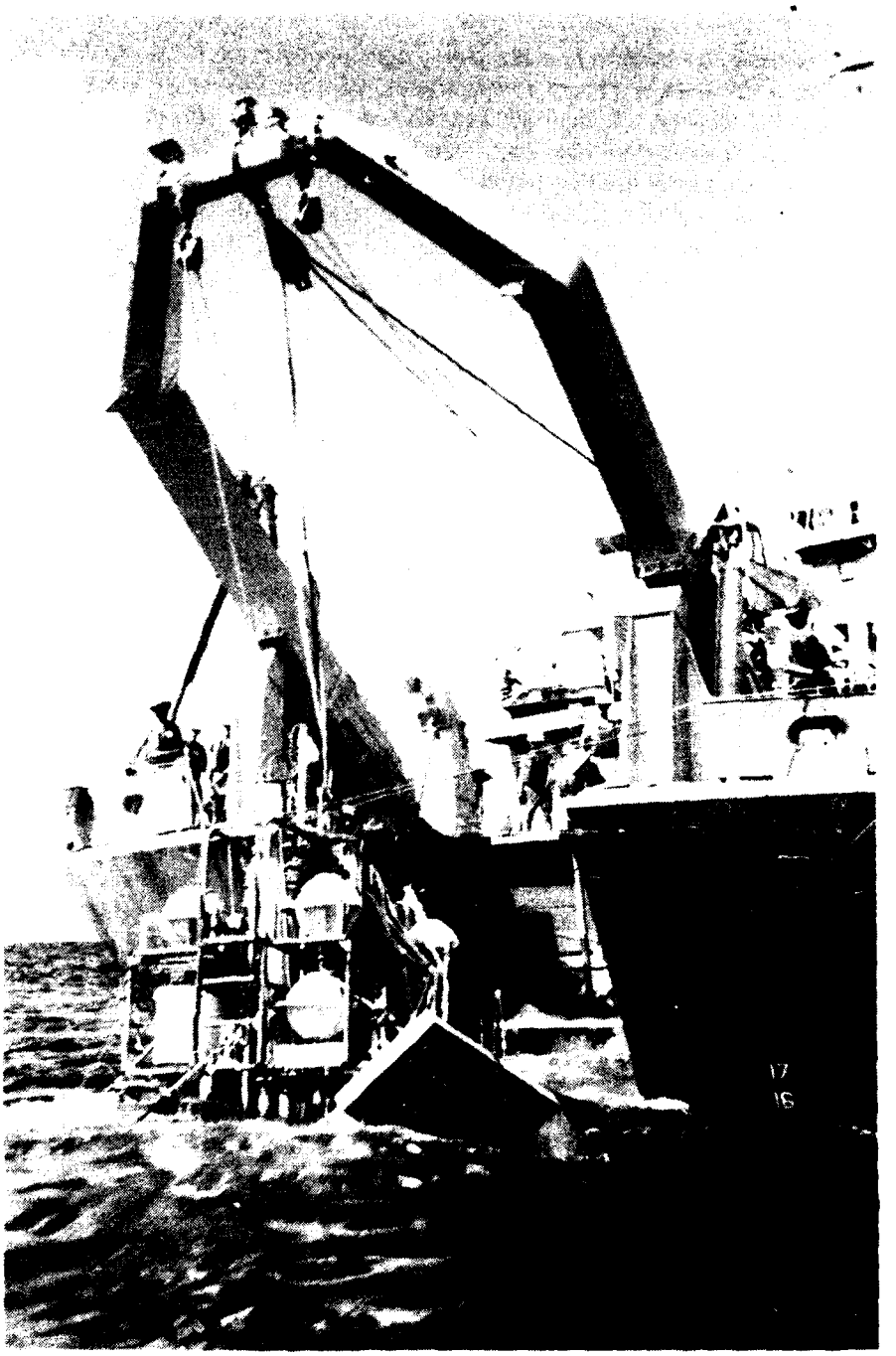

Figure 14. ISHTE platform during recovery.

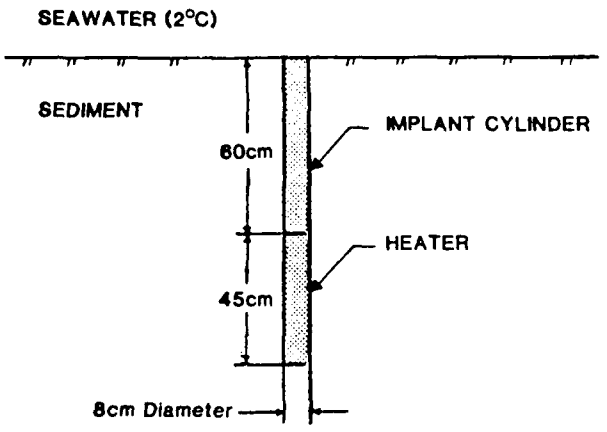

Figure 15. Schematic of heater geometry used in the numeric studies.

Two computer programs were used in the thermal analyses of ISHTE. Most of the thermal design calculations were made with a finite-element thermal-conduction code, COYOTE, developed by Gartling (1982). The finite-element grid was generated with the use of QMESH (Jones 1982). The thermal property correlations presented by Hickox et al. (1986), adjusted for temperature dependency and to the proper porosity for the experiment depth, were used in the analyses. A schematic of the ISHTE heater geometry used in the numeric studies is given in Figure 15. For the purposes of analysis, the region around the heater was defined by an appropriately selected finite-element mesh. The lateral and lower boundaries of the mesh were located far enough from the heater that the thermal field of interest was essentially unaffected by the presence of the artificially imposed boundaries. The results described in the remainder of this section were obtained from numeric studies based on the defined region.

Thermal Analyses

One of the initial considerations was the heater power requirement for the experiment. Because the experiment was intended to run for about 1 year, practical considerations of weight and volume eliminated heater power sources (electrical or chemical) other than isotopic. Previously developed, tested, and ocean-qualified 100-W fuel sphere assemblies (FSAs) (General Electric 1977) were selected for the heat source (see later section).

Calculations were initially performed for a four-sphere heater configuration. This calculation was later updated, however, to include the effects of thermal properties of a sediment based on those of reconsolidated illite (Hickox 1984a–1984g) and to include an estimated reduced power of 95 W available from each sphere at the time of ISHTE (Mondy 1985a). These results indicated a maximum temperature at the heater-sediment interface of 200° to 230°C depending on the assumed sediment conductivity. Thus, to produce a temperature greater than the 250°C minimum requirement at the heater-sediment interface, a fifth sphere was added to the isotopic heat source (IHS).

In this model the thermal conductivity is expressed by

$$\kappa = \phi\kappa_w + (1 - \phi)\kappa_s \qquad (1)$$

where κ_w and κ_s are the conductivities of water and the solids, respectively, and ϕ is the porosity of the sediment (for κ_s the properties of the solid are taken to be those of slate). This model was shown to be a good approximation of the thermal conductivity of reconsolidated illite at high temperatures (Hadley, McVey, and Morin 1980).

Figure 16 shows the values of κ_w, κ_s, and κ at a porosity ϕ of 0.72. The thermal conductivities of slate have been measured by Birch and Clark (1940) up to a temperature of 200 °C. Above this temperature the properties are assumed to be constant at their values at 200 °C as judged from the flattening slope of the curve shown in Figure 16. Properties of saltwater at 600 bar are represented by the symbols in Figure 16. These values (Riley and Skirrow 1975) are only for fairly low temperatures, but they are close to the values for pure water. The effective κ of the sediment is fairly constant up to 150 °C and then decreases as the temperature increases. Below a temperature of about 250 °C, κ from Eq. (1) is slightly greater than the 0.0091 W/(cm · °C) value given by Hickox et al. (1986).

The steady-state isotherms in and around a five-sphere IHS and obtained by assuming constant sediment thermal conductivity are shown in Figure 17 and are given by Mondy (1985b). The maximum temperature of ~319 °C occurs inside the bottom two fuel spheres. Because the seawater-sediment interface is held at 2.0 °C and is closer to the heater than the other boundaries, the isotherms are skewed downward. This causes the effective thermal midplane of the IHS to be about 9 cm below the geometric midplane. This can be seen in figures 17 and 18, where the steady-state temperatures along the surface of the IHS are plotted. Figure 19 also shows that the maximum sediment temperature, which occurs at the IHS surface, is ~286 °C. The additional power has increased the maximum temperature to >200 °C, as desired. The resulting temperatures in the sediment radially out from the center of the heat canister are shown in Figure 19 and are compared to the temperature obtained when modeling a four-sphere IHS.

Although the exact temperature dependence of the thermal conductivity of in situ sediment is not known, Eq. (1) gives a reasonable prediction based on laboratory experiments on reconsolidated sediment. As shown in Figure 20, the thermal conductivity κ predicted by Eq. (1) is greater than 0.009 W/(cm · °C) at temperatures less than ~250 °C. At the highest temperatures reached in the sediment, κ is less than the constant value used in the first case; the overall effect of using the temperature-dependent esti-

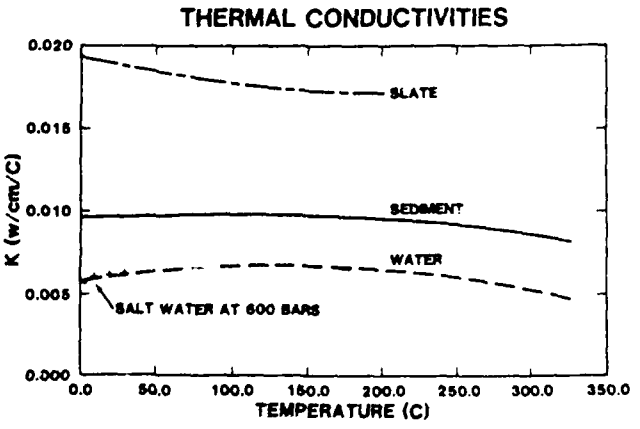

Figure 16. Values of thermal conductivities of seabed sediment as estimated from a volume average of conductivities of water and slate.

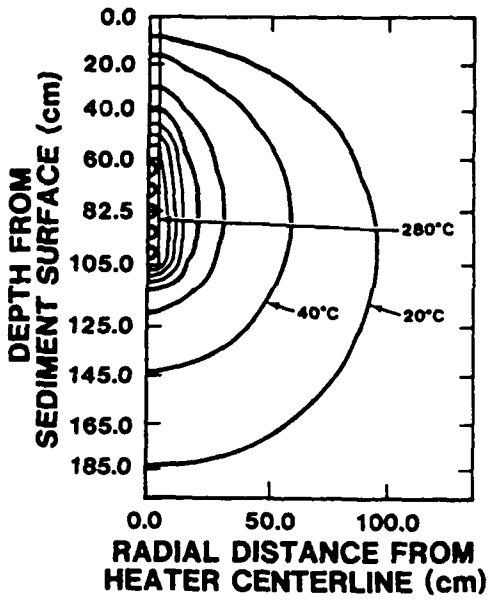

Figure 17. Isotherms in sediment at steady state; IHS dissipating 475 W. The thermal conductivity is assumed to be a constant 0.0090 W/cm°C. Isotherms are plotted in 40°C increments from 40°C to 280°C.

value used in the first case; the overall effect of using the temperature-dependent estimate for the sediment property is to lower the predicted sediment temperatures slightly, however. This is shown in Figure 20, where the predicted temperatures in the sediment at locations radially out from the heater at the level of the canister midplane are plotted for the cases with constant and temperature-dependent properties. If Eq. (1) does indeed provide an upper bound to the thermal conductivities, as indicated by recent measure-

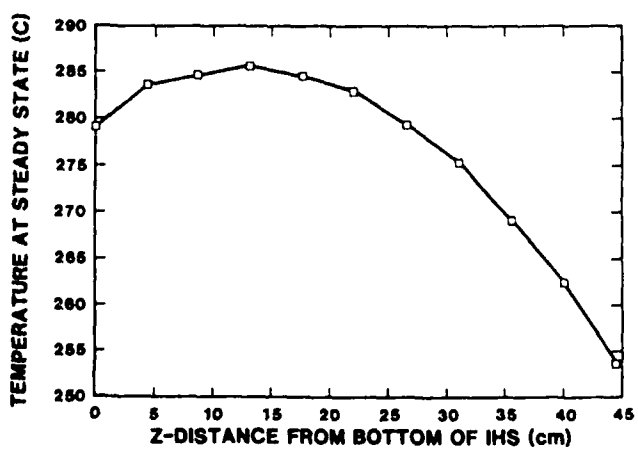

Figure 18. Temperature distribution on IHS surface (from the bottom to the connector) at steady state. Note that the hottest part of the heater is below the geometric midplane.

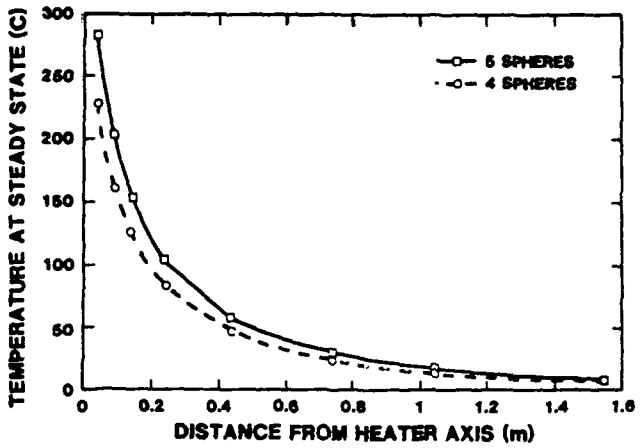

Figure 19. Steady-state temperatures in sediment out from IHS geometric midplane. The temperatures obtained with a 475-W (five-sphere) heater and a 380-W (four-sphere) heater are compared.

ments, then the temperatures in the sediment should be no lower than those shown in Figure 20.

Effects of Induced Fluid Velocity

All previous calculations assume that the thermal energy transported in the sediment is by conduction alone. This assumption may be assessed by reference to the Rayleigh number, which is representative of the relative importance of the processes of thermal conduction, natural convection, thermal diffusion, and momentum diffusion.

Analytic studies of natural convection in porous media by Hickox and Watts (1980b)

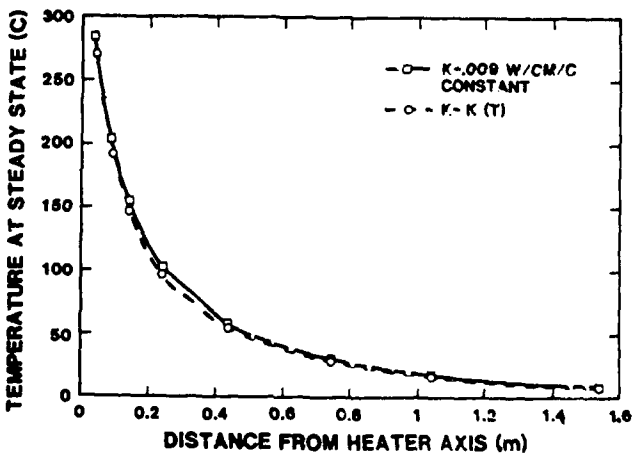

Figure 20. Steady-state temperatures in sediment out from IHS geometric midplane. The temperatures obtained assuming a constant thermal conductivity (0.0090 W/cm °C) of the sediment are compared to those predicted assuming the mixing model; average conductivity from Fig. 16.

have shown that for Rayleigh numbers less than 1, energy transport by natural convection is negligible compared with that caused by conduction. For the seabed case, the Rayleigh number can be written as

$$\mathrm{Ra} = \frac{k\rho_0\beta g Q}{\kappa\mu\alpha} \tag{2}$$

where the parameters are as defined in Table 6; numeric values are given in Table 6 for a temperature of 100°C. On the basis of the parameters in Table 6, the predicted Rayleigh number is small enough that the energy transport is by conduction. Verification of conduction behavior was one of the objectives of the experiment.

Even though the energy transport by convection is small and is not expected to influence the temperature data, finite fluid motion will occur in the sediment. The MARIAH code (Gartling and Hickox 1982a, b) was used to model the ISHTE experiment and to predict the induced fluid velocity. The vertical velocities computed at the center and corners of the heater cylinder are plotted as a function of time in Figure 21. The calculations were run for a permeability of 5×10^{-13} cm^2. The maximum predicted velocity occurs at the canister midplane and is about 2.26×10^{-8} m/s (19.5×10^{-4} m/day).

Geotechnical Effects

The heat field around the heat source may have several effects on the near-field sediment. Temperature gradients will directly cause flow of water through the sediment pores and also will give rise to pore water pressure gradients in the near field. The pressure gradients will, in turn, cause consolidation of these sediments. The consolidation process can be expected to increase the density and strength of the sediment near the heat source. Depending on the level of temperature, the sediment mineralogy also may be altered. A change in mineralogy could result in a change in permeability, strength, and other characteristics (diffusion, adsorbtion, etc.). These effects are summarized in Figure 22. As indicated above and in Figure 22, the processes and effects can be complex. Thus it is important to conduct controlled experiments carefully to determine the net results.

Table 6
Typical Numeric Values for Parameters
in the Rayleigh Number of Seabed Applications

Symbol	Definition	Numeric value (100°C)
k	Permeability	10^{-11} to 10^{-13} cm^2
ρ_0	Density of seawater	1.024 g/cm^3
β	Thermal expansion coefficient of seawater	7.5×10^{-4}/°C
g	Acceleration of gravity	980 cm/s^2
Q	Power output (thermal)	400 W
κ	Effective thermal conductivity	0.01 W/cm · °C
μ	Viscosity of seawater	2.8×10^{-3} g/cm · s
α	Effective thermal diffusivity of sediment	2.8×10^{-3} cm^2/s

Previous laboratory and physical model experiments have demonstrated that the strength of the sediment near the heater may increase by at least an order of magnitude for a maximum temperature of 400 °C. A hardening of the sediment in the near field and the possible decrease in permeability could have important beneficial effects for containment because canister migration and transport of radionuclides would decrease. There also has been some evidence of mineralogic alterations for sustained temperatures in excess of 250 °C. These and other aspects are discussed in more detail in other sections of this report.

Geochemical Effects

Geochemical experiments were included to investigate a number of phenomena associated with the heating of sediment in situ on the seafloor. It is not possible to reproduce the open system aspect of the sediments of the seafloor in the laboratory, at least from a chemical standpoint. As a consequence, it is essential to provide in situ verification of predicted chemical responses of the sediments to heating. Diffusions of ions, both into and out of the heated zone, may strongly influence the nature of the reactions occurring. Because the sorption of ions on particulate surfaces is strongly influenced by solution composition and the characteristics of the solid-phase surfaces, knowledge of the composition of the pore solution as well as of the alteration of the solid phases is essential for predicting migration rates of species in solution and the stability of canister materials and waste canister forms.

Over long time scales, particularly of the length that applies to waste disposal, diffusion through solution is overwhelmed by even exceedingly slow flow of fluid. This arises from a dependence of diffusion on the square root of time, whereas transport from flow is proportional to time. Thus it is essential to investigate the occurrence of advective transport on an extremely fine scale. Chemical tracer experiments can stand the

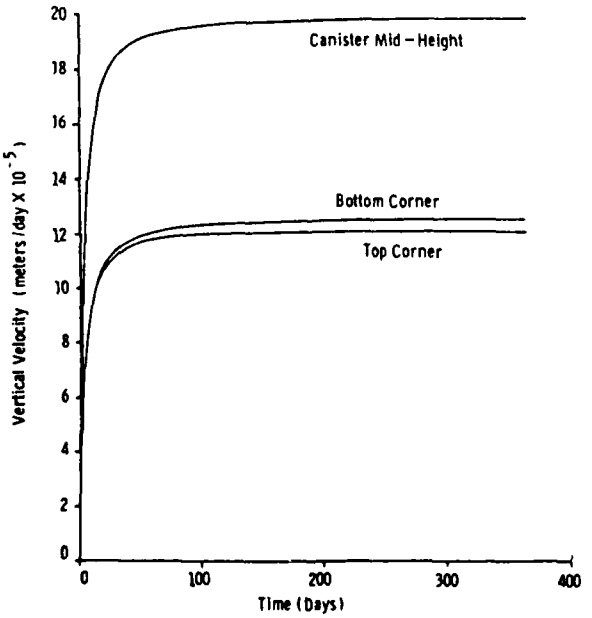

Figure 21. Computed vertical velocity plotted against time on heater surface.

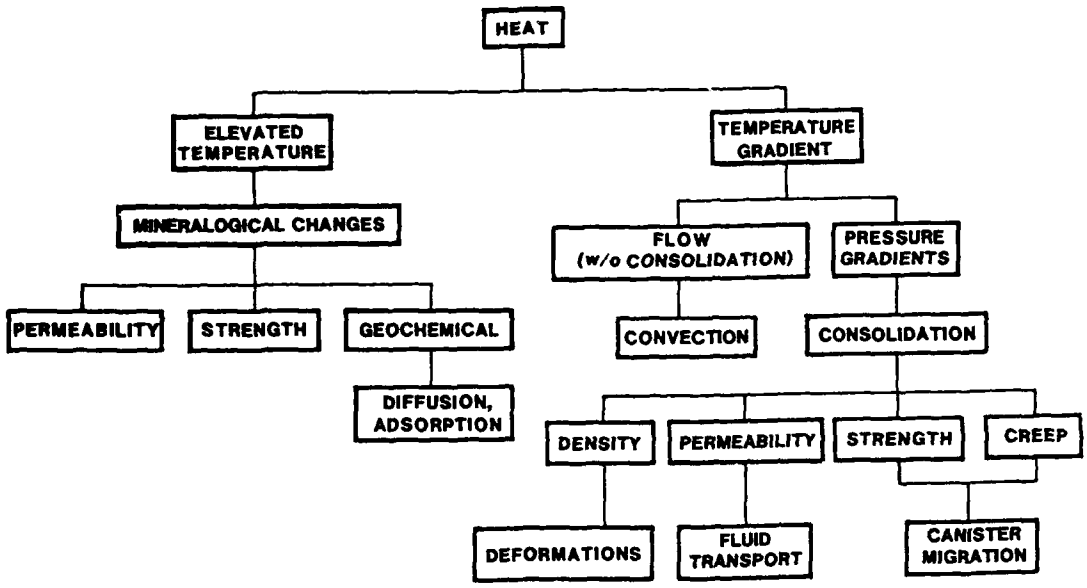

Figure 22. Effect of heat on some sediment properties and processes.

range of detection for advective flow several orders of magnitude below that achievable by thermal methods and pore pressure gradient measurements (Schultheiss and McPhail 1986). The ISHTE geochemical experiments were designed to investigate the occurrence of flow through the use of radioisotope tracers.

In addition, because the sediment is considered the primary barrier to the introduction of waste components to the ocean, the transport properties of the sediment are of the utmost concern with regard to migration of the isotopes present in waste. Experiments to define migration rates of isotopes of interest in far-field sediments under in situ conditions were an integral part of the geochemistry experiments. The migration rates derived from those experiments will form the basis for verifying the results of the numerous laboratory experiments.

In Situ Thermal Conductivity Experiment

Thermal conductivity measurements (Hickox et al. 1986) were obtained during oceanographic expeditions to a study site in the north central region of the Pacific Ocean (30°21′N, 157°51′W) ~1100 km north of the island of Oahu. The study was conducted between September 1984 and September 1985 (Olson and Miller 1985, 1986*) abroad the R. V. *Melville.*

In situ measurements of thermal conductivity were made at a nominal depth of 80 cm below the sediment surface with a specially developed line-source needle probe that incorporated three thermistors and a heater for redundancy in the measurement. For comparison, measurements in piston cores were also made with a miniature needle probe. Measurements in these cores were made at depths ranging from 8.5 to 100.5 cm below the sediment surface. In addition, one measurement of thermal conductivity was made in a box core sample (at a depth of 18.5 cm below the sediment surface) that was taken several kilometers from the study site. A summary of all measurements is given in

Table 7. Water content was determined from samples acquired during the geotechnical processing of the piston and box cores. Water contents were not available for the in situ measurements.

From Table 7 it is clear that the in situ thermal conductivity is larger than any of the values determined from core samples. Furthermore, taken as a whole the data exhibit no clear dependence on depth below the sediment surface. The cores HLC2 and HLC3 (HLC, hydrostatic core) were acquired during the same (second) lowering of the platform that resulted in the in situ measurements (APL1 to APL3). Aside from the one measurement in the HLC3 core at a depth of 100.5 cm, the data obtained during the second lowering were reasonably consistent in exhibiting a slight increase in thermal conductivity with depth. This trend, however, was not evident in the measurements obtained from the temperature, porosity, or, equivalently, water content. In situ pressure and temperature were 600 atm and 2 °C, whereas typical values for shipboard measurements with the cores were 1 atm and 25 °C. As judged from the parallel model and a mean water content of 115%, an increase in pressure from 1 to 600 atm results in an increase of 3% in the effective thermal conductivity. Similarly, a decrease in temperature from 25 ° to 2 °C results in a decrease of 5% in the effective thermal conductivity. Hence the effects of pressure and temperature tend to cancel each other. From the parallel model, a decrease of 17% in the water content is required to effect a 5% increase in effective thermal conductivity. Thus, although the data seem to suggest a lower in situ water content, no solid evidence is available to support a value low enough to account for the difference observed between in situ and shipboard core measurements. Thus we conjecture that the in situ water content is probably somewhat less than that measured in the core samples, with the additional difference in thermal conductivity being attribut-

Table 7
Summary of Thermal Conductivity Measurements

Sample number	Depth Below Sediment Surface (cm)	Initial Temperature Before Measurement (°C)	Ambient Pressure (atm)	Water Content[a] (%)	κ (W/m · K)	Sample Type
HLC1	28.5	24.5	1	112	0.823	Piston core
HLC1	63.5	24.1	2	225	0.821	Piston core
HLC1	98.5	23.8	1	115	0.818	Piston core
HLC2	13.5	24.0	1	117	0.858	Piston core
HLC2	47.5	24.9	1	121	0.864	Piston core
HLC2	97.5	27.7	1	116	0.888	Piston core
HLC3	8.5	26.4	1	112	0.884	Piston core
HLC3	45.5	26.0	1	113	0.875	Piston core
HLC3	100.5	25.0	1	120	0.810	Piston core
H-374	18.5	19.8	1	112	0.832	Box core
APL1	79.5	4.2	600		0.911	In situ
APL2	80.5	3.9	600		0.914	In situ
APL3	81.5	4.2	600		0.920	In situ

[a]Water contents were corrected for a salinity of 35 parts per thousand.

able to measurement errors. During the processing of the cores, weak regions of sediment were encountered that appeared to be the result of artifacts of the sampling procedure, further tending to support our suggestion of lower in situ water content.

Prior studies performed by Hadley, McVey, and Morin (1980) suggest that the thermal conductivity should be ~ 1.00 W/m · K. This measurement was made at a pressure of 600 atm and a temperature of 20 °C. The initial water content was 97% but decreased during the test to a value in the range of 80 to 88%. Comparing the core measurements with those of Hadley and colleagues (1980) we note that, because our cores were processed at 1 atm, we would expect the thermal conductivity to be lower as a result of the effect of pressure. Also, the higher water content in the cores can account for further reduction in thermal conductivity. We conclude that the differences in thermal conductivity between our core samples and the results of Birch and Clark (1940) can be attributed to differences in pressure and water content. Finally, we note that our measurements compare favorably with those reported by Von Herzen and Maxwell (1959) for sediment core samples obtained in the southeastern Pacific Ocean. For water contents in the range 87 to 125% those investigators reported thermal conductivities in the range 0.98 to 0.87 W/m · K, which is essentially in agreement with our results.

On the basis of our limited in situ data and their comparison with core measurements and prior laboratory experiments, we suggest that the effective in situ thermal conductivity of illite marine sediments in the geographic area of our study is 0.91 W/m · K. For the subseabed disposal of nuclear waste, it is noted that the temperature of a heat-generating waste canister depends in an approximately linear fashion on the thermal conductivity of the surrounding medium, with a lower thermal conductivity resulting in a higher canister temperature.

Temperature Field Experiment

The temperature field surrounding the heater is the most directly measurable evidence of the thermal energy transport processes in the sediment. In addition to providing data for a detailed test of the model and properties, temperature field data are necessary input for posttest analyses of the sediment cores, geochemistry samples, ion migration experiments, and pore pressure data. Furthermore, temperature data can provide evidence of and guidance to the mechanisms of any unexpected phenomena that might occur, such as sediment rupture, sediment fluidizations, large changes in permeability, and the like.

Because temperature measurements are so important, the temperature sensor array was one of the major instrumentation features of the ISHTE platform. Approximately 80 sensors were inserted into the sediment at locations away from the surface of the heater canister, and 8 sensors were installed on the heater and insertion rod. There were no thermal sensors located at the 0.10-m depth because it was possible for the nodule knockers (the probe guides) to disturb them. The locations for the temperature sensors are shown superimposed on the computed 90-day isothermal field in figures 23 through 25. Each figure shows the sensor locations in one plane. Plane A is along the center of the ISHTE platform, plane B is rotated 120° clockwise from plane A, and plane C is rotated 120° counterclockwise from plane A. The sensor array was designed to provide a detailed temperature map of the experiment region. Sensors were provided in the three planes to assess the uniformity of the sediments, to provide redundancy at the most important sensor locations, and to permit replication of data for statistical purposes.

Temperature on the heater was measured by thermocouples, and platinum resistance thermometers were to be used in the sensor probes out to a radius of 0.44 m. Thermis-

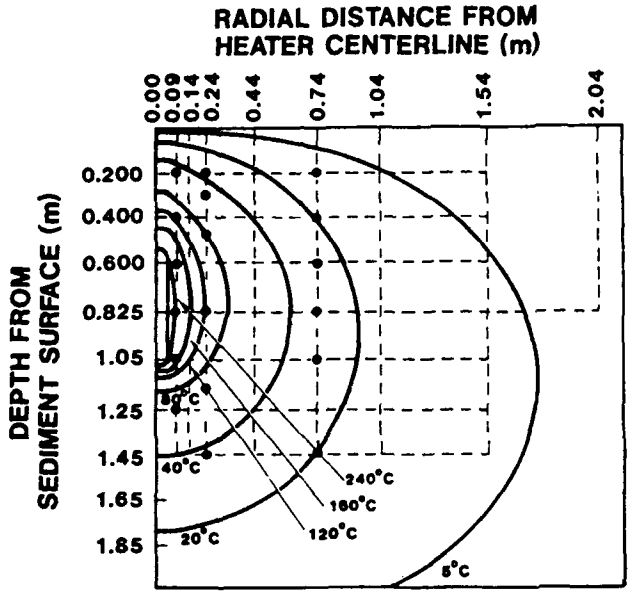

Figure 23. ISHTE thermal sensor layout (revised) in plane of ray A superimposed on base case isothermal pattern at 90 days.

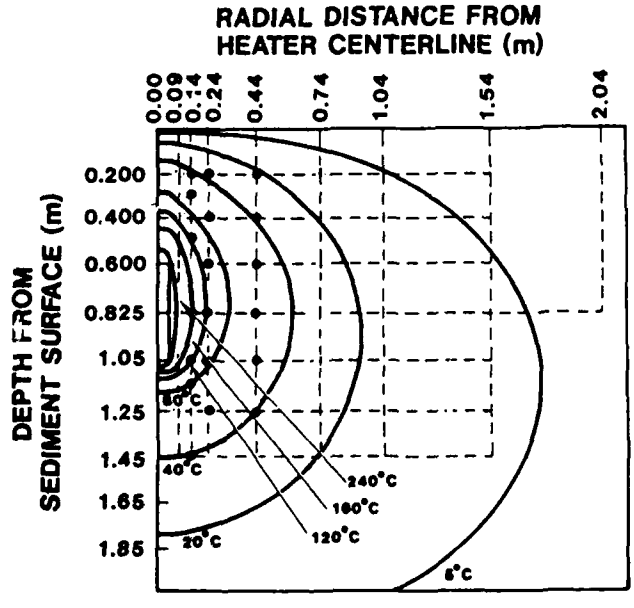

Figure 24. ISHTE thermal sensor layout (revised) in plane of ray B superimposed on base case isothermal pattern at 90 days.

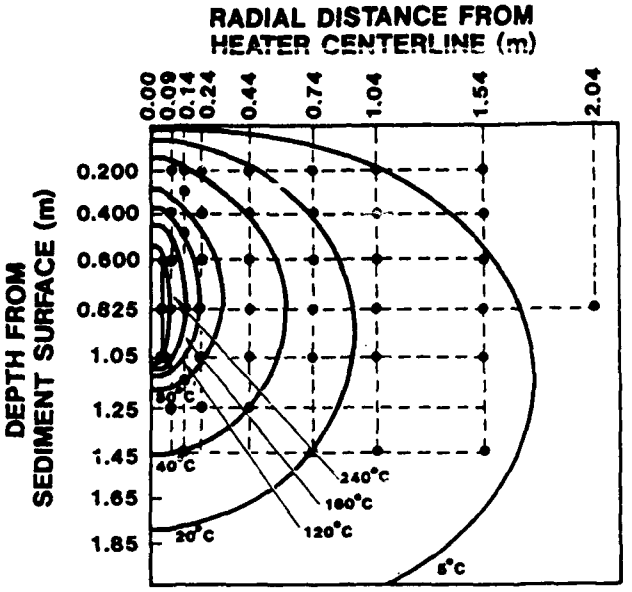

Figure 25. ISHTE thermal sensor layout (revised) in plane of ray C superimposed on base case isothermal pattern at 90 days.

tors were used for measurements at distances greater than 0.44 m from the heater. Careful calibration ensured that the temperature measurements had standard deviations of 3.0°, 0.2°, and 0.03°C, respectively, for the thermocouples, platinum resistance thermometers, and thermistors (Olson 1981). Posttest calibration of the recovered sensors along with the multiyear calibration history was to aid in evaluating sensor drift.

Each string of the platinum resistance thermometers or thermistors was inserted into a Hastelloy C-276 tube with 8.0-mm outer diameter. The space between sensors not occupied with lead wires was filled with insulation to reduce axial conduction. Hastelloy was selected for the sensor tube instead of less conductive quartz so that the units were more rugged and more likely to be recovered intact for posttest calibration (Hastelloy was more likely than quartz to survive the hostile environment of pressure and corrosion). After the platform was in place, each sensor probe was driven into the sediment by a hydraulic cylinder. The drive rate depended on sediment resistance. The anticipated drive rate was 5 mm/s.

Analyses of the temperature field data were planned as follows:

(1) In situ line-source data were used to verify low-temperature thermal conductivity models.
(2) Measured water content from cores was used to compute the product of density and specific heat.
(3) With these properties and the measured heater temperature history as a starting point, the model and parameter estimation technique was used to determine a first estimate of thermal conductivity as a function of temperature.
(4) With the conductivity estimated in (3), arrival times of thermal pulses were computed at the various sensor locations and sensor position errors were checked. During insertion, the sensors may have deflected slightly from their

planned position. If necessary, parameter estimation was used to establish correct sensor locations.

(5) Temperatures from the sensor array were used for improved estimates of thermal conductivity.

(6) Improved estimates were used to verify the laboratory data and model.

Large or consistent deviations of residuals (differences in computed and measured temperatures) would signal inadequacy of models of theory.

Parameter estimation, also known as inverse theory, is a discipline that provides tools for the efficient use of data for aiding in mathematical modeling of phenomena and in estimating the constants (i.e., thermal conductivity, thermal diffusivity, and so forth) appearing in these models. Thus the problem of estimating parameters is finding the constants.

In a parameter estimation problem, the structure of the differential equation is known; measurements of the input as well as of the initial or boundary conditions are available. Some or all of the constants or properties of the system may be unknown. In this case the problem would be to obtain the best, or optimal, estimate of these parameters by using the measured values of input or output. For the ISHTE experiment, the power input into the sediment and the location of temperature-measuring devices and the measured temperatures were known to within some measurement error, or noise. From these measurements and from the heat transfer models, the properties of thermal conductivity and thermal diffusivity could be inferred. An added complication is that both these properties are functions of temperature and thus are not real constants.

Ion Migration Experiment

Objectives

The ion migration experiment was included in ISHTE to increase the ability to detect and quantify advective flow of pore fluids as a result of heating in the sediments. The experiment also was designed to provide data for the in situ verification of migration rates of radioisotopes that were estimated from laboratory measurements. The experiment was designed to be fully integrated into and to take advantage of extensive data derived from other ISHTE experiments.

The objectives of the ion migration experiment are summarized as follows:

(1) to identify, define, and quantify the occurrence of advective transport of heat and mass resulting from the heating of sediment under in situ conditions

(2) to provide a basis for in situ verification of diffusion coefficients of interest to subseabed disposal

(3) to provide field verification of laboratory determinations of adsorption coefficients for radioisotopes of interest in the subseabed disposal of high-level wastes

(4) to determine advective velocity as a function of thermal gradient and pore pressure

(5) to determine the diffusive characteristics of marine sediment directly under in situ conditions

The ion migration system had to meet several stringent criteria for the experiments to be successful. Released radioisotopes must be recovered as closely as possible in their entirety. This requires a large and accurately located overcorer. Establishing the diffusive

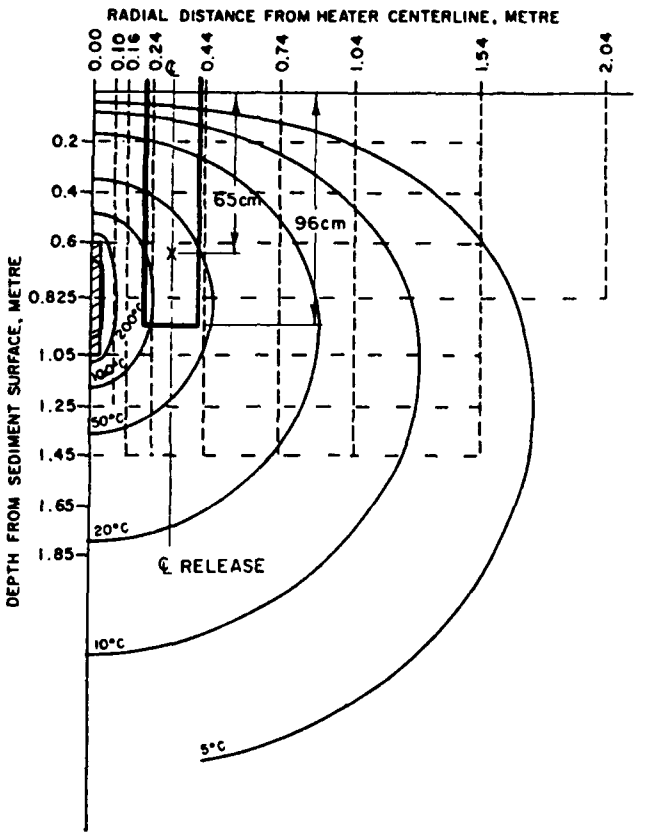

Figure 26. Position of near-field tracer release point and overcore in relation to isotope heat source and predicted isotherms in surrounding sediment. *X* inside the outlined overcore indicates release point.

properties of the sediment to quantify advection rates and defining diffusion coefficients of strongly sorbed isotopes require the release of ions with a wide range of mobilities. To provide data on the strongly sorbed species placement must be precise, particularly with regard to sampling. To avoid artifacts and to guide postrelease sampling, the release mechanism must not be disturbed after introduction of the isotopes to the sediment. Finally, the probe and overcorer must be retracted up into the platform at the completion of the experiment to protect the core and probe from disturbance during recovery.

Ion Migration Design

The ion migration experiment consisted of two coupled devices: the tracer release probe and the overcorer. There were two complete units: near field and far field. The near-field experiment took place in the area of the 75 °C isotherm, and the far-field experiment was for control in the area of temperatures less than 5 °C. The near-field release point was at a depth of 65 cm, and the overcorer penetrated to 95 cm (Fig. 26).

The tracer release and probe had to release radioisotopes with mobilities in the sediment that differed by 4 orders of magnitude. The release itself had to remain undis-

turbed in the sediment for a period of 9 months. Because the platform would settle an estimated 2 to 3 cm over the period of the deployment, it was essential that the release probes were mechanically decoupled from the platform. The faster tracers, however, were to be injected at the very end of the experiment with the release probe. Mechanical isolation was achieved by incorporating a decoupling piston into the top of the release probe. After the main implant cylinder drove the release into the sediment, the decoupler was activated to drive the release an additional 5 cm. The decoupler piston expanded after hydraulic pressure was applied to it; because it was springloaded, it retracted. This retraction left a clearance of 5 cm between the release probe and the implant cylinder shaft.

The tracer release itself was a two-stage unit and could release tracers at two different times. Because tracers remained in the release for a least several months before injection, the unit had to be sealed before activation of each section. This was achieved with a double-piston design; the capacity for two releases was accomplished simply by incorporating two units in a single body. A schematic of the release is given in Figure 27. The tracer solution was contained in v_2 and a rinse solution in v_1. Applying pressure to the top of a release piston caused the smaller piston to move down until v_2 was connected to the probe passage. At this point, the tracer solution was injected into the sediment from the probe tip. When v_2 was emptied the residual of v_1 was expelled, rinsing the probe passage. A volume of 0.28 mL was used with an injection efficiency of 95%.

The tracer overcore was a large-diameter piston core. The core inside diameter was 21 cm. This size permitted the released radiotracers to be recovered in their entirety. The release probe and the decoupling mechanism for the probe were incorporated into the piston of the overcorer; this ensured that the core over the tracer release would be centered. The relationship of the overcore to the tracer probe is illustrated in Figure 28. The overcore and contained tracer release were recovered simply by retracting the tracer probe implant piston, which was rigidly connected to the overcore piston. After retraction into the platform, a core catcher was released to cover the bottom of the core barrel; this prevented washout during ascent of the platform to the ocean surface.

The energy needed to drive the various units of the ion release and overcoring systems was derived from in situ pressure. Each implant cylinder was connected to an accumulator and to ambient seawater through high-pressure two-way valves. The valves were motor driven to provide control of the implant and retraction of the various experiments. The valves and motors along with some signal-processing electronics were housed in a set of five motor cases that were sealed at 1 atm.

Control of the motorized valves and solenoids necessary to operate the geochemistry system was accomplished with an electronics package based on a Sharp model 1211 computer. External electronics included elements for communicating with the platform's master controller and with electronics in each of the five pressure housings containing the motorized valves. Timing for the initial event sequence, including implantation of the ion migration probes and release of tracers, was provided from the master controller by sending commands to the geochemistry electronics. Communication among the controllers was accomplished by using individual lines to carry the signal for each event. When each event occurred, 1-ms, 11 ± 1V pulses were sent on the assigned lines by the platform controller. Pulses received by the geochemistry controller were tested by means of pulse-width discrimination to protect against noise; valid commands were serially encoded for transmission to the valve housings. Receivers in each housing decoded and tested each transmission. When an appropriate command was received, the receivers actuated the specified valve. The valves were driven by bidirectional dc motors through

a power transistor and timing circuit. Solenoid actuation for the tracer releases was accomplished by using the same decoding of the platform's signals, but the timers and drivers were housed in the controller case and wired directly to the solenoids.

Geochemistry events occurring near completion of the ISHTE were timed and controlled by the Sharp computer. A discrete crystal circuit provided the time base to the Sharp, with software being used to verify times for carrying out events. Commands were generated by the computer; as was the case with those from the platform's controller, these commands were serially encoded for transmission to the valve housings.

Tests and Development

The tests carried out in support of the equipment developed for these experiments fall into two categories. The first category is geochemical and release tests conducted to evaluate the release and the possible introduction of artifacts during implant as well as to

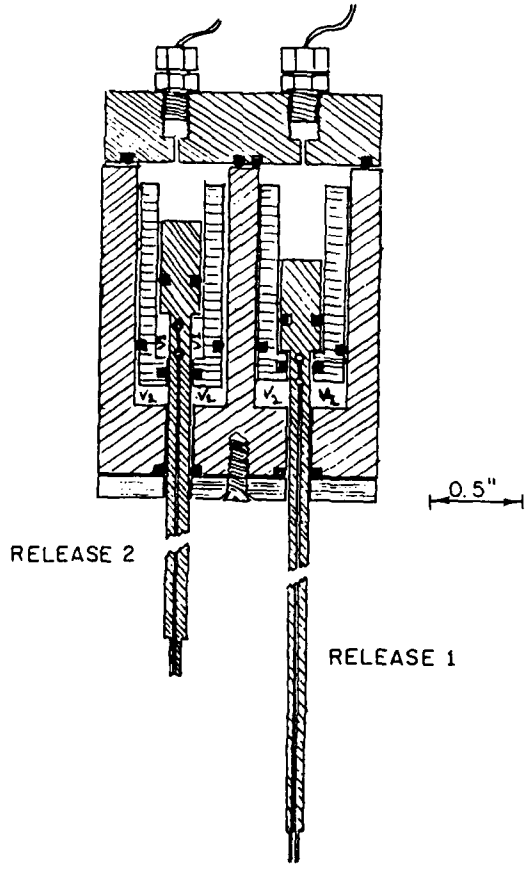

Figure 27. Drawing of two-stage tracer release used in ion migration experiments. The left release is shown in the loaded position prior to any motion. The right release is shown at the moment tracer is first injected into the sediment.

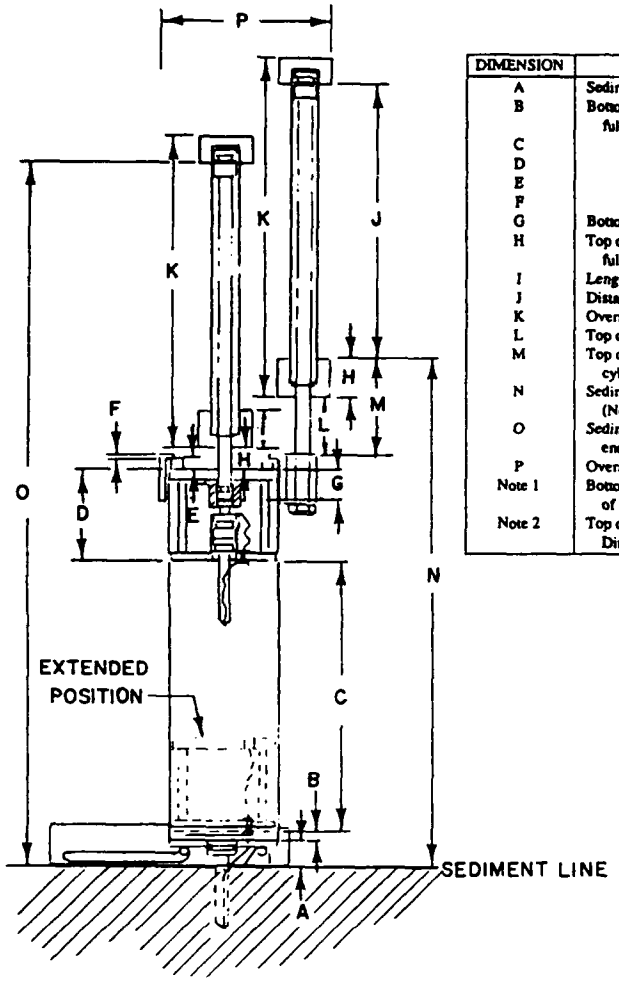

(Inches)

DIMENSION	DESCRIPTION	NEAR FIELD	FAR FIELD
A	Sediment to bottom core barrel (on deck condition)	3 1/2	3 1/2
B	Bottom of core barrel to bottom of core piston, core piston fully extended	1/2	1/2
C	Stoke of hydraulic cylinder shafts	41	27
D	Length of core piston	8 1/4	8 1/4
E	Thickness of core piston stop ring	7/8	7/8
F	Thickness of shoulder of core barrel collar	1/4	1/4
G	Bottom of Ion Migration shaft to top of core piston when coupled	2 3/4	2 3/4
H	Top of core piston to bottom of Ion Migration hydraulic cylinder, fully retracted position	3/4	1 5/8
I	Length of hydraulic cylinder lower end cap	2 5/8	2 5/8
J	Distance between end caps of assemblied hydraulic cylinders	41 5/8	27 1/4
K	Overall length of hydraulic cylinder with end caps	45 5/8	31 3/4
L	Top of core barrel collar to bottom of overcore hydraulic cylinder	3 7/8	3 7/8
M	Top of core barrel collar to top of lower overcore hydraulic cylinder and cap	6 1/2	6 1/2
N	Sediment line to top of lower overcore hydraulic cylinder end cap (Note 2)	60 7/8	46 7/8
O	Sediment line to bottom of upper Ion Migration hydraulic cylinder end cap. (Note 2)	97 7/8	70 3/4
P	Overall width of Ion Migration/Overcore assembly	11 1/2	11 1/2
Note 1	Bottom of lower clamp for hydraulic cylinder is minimum of Dimension 'N' plus 2 inches	62 7/8	48 7/8
Note 2	Top of upper clamp for hydraulic cylinder is maximum of Dimension 'D' minus 2 inches	96	68 3/4

Figure 28. Schematic drawing of ion migration probe and cylinder coupled to overcore device. Both the retracted and extended (deployed) positions of the ion migration probe are shown.

develop and evaluate sampling methods and the limits on defining diffusion coefficients through these experiments. These tests had the further objective of making basic measurements of diffusion coefficients in situ at Buzzards Bay, Massachusetts, the area where our tests were conducted. The second category is testing of the mechanical integrity of the components and the operation of the integrated system. These tests were carried out at the MPG-I site in the North Pacific on two test cruises.

A large number of experiments were carried out in the sediments of Buzzards Bay. The objectives were to look for experimental artifacts affecting tracer migration and to develop sampling techniques. Many of these experiments employed a release quite different from that described previously. This release was originally planned for the ISHTE experiment but was discarded in favor of the unit shown in Figure 27 and primarily on the basis of modeling considerations. The results obtained with the original design are, for the most part, applicable to the new release. The original design was a modification of the "peeper" concept. The release consisted of a series of chambers cut into a 1.5-in diameter rod.

Each chamber was isolated vertically and covered with a permeable membrane. The membrane permitted the chamber to be in diffusive contact with the surrounding sediment. The chambers could be covered with a shutter (in situ) to seal them from their surroundings. The middle chamber contained the radiotracer, and the surrounding chambers (10 above and 11 below) were passive; the surrounding chambers contained no spike at the beginning of the experiment. The probe (Fig. 29) was inserted into the sediment with the shutters closed; opening the shutter exposed all chambers to the surrounding sediment and initiated the diffusive spread of the radiotracer. The passive chambers equilibrated with the sediment adjacent to their surface throughout the experiment. At the conclusion of an experiment, the shutters were closed in situ to preserve the vertical profile of the tracer in the chambers. The probe was overcored by divers and sampled about the source chamber to provide an independent measure of diffusive spread. The results of the sediment distributions then provided a basis for evaluating the chambers. The sediment sampling itself was also a developmental process central to establishing techniques to obtain maximum sensitivity in determining very low diffusion coefficients.

Two deployments were made expressly to investigate the possible occurrence of enhanced diffusion in the thin skin of sediment adjacent to the probe wall that is disturbed during implant. The original design represented a worst case in this regard because its diameter was 1.5 in compared to only 0.125 in for the new probe. ^{36}Cl was used in this test because it is not sorbed by the sediment and is thus most subject to changes in the geometric factors influencing diffusion. Sediment from the radial interval 0 to 2 cm was sampled over the length of the probe for comparison with the chamber compositions. The results are given in Figure 30. As is readily apparent, the sediment data are indistinguishable from the chamber data. A quantitative evaluation of the two methods that related to the object of the geochemical experiments was done to compare diffusion coefficients calculated for the different sample sets. The data are included in Figure 30. As in the case of the graphic representation, the results are indistinguishable. In the case of the August 5 recovery, each side of the probe was sampled separately. These two sets of samples also yielded indistinguishable distributions and diffusion coefficients. We conclude from these results that the disturbance accompanying implant, even for a large probe, has no detectable influence on determining diffusion coefficients. Furthermore, the distributions about the probe are essentially symmetric.

A series of deployments was made to define the working range for which these

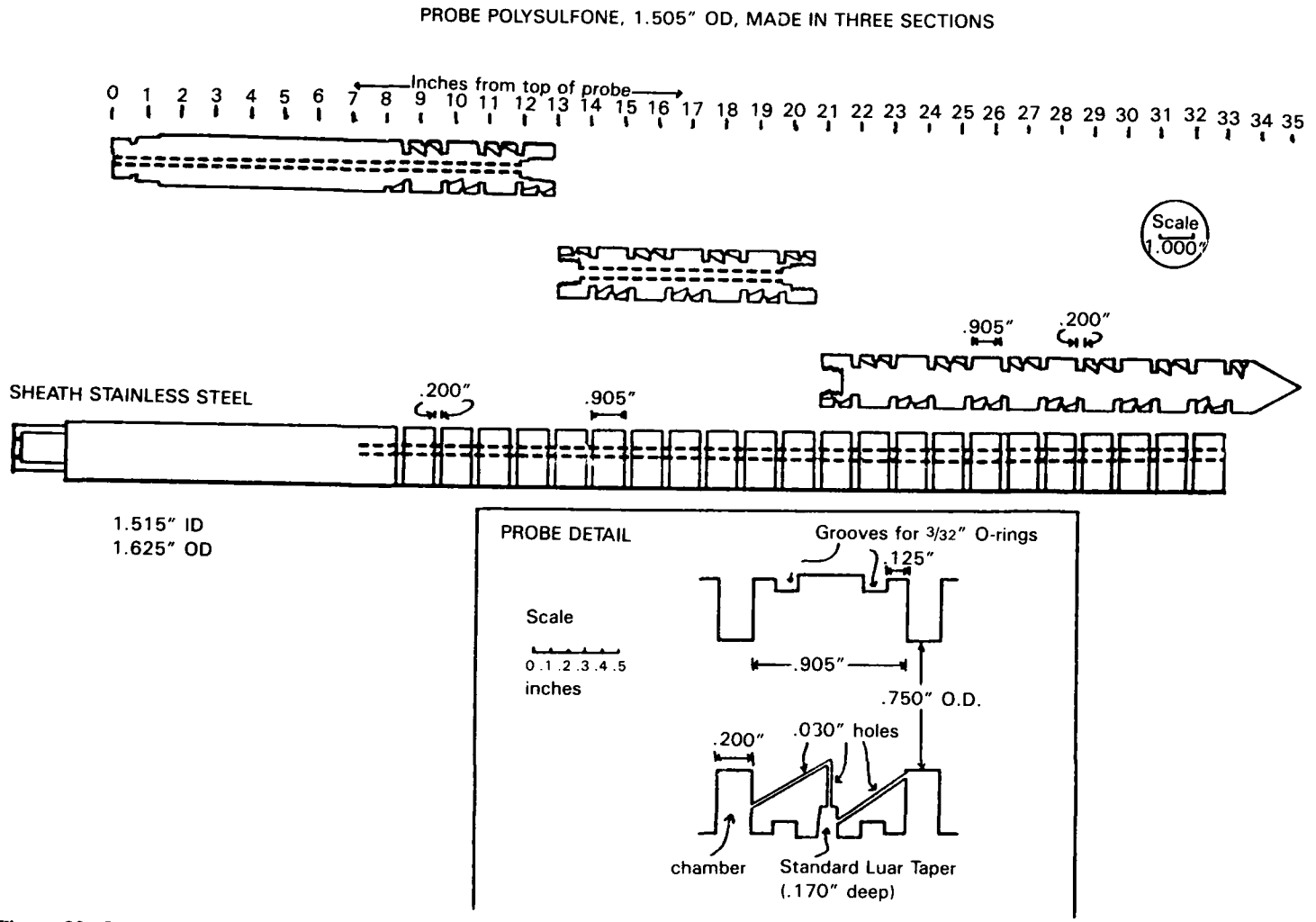

Figure 29. Peeper tracer release probe used for many of the in situ diffusion experiments in Buzzards Bay. OD, outer diameter; ID, inner diameter. The sheath is the shuttering mechanism used to isolate the chambers from any back diffusion during recovery.

experiments would be suited. In particular, it was necessary to determine whether migration of the strongly sorbed nuclides of interest in waste disposal, such as the actinides, can be resolved. Three classes of tracers were used: ^{36}Cl as a nonsorbed ion, ^{85}Sr as a weakly sorbed cation, and ^{236}Pu and ^{243}Am as strongly sorbed nuclides. The results presented in Figure 30 are representative of the ^{36}Cl data obtained. Determination of diffusion coefficients was good to about 10 to 15%. Results typical of ^{85}Sr are given in Figure 31. Data for a number of horizontal sections are included. The scatter is not all analytic but reflects real variation in the diffusion coefficients as evidenced by the consistency of individual symbols. Precision is on the order of that for Cl, ~ 10%. The data representation of Cl and Sr was derived from a spherically symmetric point-source model, in which the slope of the plot yields the diffusion coefficient. This is an oversimplification, but it is adequate for sampling on a scale of several centimeters to 10 cm.

The results of the experiment with Pu and Am are given in Figure 32. The scale of migration for these nuclides is greatly reduced; it is less than 1.5 cm. This distribution cannot be treated as a point source. The curves in Figure 32 are for a volume source of the release characteristics. The scatter is greater, which is almost certainly the result of difficulties in accurately sampling at 0.5-cm intervals. As indicated by the curves, the data are bracketed by diffusion coefficients of (2 to 4) $\times$ 10^{-9} cm^2/s. This is a fair estimate of precision (a factor of 2). The data also indicate that the lower limit of diffusion that we can work with is ~ 10^{-9} cm^2/s.

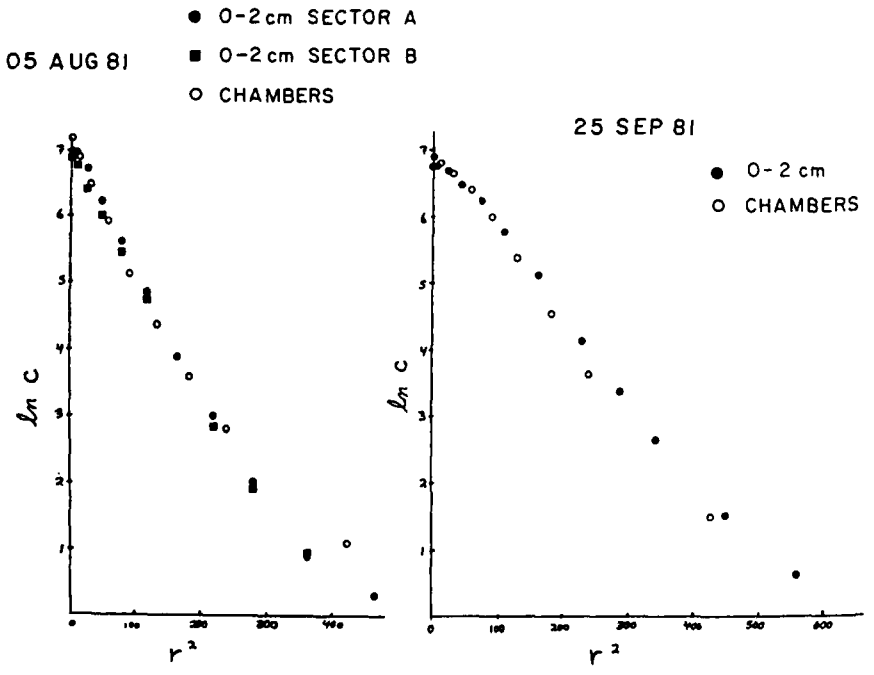

Figure 30. Graphic representation of data from two experimental releases of ^{36}Cl in sediments of Buzzards Bay. The 0–2 cm data are from analysis of 1-cm-thick horizontal sections extending out 2 cm from the probe wall. "Chambers" refers to samples taken from the chambers of the probe. Also indicated are the diffusion coefficients obtained from modeling the distribution of activity around the source as a spherically symmetrical point source, i.e., proportional to the slope of the plots of this figure.

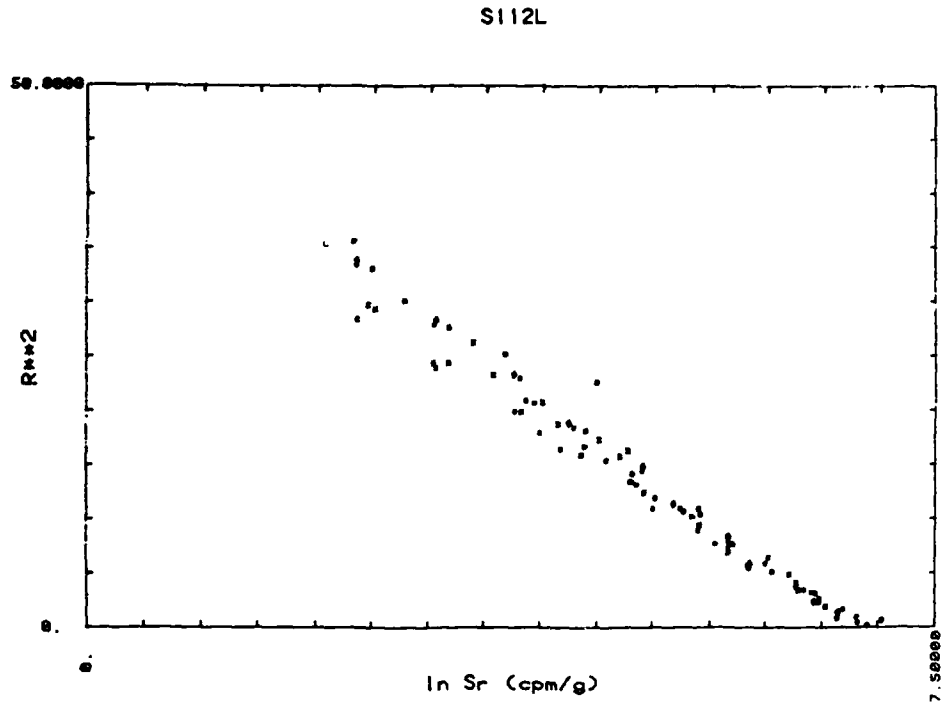

Figure 31. Plot of ^{85}Sr activity around source chamber as in Fig. 30. The various symbols are used indicate the separate horizontal sections above and below the source for which data were obtained. All t data were obtained from sediment samples in the radial interval 0 to 4 cm.

To be successful, the tracers must stay in solution while they are contained in the release. Tests were carried out to ascertain the conditions that would ensure this. Solutions were stored in tubing of the same material as the releases and with the same surface-to-volume ratio as the release chambers for a period of several months. These tests indicated loss of the actinides at pH >3.5. Consequently, we used a tracer solution with the pH of 3.0 for ISHTE. The solution is stable in the 316 stainless steel from which the releases were made. The effects of pH from the release of 0.28 mL of such a solution were dissipated within a few days and thus did not affect the long-term migration of the radioisotopes. Tests of migration after a 10-day deployment showed no significant early migration that could be attributed to pH-induced artifacts.

The near-field ion migration system was mounted on a platform of its own for the component test cruise at MPG-I. This was the first deep-sea deployment of the equipment that included the ion migration and overcore systems along with the required electronics controller and valve housings. For the experiment to be successful, the ion migration probe had implant, decouple, release the tracer, and retract with the overcore. This failed on all three platform launches. The valves controlling implant did not respond to the implant signal. As a result, the probe was not implanted in the sediment on the first two deployments. The decoupler was activated and operated as designed. The release also operated successfully when set to release and when not triggered (the latter operation established that no premature release would occur).

On the third deployment, the control valves for the pore water system were used to

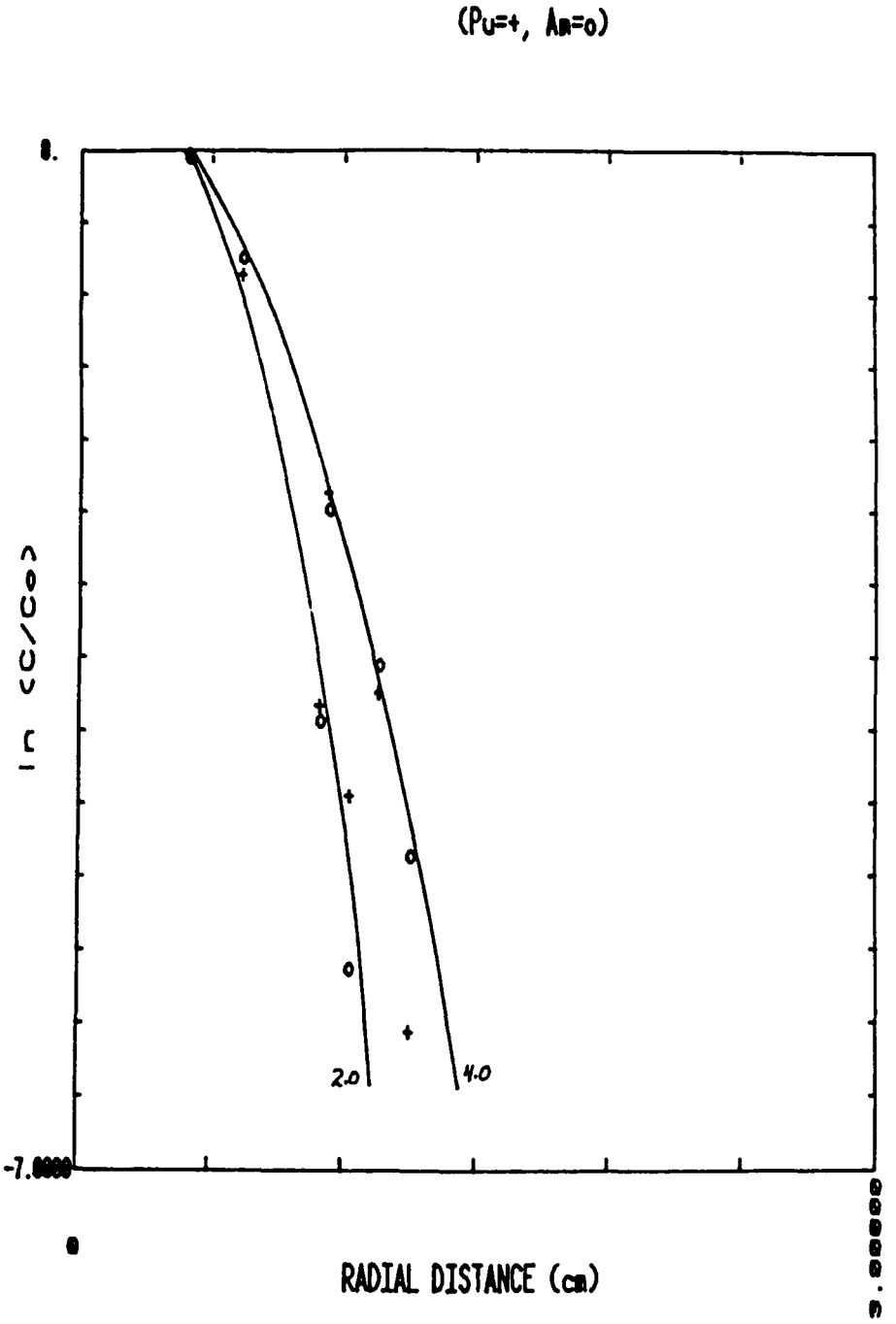

Figure 32. Plot of distribution of Plutonium (^{236}Pu) and Americium (^{241}Am) in sediments about release point. The solid lines are model calculations of predicted distributions for a volume source with the geometry of the release. The values adjacent to these curves are the diffusion coefficients used for the calculation in units of 10^{-9} cm^2/s (2×10^{-9} cm^{-2}/s).

control most of the ion migration–overcore operation. In this configuration, operation was largely successful. Implant, decoupling, release, and retraction occurred as designed. The failure of one of the original implant valves after the experiment caused the extrusion of the core and prevented recovery of the sediment. In each deployment, the core catcher was successfully closed.

Overall, the cruise pointed up one specific deficiency. The hydraulic control that interfaced the various components was inadequate. Specifically, one of the 15 valves leaked through the packing, and the electrical capacitance at in situ pressure and temperature was sufficient to make the signal strength marginal. In addition, difficulties in communicating with the platform through the platform's acoustic link led to the development of a default control that would cause the WHOI controller to take command of the final sequence. This was done to protect against the eventuality that the acoustic signal could not be received by the platform's master controller.

A test of the complete ISHTE platform with all the experiments on board was planned for the ocean test cruise. For the geochemistry program, this included both the near-field and the far-field systems for the ion migration experiment. In many respects, this test was less successful for the geochemistry experiments than the component test cruise. The failure of the acoustic signals to be received for the initiation of the geochemistry experiments short-circuited much of the evaluation program. The default portion of the sequence was initiated, but leaking valve packings that flooded one pressure housing prevented proper operation. Those signals actually sent from the WHOI controller were received and acted on by the proper valve controllers, but the short in the electronics also caused a number of random signals to be received and acted on.

As on the previous deep-sea test, the valves necessary to interface the system as a whole failed. All valves had to operate for the experiments to be carried out successfully. The repeated failure of two valves despite specific corrective efforts led to the conclusion that the valves could not be used in their present configuration. The pressure across the valve packings will have to be eliminated by placing them in oil-filled cases.

With one crucial exception, the various components were successfully tested in the deep sea. The one exception was the valve control system essential to integrating the entire collection of equipment. Because of this failure, the integrated operation of the entire system could not be satisfactorily demonstrated. The valves controlling system integration must be modified and a field operation of the entire package successfully demonstrated before any full-scale experiment is attempted.

Pore Pressure Experiment

Measurement and careful assessment of the pore pressures developed during ISHTE were crucial because excess pressure reduces the strength and effective stress of the sediment and because water flow will occur away from the heater as the thermal gradients develop around the heat source or canister. Pore pressure increases can cause time-dependent changes in the physical and mechanical properties of the sediment and thus affect its isolation capacity for the waste. The pore pressure measurements were used to check computer models developed for ISHTE and the SDP (Percival 1982; McTigue and Gartling 1986). The ISHTE platform had five piezometers to measure insertion pressures (excess pressures generated during sediment penetration), their pressure decay characteristics, and the pore pressure field resulting from the induced thermal field. The probe locations were selected to be at the heater middepth and at the following radial

distances, which correspond to various predicted sediment temperatures after steady state is realized:

- one probe at 14 cm (190 °C)
- three probes at 54 cm (40 °C)
- one probe at 154 cm (10 °C)

Pore pressure measurements provide not only ambient static, dynamic, and transient pore water pressure conditions but also a means of determining the in situ permeabilities, undrained shear strength, and soil bulk and elastic properties (Bennett et al. 1982, 1986a, 1986b, 1989; McTigue, Lipkin, and Bennett, 1986; Lipkin, Bennett, and McTigue 1986).

The piezometer probe(s) consisted of an 8-mm diameter Ti tube that attached to a tip with a cone angle of approximately 5.3° (Bennett and Faris 1979). A porous stone filter, which allowed pore water pressure to be transmitted to the pressure sensor, was fastened between the Ti tube and the probe tip (Fig. 33). Pore pressure was transmitted through the porous stone to an internal tube fastened to the positive side of the pressure sensor. The differential pressure sensor was pressure balanced by a similar internal tube that ran from the negative side of the pressure sensor to the top of the porous stone retainer but was isolated from the porous stone. The pressure sensor was enclosed in a stainless steel housing that was pressure compensated to in situ hydrostatic pressure (Fig. 33). The stainless steel pressure sensor housing was physically separated from the Ti by high-dielectric polycarbonate material.

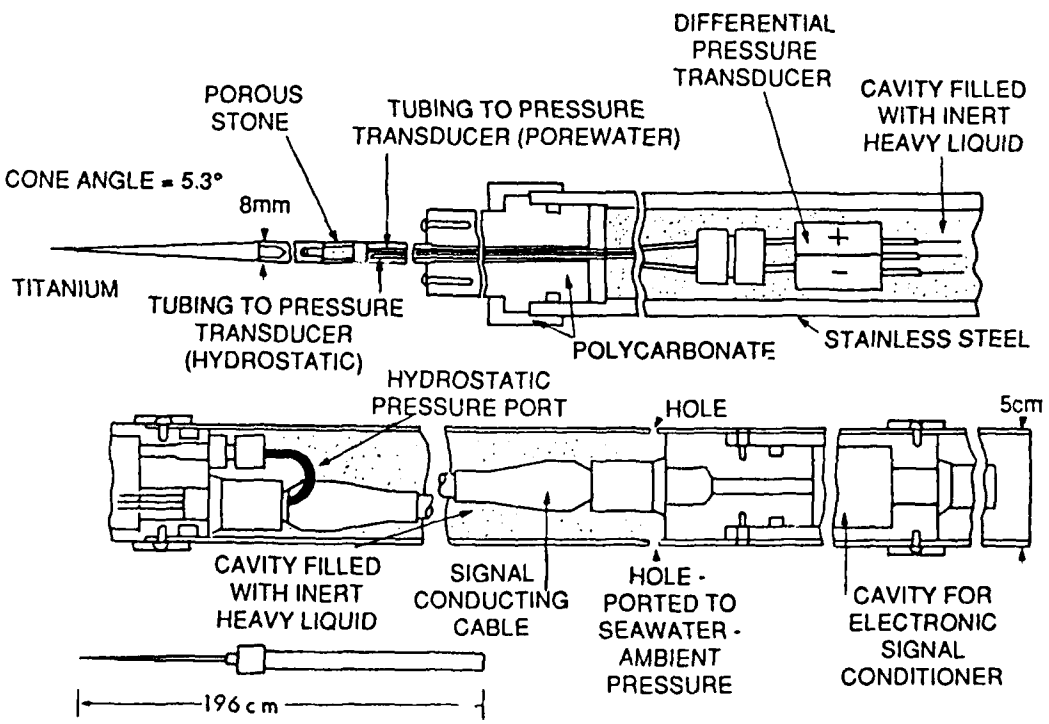

Figure 33. General mechanical configuration of deep ocean piezometer probe developed for ISHTE.

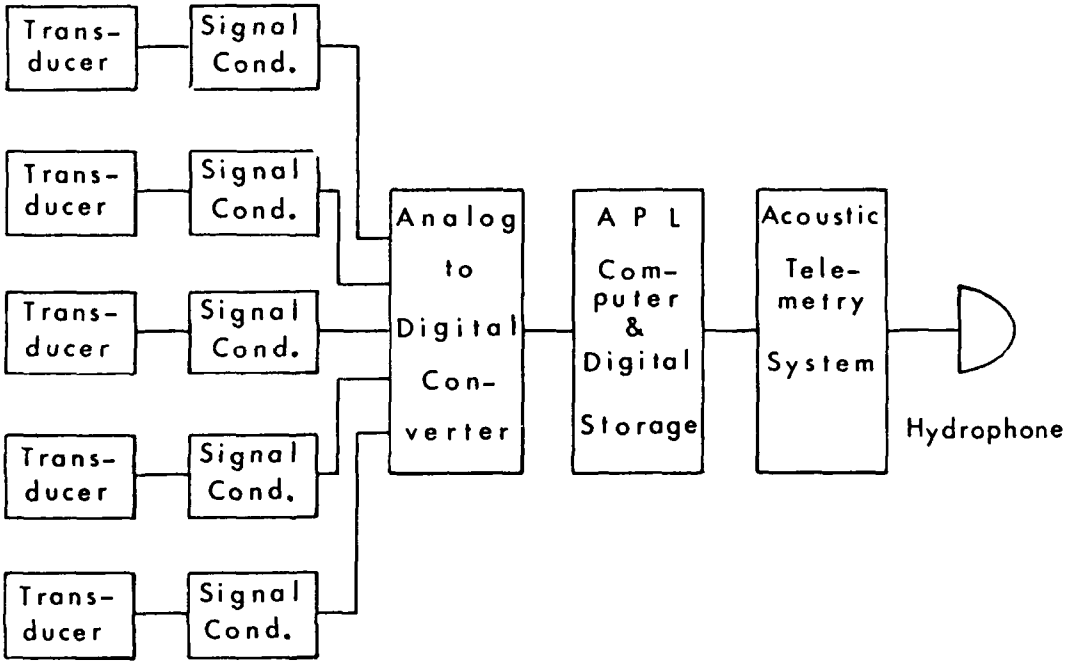

Figure 34. Block diagram of major components of deep ocean piezometer probe system and interface with APL data acquisition systems.

The piezometer electronic system consisted of three main components: pressure sensor, signal conditioner, and interface. Solid-state signal conditioning-electronics were enclosed (at atmospheric pressure) in a stainless steel capsule and located directly above the pressure sensor capsule. Figure 34 depicts the major components of the system and their interface with the ISHTE platform data logging system. A variable-reluctance, differential pressure transducer measured excess pore water pressure directly (differential above hydrostatic). Further details of the piezometer system's mechanical and electronic components and performance can be found in Bennett et al. (1985b).

Comprehensive piezometer testing and evaluation were completed in support of ISHTE objectives. Two laboratory and two field experiments were conducted from 1981 to 1985. Piezometers were deployed during field exercises at MPG-I in 1984 and 1985. The probes were an integral part of the ISHTE simulation (ISIMU) at David Taylor Naval Ship Research and Development Center (NSRDC) in Annapolis, Maryland in 1981 and at a post-ISIMU experiment at SNLA in 1984. Details of these activities, including objectives, piezometer performance, precision, data analysis, and significance of results, have been thoroughly documented (Percival et al. 1980; Percival 1982; Valent et al. 1985; Bennett et al. 1982, 1986a, 1986b, 1989, in press; Lipkin, Bennett, and McTigue 1986; Riggins et al. 1985; Walter, Burns, and Valent 1986).

Extensive in-house testing of piezometer components at high pressure (69 MPa) was completed to assess performance stability, reliability, and sensitivity of pressure sensors (Bennett, Burns, and Lambert 1981a, 1981b; Bennett et al. 1983; 1989). Testing was carried out with a high-pressure calibrator designed to operate in a pressure chamber. The calibrator loads a differential pressure transducer by increasing or decreasing the

static loads incrementally. Static loads can be held for periods of several hundred hours (Bennett et al. 1986a; 1985b; in press).

During the ISIMU test, pore water pressures were monitored with two piezometer probes placed at selected radial positions from the heater (Percival 1982; Bennett et al. 1985b). Each probe was inserted independently at atmospheric temperature and pressure. During probe insertion sediment deformation occurred, and excess pore water pressures (U_i) were generated. These pressures reached a maximum along the probe-sediment interface. Maximum insertion pressures were different for probes 1 and 2 (Fig. 35). These differences may have been caused by greater sediment disturbance around probe 1 from remolding by the heater. It should be noted that probe 1 was inserted to 16.9 cm and probe 2 to 26.4 cm below the sediment surface. In a normal and consolidated, cohesive, fine-grained sediment, the time required for these induced excess pore pressures to dissipate to ambient pressure is, to a first approximation, a function of the probe radius and the sediment coefficient of consolidation and is thus dependent on the permeability of the material (Soderberg 1962; Wroth, Carter, and Randolph 1979). Figure 35 depicts these characteristics for the ISIMU experiment. Data analyses are discussed by Percival (1982) and Bennett et al. (1985b, 1986a, 1986b). Important geotechnical properties such as permeability (k), induced excess pressure (U_i) and ambient excess pressure (U_e), effective vertical stress (σ'_e), undrained shear strength (S_u), and the coefficient of vertical consolidation (C_v) can be derived from piezometer measurements (Bennett et al. 1982, 1986b, 1989; McTigue, Lipkin, and Bennett et al. 1987;

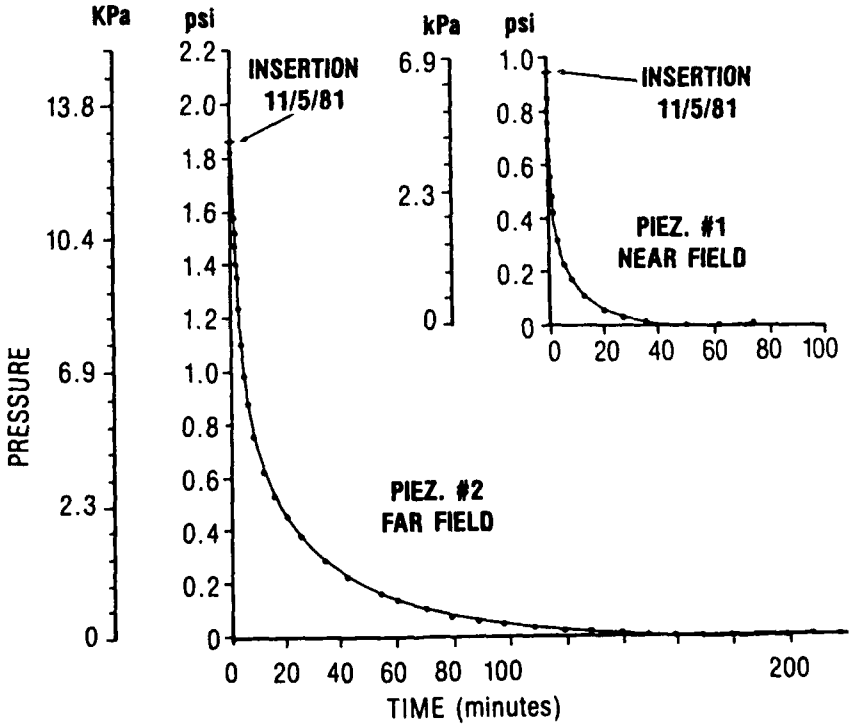

Figure 35. Dissipation of excess pore pressures from 8-mm diameter probe inserted into reconstituted illitic red clay soil measured by differential pressure sensors.

Lipkin, Bennett, and McTigue 1986). C_v and C_h (coefficient of horizontal consolidation) are considered essentially identical (Bennett et al. 1986b; Burkett et al. 1987).

After pressurization of the ISIMU sediment tank and instrumentation, on 11 November 1981 heater power was initiated to induce thermal gradients in the illitic sediments (Percival 1982). The power selected was 115 W, which generated a maximum temperature change of ~206 °C.

Excess pore pressures in the near field (piezometer 1) responded, reaching a maximum of ~07 psi (4.8 kPa). The far-field piezometer detected excess pore pressures after ~240 to 300 minutes as depicted in Fig. 36. After stabilization of the thermal field (steady state, 211 °C) the near-field pore pressures diminished and approached stable excess pressure, and the far-field pore pressure increased and also stabilized with a slight excess pore pressure (Fig. 36). Later in the experiment, an increase in heater power was generated; it was generated with a smaller change in temperature (Δ80 °C with power at 160 W; steady-state temperature, 291 °C), however. Excess pore pressures followed the same general trends, with maximum U_i reaching ~0.2 psi (1.4 kPa) above the steady-state excess pore pressure established during the first stage of induced thermal gradients at 211 °C. Clearly, the piezometers responded to the insertion pressures and thermal gradients as expected.

Three piezometer probes were field tested during the 1984 ISHTE component test cruise to MPG-I. Two probes (PP-1 and PP-3) were implanted in undisturbed sediment at radial distances of 10.7 cm and 67.0 cm from the heater surface. The other piezometer, PP-2, was inserted 10.8 cm from the heater surface after implantment of the heater. The objective was to measure possible effects of sediment disturbance caused by heater insertion as detected in the excess pore pressures generated by piezometer PP-2 insertion. PP-2 insertion pressure (approximately 2.4 psi or 17 kPa) was less than the insertion pressure generated by PP-3 (4.3 psi or 30 kPa) but slightly more than the induced pressure observed for PP-1 (2.2 psi or 15 kPa). These differences probably reflect differences in sediment variability.

PP-1 pore pressure response to probe insertion and its decay characteristics are depicted in Fig. 37. Approximately 1 hour into the dissipation of U_i the heater was inserted, and its induced pressure was recorded as measurable by PP-1. Before the complete dissipation of U_i generated by the heater and measured by PP-1, piezometer PP-2 was inserted, its induced pressure was only slightly measurable by PP-1. As clearly indicated, the heater required considerably more time (as predicted by theory) for dissipation compared to the smaller-diameter probes.

During 1985 an ISHTE ocean test cruise to MPG-I was completed with all the planned instrumentation, including five fully operational piezometer probes. The insertion pressures appeared to be reasonable; nevertheless, these pressures were slightly less than the pressures observed for the three piezometers during the previous component ocean test. This may indicate that the sediments tested on the 1985 cruise were of slightly lower strength than those tested during 1984 or that the piezometer filter may have penetrated to a slightly greater depth below the seawater-sediment interface during the 1984 test.

Laboratory and field investigations with deep-ocean piezometer probes have shown the importance and feasibility of making pore pressure measurements for sea-floor engineering applications and other geotechnical site evaluations. In situ pore water pressure measurements provide a quantitative means of assessing the consolidation state of sedimentary deposits and time-dependent changes in vertical effective stress in response to human-induced and naturally occurring environmental forcing functions. Pore pressure

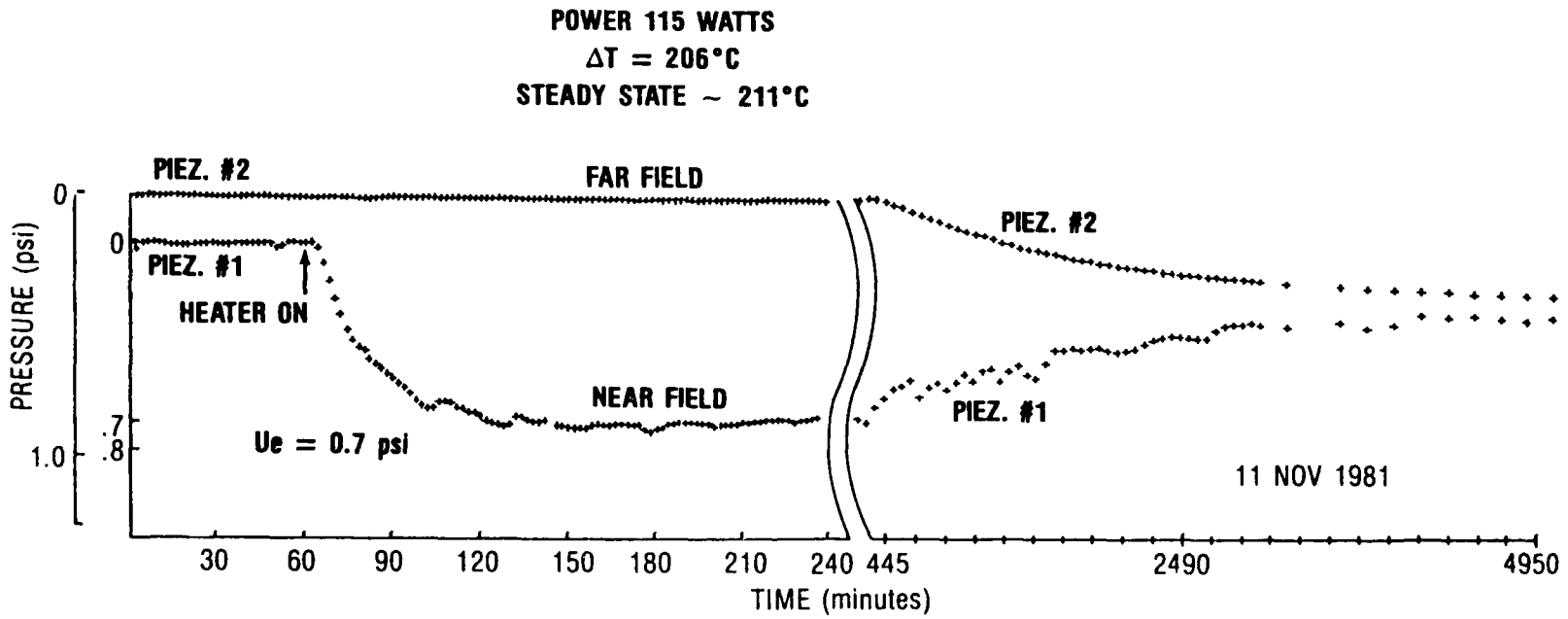

Figure 36. Pore pressure response to induced thermal field as measured by piezometers 1 and 2 during ISIMU-I (power of 115 W).

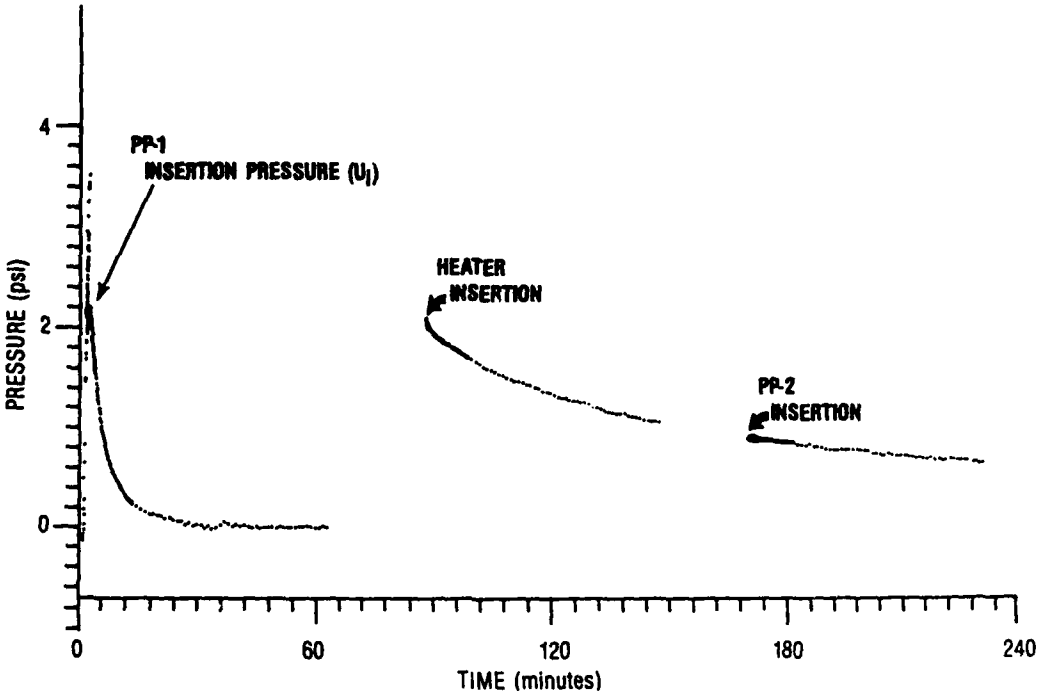

Figure 37. On-bottom data history for piezometer 1 (1984).

tests during ISIMU demonstrated the importance of these measurements in evaluating the influence of thermal gradients induced in the sediment because of temperature increases generated by a heat source (e.g., heat probe, radioactive canister, and the like). Pore pressure measurements make it possible to evaluate the in situ permeability, the undrained shear strength, and the elastic properties of submarine sediments.

Shear Strength Experiment

It is anticipated that the sediment strength will increase appreciably because of the high temperature around the heat source. The changes in sediment shear strength must be measured in situ because it is difficult to duplicate the ISHTE conditions in the laboratory. Data on these changes will be important in assessing the behavior of the canister and surrounding sediments over long periods of time. Initial modeling studies indicate that the canister will move relative to the sediment because of the accumulation of creep deformations resulting from imposed stresses. Nevertheless, the increased sediment stiffness, manifested by an increase in strength, will tend to counteract these long-term creep effects. Therefore, the changes in strength properties must be determined to complete the modeling studies.

Initial laboratory experiments at high pressure indicated that heating of illite sediment to 400 °C results in an increase in shear strength by a factor of 6 to 10 (Hadley, McVey, and Morin 1980). In these experiments, however, it was necessary to cool down and depressurize the sediment sample before conducting strength tests. Therefore, it is not possible to determine what the actual effects were while the sediment was at high pressure and high temperature.

ISIMU provided the first opportunity to measure strength properties at various temperature conditions while the sediment was at high pressure. An in situ vane (ISV) probe designed for ISHTE was modified and used in the simulation experiment. This experiment indicated that heat had a marked effect on the shear strength of the sediment (Babb 1982; Silva et al. 1985). The results are summarized in Figure 38.

The pretest and unheated zone posttest measurements were made at atmospheric pressure at a considerable distance from the heater. The heated profile was taken at 55 MPa just before the heater was turned off, with the closest proximity of the ISV to the heater surface being 0.6 cm. These initial results clearly show that the sediment strength changes dramatically because of high temperatures, with an approximate tenfold increase at the closest point (Babb 1982). It appears that the strength changes may be caused by a combination of thermal consolidation and alteration of illite to a more smectite-rich mineralogy (Burkett et al. 1987). Results indicate that the near-field sediment around the heater will undergo considerable increase in shear strength and, therefore, will be much stiffer than sediments in the far field.

The original plan called for two ISV probes on the ISHTE platform. The two devices were to be coupled to a single microprocessor and power unit. One probe was to be used in the far-field sediment before emplacement of the heater to obtain a baseline shear strength profile at the actual ISHTE site. The final plan was to have only one probe implanted at the end of the experiment (1 year) in the near-field, heat-affected sediment.

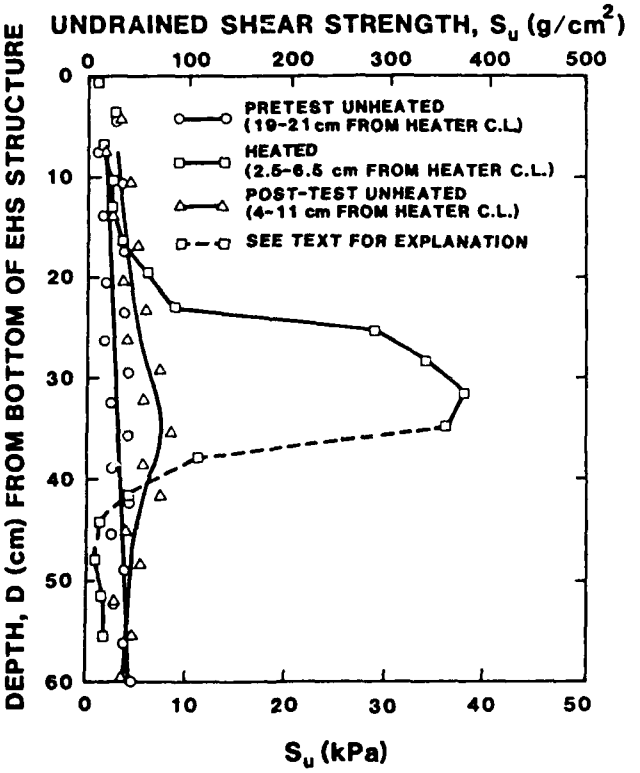

Figure 38. Undrained shear strength plotted against depth from ISIMU showing increased shear strength in heated region. EHS was the electric heat source.

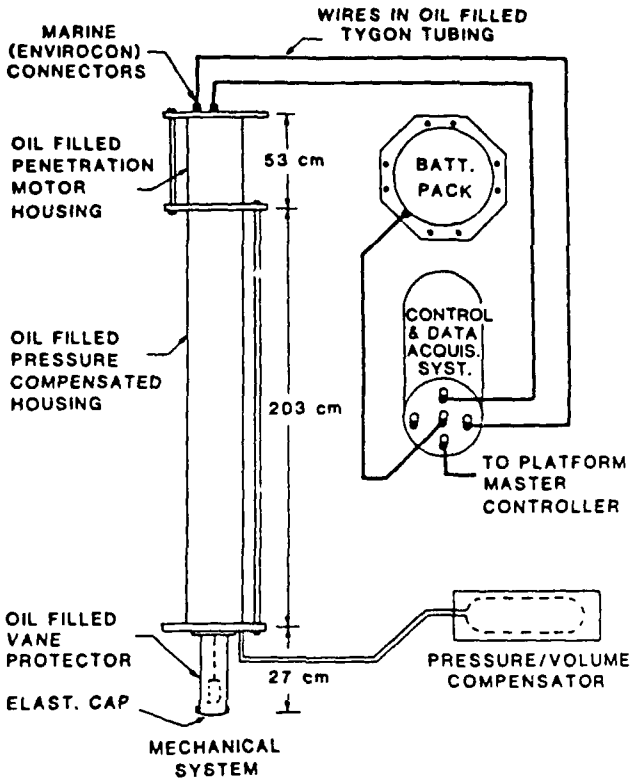

Figure 39. Schematic of ISV system.

The vane shear device was programmed to make an entire series of measurements after being activated by the central control system. All the data obtained would be stored on tape in the control housing, and a smaller data set would be sent to the platform logger for transmittal to a surface ship through the acoustic link. The data would include torque and rotation for each test site and force during each penetration cycle. From these data, the following geotechnical information can be determined:

- undrained shear strength (from maximum torque)
- stress-strain parameters, such as elastic and shear modulus (from torque-rotation data)
- residual shear strength (from large-deformation torque readings)
- penetration resistance (from force displacement data)

Twenty-two ISV measurements at progressively greater depths were to be recorded at an angle of $\sim 15°$ from the vertical so that the vane would pass just above the midplane of the heater at a distance of 1.0 cm from the heater surface. In this way, a large range of temperature conditions could be sampled to a depth of ~ 1.6 m.

The ISV system consisted of four integrated packages: mechanical system, electrical controller and data acquisition system, volume compensator, and power supply (Fig. 39). The system could be operated autonomously with its own power, controller, and data acquisition system. In ISHTE, the system could be initiated by the ISHTE central control

system; also, a back-up timer system in the ISV controller would be available in the event of a problem with platform commands.

Both the mechanical system and the volume compensator were oil-filled and designed to operate at deep-ocean pressures. Because the power supply and controller operate at atmospheric pressure, they were contained in high-pressure housings on the platform. The cabling connecting these packages was oil filled to provide volume compensation and to make use of special marine connectors.

The mechanical system drew on the experience of the ISV device developed for ISIMU. Many of the individual internal components remained the same, but some significant overall design modifications and refinements were made to meet the requirements of ISHTE. The internal arrangement of the apparatus is shown in Figure 40.

The system controller was basically an Intel 8751 microprocessor, which allows the user to change configuration characteristics easily; these characteristics may include the

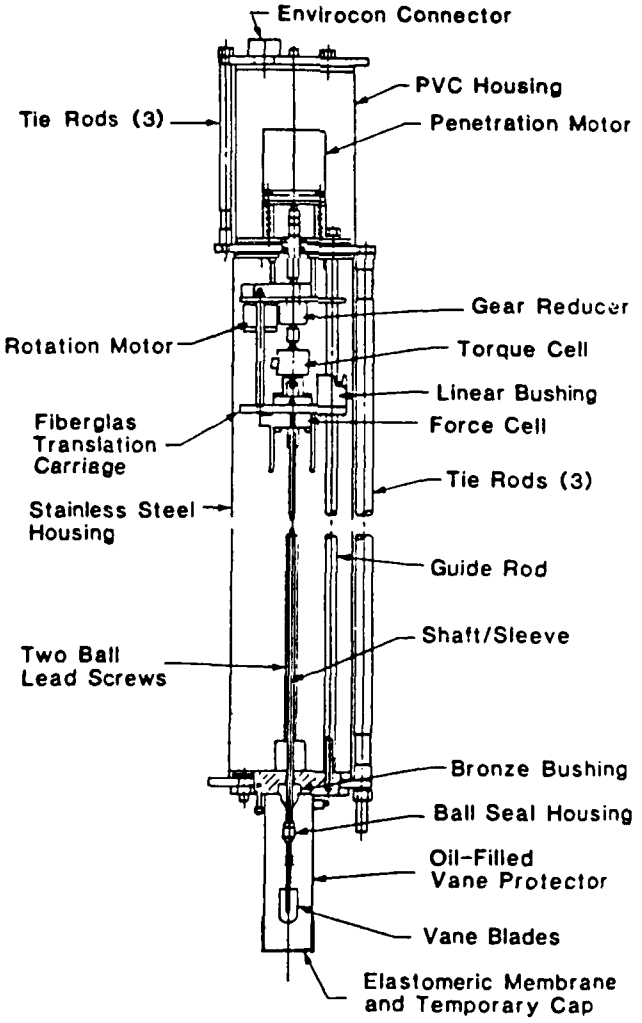

Figure 40. Assembly drawing of ISV model B. Penetration depth of 1.5 m.

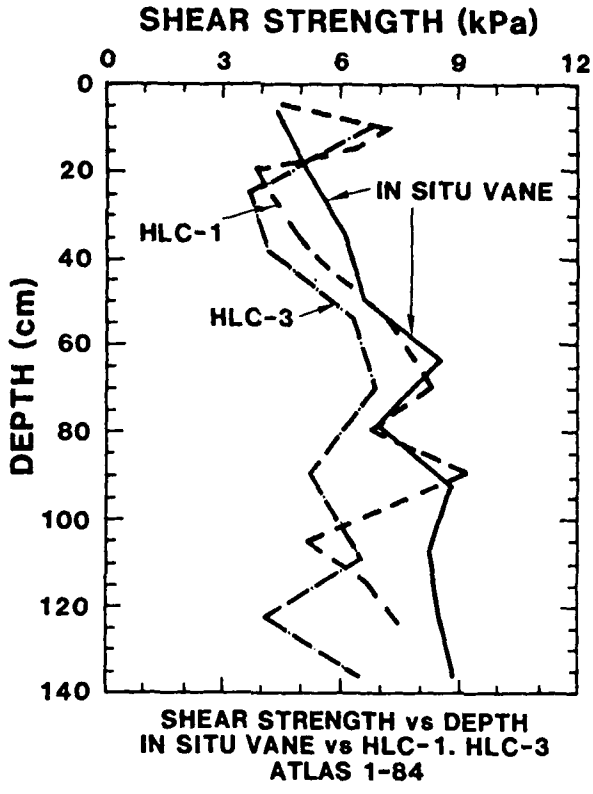

Figure 41. Shear strength plotted against depth.

number of sample sites, their locations, gear ratios, output data format, and the like. The microprocessor also interfaced with the force and torque transducers in the mechanical housing to measure the penetration force and shear torque. A cassette tapedeck for data storage and stepper motor drive cards were in the same pressure housing as the controller.

Power for the entire system was provided by batteries housed in a 0.43-m diameter Benthos glass sphere. The sphere contained three separate battery packs: one 18-V pack with a 10-Ah capacity for vane electronics and two 18-V packs with a 40-Ah capacity for the motors that drove the system.

The ISV system was fully tested on the 1984 ISHTE component test cruise in a water depth of 5850 m. During the component test cruise, the platform was lowered twice. For this test the ISV was vertical, and the system was programmed to take only 10 measurements in the 1.4-m depth. The ISV performed successfully and obtained a full data set. In addition, the ISV has been extensively tested and calibrated in the laboratory. An algorithm nas been developed for interpreting data.

The results of ISV measurements during the ISHTE component test cruise are compared with results of shear strength measurements on two hydrostatic cores, HLC-1 and HLC-2 in Figure 41. HLC-1 was taken on the same lowering as the ISV measurements, and HLC-2 was taken on a lowering 66 m away. The strengths of the two hydrostatic cores show trends similar to the trend of the ISV for most of the 1.4-m depth measured.

The ISV profile generally shows higher strengths than the values obtained from the hydrostatic cores, however. These and other comparisons indicate that the in situ strengths are 15 to 40% higher than in good-quality cores. Some of the extreme variability in the lower parts of the two cores does not show up in the ISV profile. It is likely that the lower shear strengths in the cores are caused by disturbance rather than by actual sedimentary conditions. Additional details are discussed by Silva et al. (1985).

Pore Water Sampling Experiment

Objectives

The objective of the ISHTE pore water sampling experiment was to define the chemical environment of the near field to a waste canister after sediment heating has taken place. Laboratory studies of seawater-sediment mixtures have been limited to closed systems. It is unclear to what extent the results can be used to predict the chemical behavior of the open system that would exist around a heat source emplaced in deep-sea sediments. At the very least, ions will diffuse into and out of the near field. Advection of pore fluids could further modify the chemistry from that predicted by experiments in the laboratory. Pore water samples are essential for understanding chemical processes associated with the near-field environment, and in situ measurements would help establish validity for laboratory studies of seawater-sediment-waste package interactions.

In addition to evaluating the chemical environment around the heat source, the pore water sampling of ISHTE would be helpful in interpreting the results of the ion migration experiments, especially if the results of the ion migration experiments differ significantly from the results of laboratory studies and tests in shallow-water environments.

Hardware

The pore water sampling systems were mostly based on standard technology and required only limited special consideration for use on ISHTE. Two pore water samplers were utilized on the platform: one for near-field samples and the other for far-field samples of water from the heated volume surrounding the heater. The far-field sampler was meant to provide a control sample and lay outside the 5 °C isotherm. The near-field sampler assembly is shown schematically in Figure 42; the far-field unit was analogous in design. The near-field unit was angled 22 ° from the vertical in the plane of the heater to intercept the heater 5 cm above the midpoint of the heat source (Figure 43); the far-field unit was inserted vertically to a depth of 60 cm.

Samples were obtained by drawing pore fluid into the samplers through filter elements spaced at intervals along the shaft. The suction to achieve this was provided by a master cylinder that was springloaded and controlled by a valve on the high-pressure side of the cylinder. When the valve was opened to ambient, suction was supplied to each filter element through a manifold. Each port of the sampler was connected to a slave cylinder that limited volume intake at each port to 21 mL. The extracted pore fluids were led to these cylinders through capillary (0.030-in internal diameter) tubes and stored in them for analysis once the platform was recovered at the termination of the experiment. The filter elements were sintered Inconel sleeves with nominal pore diameters of 0.5 μm and an outside diameter the same as that of the pore water probe shaft. They were sealed with O rings on the inside. The near-field unit had 10 sample ports, and the far-field had 7. The concept of in situ filtration of pore waters has been used for

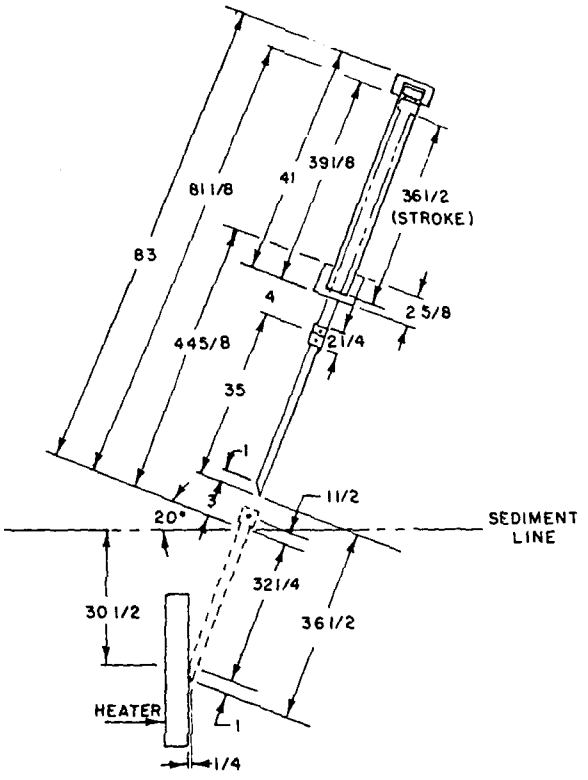

Figure 42. Schematic drawing of near-field pore water probe and implant cylinder. The position of the probe relative to the heater is also indicated. (Units are in inches).

nearly a decade in the collection of interstitial solutions free of artifacts that affect samples collected in cores. The criteria for the ISHTE samples were similar with regard to sample collection and storage. In addition, the near-field probe was designed to withstand sediment temperatures in excess of 250 °C. Placement of the near-field sampling probe was crucial because the high-temperature isotherms are closely spaced. Location had to be within 0.5 cm precision.

The implantment equipment for pore water sampling used the same type hydraulic actuation as the ion migration equipment and the same computer control as discussed elsewhere in this report.

Tests and Development

The first test of the pore water sampler was a prototype scaled to operate in the ISIMU experiment. This unit operated as designed in the month-long ISIMU experiment. Although there is no a priori method of determining the absolute accuracy of the samples collected in such an experiment, the marked chemical gradients sampled do not indicate sampling artifacts. Sampling was done over a range of temperatures from ~200° to ~5 °C in the sediment. The results identified a strong effect from thermal diffusion that had not been included previously in seabed near-field considerations.

The first deep-water deployment of the pore water sampler was on the chemistry

lowerings, the pore water system worked as designed. The probe was implanted, activated, and retracted back into the platform.

A final deployment of the pore water sampler in deep water was performed on the 1985 ocean test cruise to MPG-I. Both the near-field and the far-field probes were mounted on the ISHTE platform and bench-tested at the dock in Honolulu. During the platform test on the seafloor, the pore water sampler was not supplied with an initiation signal from the platform control system. Thus no water samples were obtained on deployment. Changes will need to be made to the implantment and retraction control valve system. At least one final test of the near-field and far-field probe should be performed from the fully instrumented ISHTE platform before a long-term experiment is initiated.

Posttest Coring Experiment

Posttest cores were planned to be taken as part of ISHTE for laboratory analysis. Analysis of these cores would help determine changes in sediment characteristics in the heat-affected zone. The cores would be situated, subsampled, and tested so that a good representation of the sediment changes can be determined. Previous laboratory experiments (Hadley, McVey, and Morin 1980; Babb 1982; Seyfried and Thornton 1982) have shown significant changes in physical properties and mineralogy resulting from the

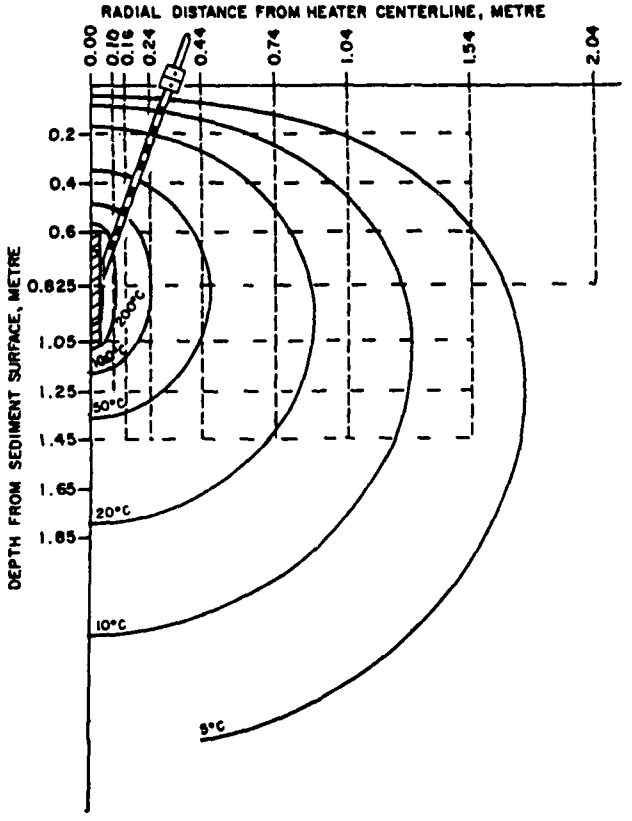

Figure 43. Location of near-field pore water sampler relative to predicted isotherms about isotope heat source.

heating of remolded illite sediment up to 400 °C at 60 MPa. Although the in situ changes may not be of the same magnitude as those encountered in the laboratory, the results of these previous laboratory experiments indicate that a detailed analysis of sediment properties in the heat-affected zone is necessary.

Five large-diameter cores and one small-diameter core were planned to be taken at various locations in the heat-affected zone once the experiment was completed. These cores were to be recovered with the platform. In addition, two larger-diameter cores were to be obtained with the ion migration experiment.

The six cores were oriented so that a continuous radial sample, with some overlap, could be recovered out to a distance of 32 cm, with two additional samples being recovered at 47 and 100 cm from the heater (Fig. 44). Five of the six corers were obtained from 10-cm diameter hydrostatic corers. The sixth corer, 5 cm in diameter, was attached to and driven with one of the hydrostatic corers (number II). The intent of using the smaller corer was to obtain a continuous sediment sample right along the sediment-heater interface. Because this sample was smaller it was probably disturbed in terms of strength properties, but the material should be representative.

The cores were extruded hydraulically, bottom first. As the core was extruded, undisturbed samples in thin-walled, stainless steel tubes were taken with a special piston core subsampling device. These undisturbed samples were of various sizes for different geotechnical tests and other analyses and were both horizontally and vertically oriented; the horizontally oriented samples were used for analysis of anisotropy effects. Measurements of shear strength with a miniature vane shear device and thermal conductivity with a needle probe were taken while the sediment was still in the core tube. Sampling for water content, bulk density, and classification was done periodically down the length of the core. All these sampling and testing procedures were successful on the 1984 component test cruise.

The laboratory testing program for the acquired samples focused on the physical and chemical properties of the sediment as they relate to sediment and canister interaction. These properties include shear strength, permeability, compressibility, creep, thermal conductivity, sediment microstructure, geochemistry, and ion migration. Laboratory tests that were run parallel to previous tests were performed for comparison.

Hydrostatic cores were obtained during the ISHTE component test cruise and were subsampled and tested in the manner described previously. The water content and shear strength results shown in Figure 45 are typical profiles. As an example, the HLC-1 hydrostatic core yielded 13 shear strength measurements, 6 conductivity measurements, and numerous water content, bulk density, and classification samples. The laboratory analysis combined with the in situ tests provided an accurate measurement of changes in sediment properties in the heat-affected zone.

Isotropic Heat Source

The reasons for the amount of thermal power (4.5 MW-h of total thermal energy) desired for the ISHTE (500 W) and the duration of the experiment (1 year) are discussed elsewhere in this report. The options available to provide such power are:

- batteries such as those used in normal oceanographic experiments
- fuel cells such as those used in the space program
- exothermic chemical reactions

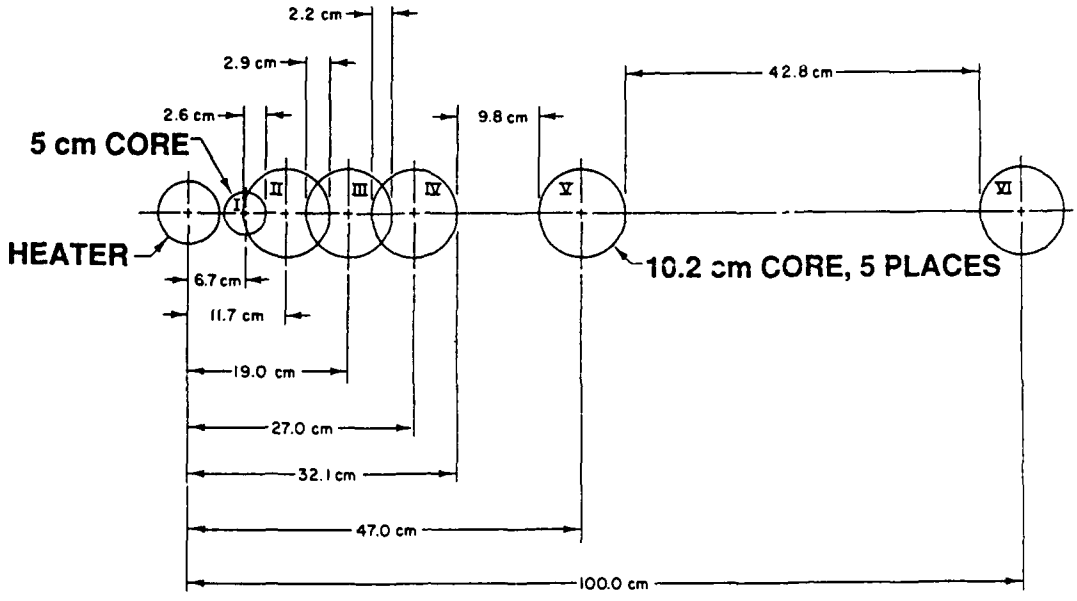

Figure 44. Schematic of radial core distances.

- power cables to the shore or a surface buoy
- radioisotopic thermal power

The common battery energy source for the deep-ocean application comprises pressure-equalized lead-acid or Ni-Cd batteries. Optimistic calculations showed that the in-air weight of enough such batteries to provide the total energy required would be 2×10^5 kg (220 ton), without allowing any excess energy for contingency or considering that the efficiency of the battery system would decay over the duration of the experiment. Neither did the calculations include any considerations of reliability. Also, the transportation, handling, and deployment problems certainly precluded the use of such batteries on the small platform envisioned for ISHTE.

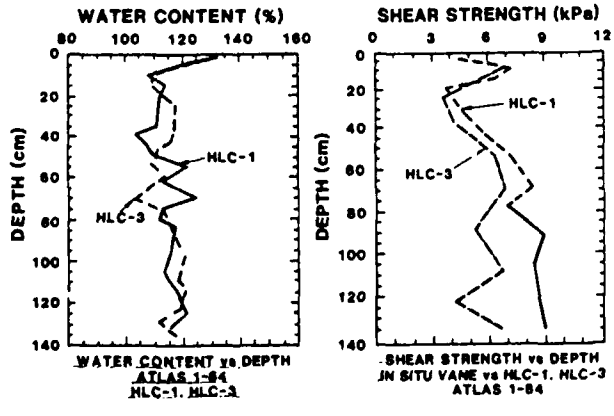

Figure 45. Water content and shear strength plotted against depth.

The use of fuel cells or exothermic reactions was rejected because of the same two major limitations. The technology to operate these systems at high ambient pressure is considered at best state of the art. Inquiries brought responses indicating that such operation might be possible, but the particulars of a workable design were not known. Thus the cost of development was not bounded, and all indications were that it would be high. The safety and reliability of the systems were of great concern. Handling, storing, and deploying the large quantities of the reactive chemicals required would present hazards that had not been addressed by the oceanographic research community. Also, there was no reasonable way to test these systems for long-term reliability except by costly, long-term deployment.

Running a power cable from an energy source on the shore or on a surface buoy was deemed impractical. It was considered mandatory that ISHTE be performed at high pressure (typical of that to be expected in the anticipated repository sites) and that the sediment type be typical of the red clays in those areas. Details of the nature of these red clays are discussed by Bryant and Bennett (1988). No sites meeting these criteria exist close enough to a shore that it would be economically feasible to run a power scale.

If power were to be supplied by running a cable to the ocean floor from a surface buoy, the power would be generated by a motor generator set and transmitted to the bottom by an electrical-mechanical cable. Cost and reliability were the deciding factors. The cost to keep a manned ship on station for 1 year would be prohibitive. Likewise, the cost of mooring an unmanned buoy in water of sufficient depth was high, and the reliability would probably be quite low. Experience has shown that unmanned buoys, particularly of the size required here, have a poor record of staying anchored and, because they attract the attention of passing ships, are subject to damage or pilfering. Also, there is no known previous experience in deploying a power cable to these extreme depths for 1 year. This would be another open-ended development problem with no reasonable cost limit.

The only alternative left for providing thermal power to ISHTE was the use of radioisotopic material. This source is already considered the most practical when energy is needed at some remote location or in a particularly hostile environment. In such cases the power needed is usually electrical, and a thermoelectric generator must be included in addition to the isotopic power. There are instances (in space vehicles in particular) when radioisotopic power is used to provide thermal energy to protect electronic hardware from a cold environment.

An IHS was designed on the basis of the existing technology of FSAs as used in multihundred-watt radioisotopic thermoelectric generators for space flight applications. Considerable testing has been done to qualify the FSA for space flight (General Electric 1977); eventualities considered have included fire, aborting a flight, and ocean impact. The use of FSAs in the IHS for ISHTE drew heavily on previous work.

The IHS, which contained five FSAs, is shown in Figure 46. Each FSA had a thermal output of 100 W, for a total of 500 W, and was composed of a 3.72-cm diameter PuO_2 sphere (80.2% ^{228}Pu) encased in a thin Ir shell. An external graphite impact shell around this assembly provided additional protection. The use of Inconel 625 was dictated by its combination of high-temperature strength and corrosion resistance. The necessary conditions for the IHS were 59 MPa external pressure and a maximum temperature of 400 °C. Stress analysis of the IHS design was completed, and an unfueled prototype was fabricated at Monsanto Research Corporation and tested at Battelle Columbus Laboratory. The test conditions included a maximum external pressure of 76 MPa at 515 °C; no yielding was indicated.

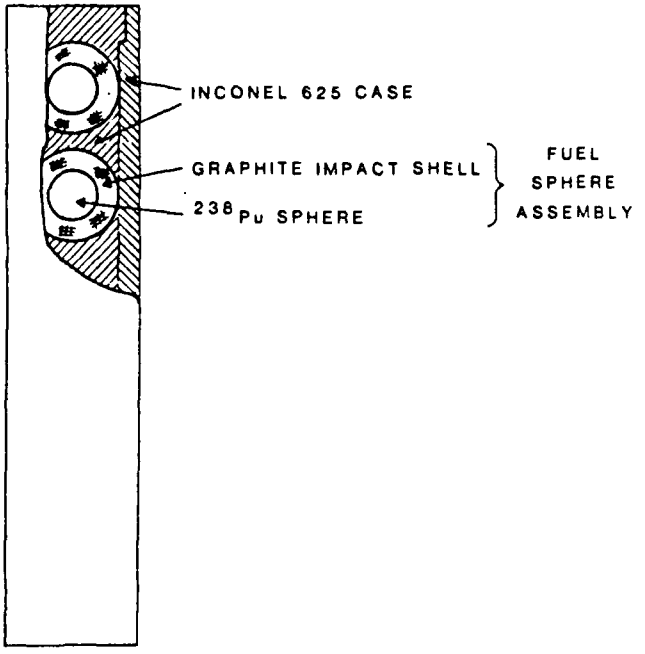

Figure 46. ISHTE IHS.

ISHTE Simulation Experiment (ISIMU)

One of the most significant events that occurred on the ISHTE project was the planning, preparation, and completion of ISIMU. This simulation was a 0.2387 : 1.0-scale ISHTE conducted in the large pressure vessel at David Taylor NSRDC in Annapolis, Maryland during the latter part of 1981. The following reasons dictated that this laboratory simulation be performed before the complex, long-term ISHTE was fielded:

(1) Such a simulation would help ensure the success of ISHTE by uncovering unanticipated responses as well as by checking the validity of the ISHTE experiment concept.
(2) Good correlation between the smaller-scale laboratory simulation and ISHTE would lend credence to laboratory-scale testing of other SDP thermal problems.
(3) The simulation experiment would provide an opportunity to test several prototype ISHTE components at deep-ocean pressure and temperature.

The pressure vessel, containing a tank of reconsolidated sediment, was maintained at 55 MPa and 4 °C to simulate in situ deep-ocean conditions. One month was the longest that these constant environmental conditions could be maintained. This resulted in a scale factor of 0.2387 : 1.0. With this scale factor, the boundaries of a 1-m diameter by 1-m deep sediment tank had little effect on the thermal response of the heater and sediment. Figure 47 shows predicted comparison plots of the isotherms for ISHTE and ISIMU. Note that the ISIMU calculations show a change in shape of the outer isotherms because of the finite tank boundaries. It is obvious, however, that the relative shapes of the isotherms inside the 20 °C isotherm are similiar.

A top tank above the sediment tank provided a seawater cover over the sediment and allowed the use of freshwater in the pressure vessel. Figure 48 shows the schematic of

the ISIMU experiment. Sediment dredged from the proposed ISHTE test site, MPG-I, was processed and then reconsolidated over a 10-week period to approximate in situ overburden pressure (Silva, Jordan, and Levy 1982; Silva et al. 1982). A heater probe, various thermal sensors, a line-source thermal conductivity probe, pore pressure probes, and a pore water sampling probe were inserted into the reconsolidated prepared sediment. A displacement device measured the motion of the sediment-water interface, and a vane shear measured the sediment shear strength. Closed-circuit television monitored the experiments.

An initial power of 115 W was supplied to the heater until essentially steady-state conditions had been attained after a period of 9 days. This power level was scaled to reflect the 400-W power initially anticipated for ISHTE. The maximum heater temperature produced at this power level was ~210 °C, which was roughly 25% lower than the pretest prediction based on initial measurements of the thermal conductivity. To produce a maximum heater temperature close to that predicted for the ISHTE, the power level was increased to 160 W 9 days into the test. At this power, a maximum steady-state heater temperature of ~290 °C was produced. The power was maintained constant at this heater power level for the remainder of the 1-month duration of the experiment. A period of 1 month was selected to represent a scaled time of 1 year for the ISHTE and to allow sufficient time for chemical changes in the sediment-seawater system to progress to an observable level. On termination of the experiment a thorough posttest inspection was conducted, thermal conductivity measurements were made, and numerous cores were taken for subsequent analysis. Initial evaluations indicated that all instrumentation functioned properly throughout the test. A preliminary data transmittal report that summarizes the important aspects of the experiment has been prepared by APL (Miller, Miller, and Olson 1982).

The primary objectives of the experiment were:

- to determine transient temperature distribution in the sediment
- to measure the effective thermal conductivity of the sediment
- to measure transient pore pressure
- to measure transient sediment response to the applied pressure

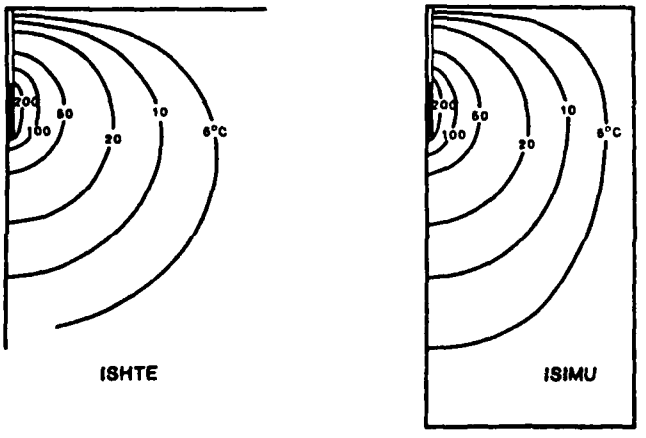

Figure 47. Comparison of thermal fields for ISHTE and ISIMU.

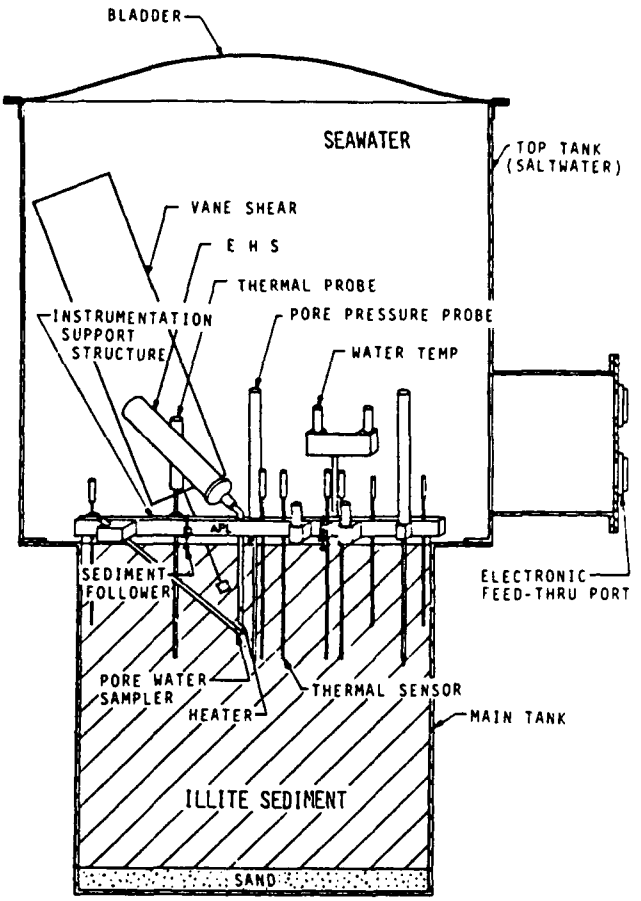

Figure 48. Schematic view of ISIMU.

- to measure sediment shear strength
- to study pore water chemistry

During ISIMU it was observed that, for a given heater power level, the maximum heater temperature was ~25% lower than predictions based on pretest measurements of sediment properties. It was originally conjectured that this behavior could be attributed to:

- measurement errors (temperature or thermal conductivity)
- thermally induced convection or pore fluid
- nonhomogeneity of the sediment (thermally induced porosity or structural changes)
- local fluidization of sediment near the heater
- thermal energy transport due to concentration gradients (Dufour effect or diffusional transport)
- temperature- and pressure-dependent sediment properties (water or sediment)
- thermal conduction in the implant cylinder (possible convection in the cylinder)
- convection transport of thermal energy in annular gaps or radial cracks near the heater and implant cylinder

A small-scale experiment was conducted by SNLA to investigate further the underlying reasons for the discrepancy (Percival 1985b). The experiments were conducted with the same heater assembly and sediment originally used in ISIMU at Annapolis. The heater assembly was implanted vertically in reconsolidated illite sediment, which was consolidated in a manner similar to that used in the original ISIMU. The major difference in the two experiments was that the studies at SNLA were conducted at atmospheric pressure and temperature whereas those at Annapolis involved conditions (55 MPa and 4 °C) closely approximating the ambient environment of the seafloor. Consequently, the studies at SNLA were conducted at a significantly lower power level to prevent boiling in the sediment. The thermal conductivity of the sediment prepared was within 3% of the thermal conductivity measured in the original ISIMU experiment. Likewise, the permeability of the sediment was within the range of values normally quoted for illite sediments. In all important features, the experiments performed at SNLA produced thermal responses essentially identical to those observed previously at Annapolis.

Observations during the SNLA experiments suggested that a significant portion of the electrical power supplied to the heater was being dissipated by resistance heating in the portion of the sheathed heating element that was exterior to the heater block. It was found that the resistance of the primary heating element (which fit in the heater block) was 0.602 Ω at 23 °C. The total electrical resistance of the entire sheathed heating element assembly (consisting of the primary heating element, Ni alloy leads, and Cu leads) was 0.831 Ω. Hence 27.6% of the total dc electrical power supplied to the heater was dissipated by resistance heating in the leads to the primary heating element. It was further observed that the heating element did not occupy the entire length of the heater block and was slightly asymmetrically located in the block.

The correct power distribution and heater block geometry were incorporated in the numeric simulation. It was assumed that the distribution in the heater used in both the SNLA and the ISIMU experiments was the same as that determined for the back-up heating element assembly. This refinement in detail resulted in an accurate prediction of the heater's thermal response for both experiments.

On the basis of the results of the SNLA studies, numeric predictions for the temperature distribution were made with the finite-element thermal-conduction computer program COYOTE (Gartling 1982). To describe the results of this simulation as briefly as possible, only the steady-state results for a total power of 115 W are considered. The results of the simulation are thus compared with the experimental data obtained 8 days 23 hours after the initiation of heating in ISIMU. These were the last data obtained before the total heater power was increased to 160 W. In Figure 49, the measured temperature profiles are compared to the predicted profiles. The predicted temperatures generally agree with measured values to within 10% for the higher temperatures. The larger differences, which occurred at the lower temperatures, can be attributed to the lower accuracy associated with the measurement of these quantities. It should also be noted that the temperature distribution on the heater was accurately predicted.

It is concluded that the insertion of the heater assembly into reconsolidated illite sediment did not alter the sediment in the vicinity of the heater assembly (Burkett et al. 1987). Hence it is now believed that the thermophysical properties of the sediment are unaffected by the insertion of the heater assembly and that any thermally induced fluid motion that may exist in the sediment is too weak to alter the thermal field established by conduction. The good correlation between the predicted and measured values of temperatures in the sediment indicates that the possible disturbances of the temperature field must be of insignificant magnitude.

Results from ISHTE reveal complex alteration and mass-transport processes due to thermal diffusion, convection, and solution mineral equilibria. Sediments altered at temperatures $<170\,°C$ remained unconsolidated even though important mineralogic and chemical changes occurred. For example, sediments from the hottest portion of this unconsolidated zone exhibited the formation of chlorite and calcite and dissolution of Na- and K-rich mineral phases. Pore fluids were characterized by compositional gradients, including large decreases in Na^+, Cl^-, Mg^{2+}, Ca^{2+}, and SO^{2-}_4 with increasing temperature. These changes are consistent with thermodiffusional transport (the so-called Soret effect) and rock-water interaction. Cl^- was the only component unaffected by rock-water interaction and responded only to thermodiffusional processes.

At temperatures of alteration $>170\,°C$, a baked zone formed. The consolidated nature of this zone appears to have resulted from extensive secondary mineralization, the most important being analcime formation. The sediment-water content, however, instead of decreasing as one might expect, actually showed an increase of $\sim 20\%$ relative to that of unaltered sediment. Apparently this was due to the existence of water-filled microcracks. These cracks may have initially resulted from sediment deformation associated with heat probe emplacement in the sediment but were maintained and possibly enlarged by dissolution of selected minerals in sea-salt solution convectively circulating near the heat source. Some microchannels were observed by transmission electron microscopy analyses (Burkett et al. 1987, in press).

Convective circulation of the sea-salt solution in the immediate vicinity of the heat source occurred on a relatively large scale. For example, mass-balance constraints indicate that ~ 641 effective volumes of the sea-salt solution passed through this baked zone

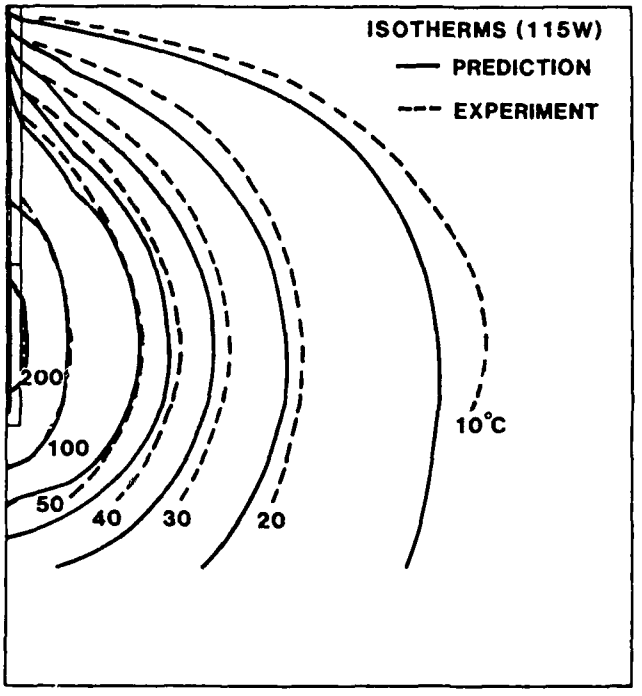

Figure 49. ISHTE simulation isotherms.

during the 30-day experiment. In addition to supplying Na for analcime formation, seasalt solution convection resulted in nearly total elimination of quartz as a reactant in sediment immediately adjacent to the heat source. Circulation of solutions having relatively low concentrations of SiO_2 caused chlorite to form at the expense of smectite. Mineralogic and, to some extent, chemical changes in baked-zone sediments from ISIMU are similar to those recorded for sediments in contact with dolorite sills in the Guaymas Basin of the Gulf of California.

Results from the ISIMU experiment must be cautiously applied to subseabed disposal concepts because we are unsure of the likelihood of seawater convection near a buried waste-containing canister. If convection occurs, it is localized and closed to recharge pathways; if convection does not occur, the pH of the near-field hydrothermal fluid at temperatures >250°C will be mildly acidic. The redox intensity will be constrained by sediment chemistry and mineralogy.

Component Test Cruise

The component test cruise (Percival 1985a) was a deep-ocean test of ISHTE components before the total ISHTE platform was assembled. The principal purposes of the test were to evaluate the operation of the various components at the proposed water depths and to check the interfaces between the experimental components and the platform controller and data acquisition systems. The successful completion of component testing was necessary to continue developing ISHTE with confidence. During this cruise, values of in situ sediment properties were obtained for finalizing the ISHTE design.

The ISHTE components were tested with two separate platforms. This enabled personnel to test one set of ISHTE hardware while another set was being prepared for testing. The actual ISHTE platform was to have redundant platform controller and data acquisition systems. Both systems were available for the component test cruise. Each test platform used one of the ISHTE platform controller and data acquisition systems to interface with the experiments. One platform, the small one, was used to test the geochemistry experiments. The other platform, the large one, was used for all other experiments.

There were two significant disappointments with regard to the operation of the ISHTE tests: failure of the battery system, and limitation in the range of the acoustic telemetry system.

There was a failure of the battery system being used to power the heater. This system was not part of the ISHTE platform but was included to test the thermal sensors on the heater. The failure of the battery system did not represent a failure of a regular ISHTE component, but it did limit the testing that was scheduled for the thermal sensors. All other indications suggested that the sensors worked properly. There were other minor electrical problems that were probably the result of stray electrical currents caused by the battery failure. These were corrected and did not compromise the test.

The second disappointment was a limitation in the range through which the acoustic telemetry system would send data to the ship. The limitation was apparently due to background acoustic noise originating in the ship. Previous measurements of the acoustic background for the R. V. *Melville* indicated that sending acoustic signals between the platform and the ship would not be a problem. During the component test cruise it was found that data could not be sent reliably from the platform to the ship. Once it was discovered that signals could be sent to the platform, however, the tests were conducted

as planned. The data were recovered from the platform at shallower depths and on the deck of the ship.

The overall platform system performed extremely well, particularly the command and control systems, which had not been tested before in the deep-ocean environment. The software to interface the various experiments with the ISHTE platform was found to be user friendly and essentially bug free. The command, control, and data acquisition interfaces to the platform worked well. All the piezometer probes produced good raw data. The data were analyzed for detail that could help define the character of the in situ sediment.

Three cores were taken with the ISHTE hydrostatically actuated corers on the large platform. These cores, along with three of the box cores taken by biologists from Scripps Institution of Oceanography, were processed on board the ship. Shear strength and water content profiles for the three ISHTE cores were obtained as well as a significant number of undisturbed samples for laboratory analysis and testing.

The ISV system worked on the first lowering of the large platform. The shear strength for the sediment as determined in situ was compared to the data from the three hydrostatic cores. The in situ measurements gave a higher value for shear strength than that obtained from the cores.

Several thermal experiments were conducted on the component test cruise. The thermal conductivity of the illitic sediment in MPG-I was measured both in situ and in the processed cores. The in situ value was 0.91 W/m · K. The values measured in the cores ranged from 0.88 to 0.97 W/m · K. These values agree favorably; they are slightly lower than the values measured for reconstituted illite in the laboratory.

One of the ISHTE thermal probes was used to measure the thermal gradient in the sediment. These measurements were used along with the thermal conductivity to predict the naturally occurring heat flux in the MPG-I region. The value obtained was 1.4 $cal/cm^2 \cdot s$. This compares favorably with the previously measured values of 1.24 to 1.70 $cal/cm^2 \cdot s$.

Ocean Test Cruise

The objective of the ocean test cruise (Percival 1986a) was to perform a test of the complete ISHTE platform with time for modifications before the 1-year experiment. The plan for the cruise was to deploy the ISHTE platform twice, with time between to correct problems from the first lowering. During these deployments all various ISHTE systems, including the deployment and recovery system, were to be tested. The software program to operate the platform's control system was to be exercised by using abbreviated ISHTE sequences. On each lowering, the heater was to provide power for only 8 hours; thus electrical heater and battery power could be substituted for the IHS of ISHTE.

The final preparation for the cruise and the first assembly of the equipment on the ISHTE platform were completed at the staging area in Hawaii. This operation went smoothly and on schedule. Loading on the ship and final checkout of the ISHTE platform began on 9 September 1985.

Nine days were spent on station. The first 3 days were spent deploying the acoustic tracking system, testing some ISHTE components (in 5800 m of water) on a line, and preparing the ISHTE platform for deployment. Deployment began with the launch of the ground line for the back-up recovery system. After the 6400 m of ground line was deployed, the platform was attached and lowered to the sea floor. It took 19 hours to

fully deploy the ISHTE system in 5900 m of water (see Figure 9). The deployment configuration was perfect, and the locations of the platform and ground line were exactly as planned.

Because this was the first test of the system, the nylon line used to lower the platform was secured to the ship while the platform was tested on the sea floor. The plan was to test the release on the platform at the end of the operation and to allow the recovery line to feed out of the line bin. The end of the line from the bin was attached securely to the platform for recovery. After 5 hours of a planned 18.5-hour operational test of the platform, the acoustic command link stopped functioning. The hydraulic release on the platform could not be commanded to operate and so had to be used to raise the platform to the surface. As the platform was held at the surface during recovery, the release malfunctioned.

The platform was dropped to the ocean floor with the ground line still deployed and the associated acoustic transponders in working condition. The acoustic transponder at the midpoint of the ground line was tracked acoustically during the fall. By using the ship's location at the time of the fall and the final location of the transponder and the lengths of line involved, it was possible to plot the location of the platform on the bottom and the new orientation of the ground line.

By this time, the entire ISHTE crew was tired from three continuous days of operation, and everything seemed to be secure. While the ISHTE crew rested, the ship was used by a group of biologists for a deep-towed camera operation. The recovery of the platform would be accomplished the next morning by acoustically releasing the ground line.

Early the next day the ship was positioned over the ground line anchor, and the acoustic releases were actuated to drop the anchor. The ground line was not expected to reach the surface for at least 4 hours because of drag. Instead, the floats broke the surface in just over 1 hour. The line was hauled in with little tension. After 600 m, the cut end of the ground line was hauled aboard. All indications were that the biology camera tow had crossed the ISHTE ground line and cut it. The transponder on the back-up recovery line was still functioning and indicated that the ground line was in a taut moor above the platform.

Preparations were made to grapple for the recovery line. The grappling system consisted of a 69-kg grapnel hook with a 186-kg ball 1 m below it. An acoustically tracked object was placed 250 m above the grapnel. A spare tracked object was located 50 m above the first. The tracked objects allowed the grapnel to be tracked with respect to the platform and the recovery line.

The grapnel was towed along the bottom for 24 hours, the ship making six circles about the taut moor and the platform. The grapnel was then retrieved and, with it, the end of the back-up recovery line. With this line the platform was recovered. This episode indicates that with an accurate navigational system and tracked objects an ISHTE-type platform can probably be recovered from the sea floor under most circumstances. More extensive testing of the back-up recovery modes for ISHTE was performed than was planned.

The time required to drop and recover the platform prevented a second full deployment of ISHTE. Of the platform systems tested, most performed satisfactorily. Except for the acoustic telemetry, it was fairly obvious what caused malfunctions in one camera system, the heater implantment system, the recovery line release, and the chemistry experiments. These problems could be corrected with fair confidence, but the acoustic telemetry link problem is more difficult because it started working again at 3 km when it

was turned on during recovery. The remainder of the cruise time was spent testing this acoustic telemetry system on a line at depth. It operated satisfactorily to the full depth of the ocean when separate from the platform. The best guess is that the transducers, which were floated above the platform, had a geometry problem with respect to the instruments on the platform.

After the cruise, some minor design flaws were found in the acoustic system hardware; these have been corrected, but we have no clear answer about the reason for the failure. An additional test of a fully instrumental platform must be performed before an ISHTE-type system can be deployed. In summary, the ocean test cruise seemed to be successful in demonstrating the ability to field a complex ISHTE platform in the deep ocean and to recover the equipment. Valuable data were recovered on thermal conductivity of the in situ sediment and the pore pressure response to driving probes.

Concluding Remarks

This report is a description of the final status of ISHTE, which had been under development by the SDP for 9 years (1978 to 1986). The work was a joint effort by several institutions and thus is not intended to relate the evolution of ISHTE. These details can be found in the SDP Annual Reports for the years 1978 through 1986 and in the minutes of the ISHTE Project Planning Group Meetings. Many other reports and papers have been written that cover the details of ISHTE. Many of these reports are included in the reference section.

Much effort has gone into ISHTE over the past years, and many new ideas and concepts related to ocean engineering and marine science have been developed and tested. Each individual system on ISHTE represents state-of-the-art technology and required significant analysis, engineering, and testing. The success of ISHTE is actually a summation of the successes of the many systems that make up ISHTE. The major testing milestones for ISHTE are listed below:

- 4/80 Site selection cruise: Bathemetry and coring
- 7/80 Tracking system test cruise: Test tracking and deploying long-term mooring
- 5/81 Coring system test cruise: Test-coring, acoustic telemetry, and recovering long-term test mooring
- 12/81 ISIMU: Long-term laboratory testing of experimental concept
- 9/84 Component test cruise: Testing of individual components interfaced with controller and data loggers
- 9/85 Ocean test cruise: Completing test of ISHTE including deployment and recovery systems

The future milestones for ISHTE were:

- FY87 Deployment: Deploying ISHTE for 1 year with isotopic heater; beginning data acquisition by means of telemetry
- FY88 Recovery: Recovering ISHTE and making a laboratory analysis of samples
- FY89 Analysis: Data analysis and reporting

With the completion of the ocean test cruise, the various systems for ISHTE were evaluated with regard to their readiness for long-term deployment. Some systems had deficiencies that need to be corrected. It was felt by the ISHTE Project Planning Group

that an additional ocean test of the complete ISHTE with an electric heater is quite important and could provide a high level of confidence for a 1-year deployment.

During the November 1985 to March 1986 time frame, the future of ISHTE and the SDP was debated. The decision was that the SDP, and thus ISHTE, would be terminated at the end of September 1986. Because of this termination date, it would not be possible to complete any significant further testing of ISHTE components. The time since the announcement of the termination has been spent evaluating the data from the ocean test cruise, reworking some components, and writing the final reports.

Even though the major goal of ISHTE to deploy the experiment for 1 year on the seafloor was never accomplished, the project had a lot of success with state-of-the-art equipment. These new deep-water tools were all developed and tested in the field with a high degree of success for most systems. In addition, the project has gathered a fair amount of in situ data on seafloor sediments and has demonstrated that meticulous experiments can be performed in the great depths of the abyssal plains. To date, the data gathered have reinforced and refined the values for sediment properties used in laboratory models and in computer codes. No unanticipated phenomena have been uncovered with the work, but working in the field has provided valuable insight into the problems that need to be solved for reliable operations in a hostile environment. No in situ data have been obtained on how inhospitable the environment will be when the sediment is heated to several hundred degrees for several months.

Acknowledgments

ISHTE, which was part of the SDP, was supported by funds from the Department of Energy through Sandia National Laboratories under the administrative direction of Dr. D. A. Anderson. Editing and preparation of this final report for *Marine Geotechnology* was supported by NOARL, Stennis Space Center, Mississippi. The authors appreciate the professional assistance in editing and preparation of the illustrations and proofing by Ms. F. Lee Nastav and Dr. Huon Li, both of NOARL. Mr. Carl Mueller, head of the Technical Information Branch, NOARL, assisted in the original conversion of the computer copy of the text. Mrs. Ethel Shields and Mrs. E. Fay Ladner, of LOARL's Seafloor Geosciences Division, typed various versions, corrections, and changes of the text. NOARL supported the special editor of this issue in the preparation of the final version and editing of this report for *Marine Geotechnology*. The authors wish to acknowledge the reviewers of the early version of the text.

References

Anderson, D. R. 1979. *Nuclear waste disposal in sub seabed geologic formations: The Seabed Disposal Program.* SAND78-2211. Albuquerque: Sandia Laboratories, May.

Babb, J. D. 1982. Development of a probe for in situ strength measurements of deep-sea sediments. Master's thesis, University of Rhode Island, Kingston.

Backes, J. L., B. M. Bell, and J. B. Miller. 1983. Implementation of error detection and correction codes for acoustic data telemetry. In *Oceans 1983*, vol. 1, 167–175.

Backes, J. L., B. M. Bell, and L. O. Olson. 1981a. ISHTE system tests at MPG-1, May 1981: Cruise report, APL-UW 1381. Prepared for Sandia National Laboratories by the Applied Physics Laboratory at the University of Washington in Seattle, November.

Backes, J. L., B. M. Bell, and L. O. Olson. 1981. Long baseline deep ocean acoustic tracking and telemetry system. In *Oceans 1981*.

Bennett, R. H., and J. R. Faris. 1979. Ambient and dynamic pore pressures in fine grained submarine sediments: Mississippi Delta. *Applied Ocean Research* 1:115–23.

Bennett, R. H., J. T. Burns, and D. N. Lambert. 1981a. *Design and development of deep-water piezometer for the Sandia Subseabed Disposal Program: Subseabed Disposal Program annual report, January–December 1980, vol. II, part 1 and 2.* SAND81-1095/II. Albuquerque: Sandia National Laboratories, July.

Bennett, R. H., J. T. Burns, and D. N. Lambert. 1981b. *Fabrication and testing of deep-ocean piezometer system and components for the Sandia Subseabed Disposal Program (SDP): Status report, January–September.* Albuquerque: Sandia National Laboratories, November.

Bennett, R. H., J. T. Burns, and D. N. Lambert. 1982. *Fabrication and testing of deep-ocean piezometer system and components: Subseabed Disposal Program annual report, January–September 1981, vol. II, part 1 and 2.* SAND82-0664/II. Albuquerque: Sandia National Laboratories, July.

Bennett, R. H., W. R. Bryant, P. J. Burkett, and L. E. Shephard, 1985a. Microstructure of red clays from Northwest Pacific Deep Sea Basin. Presented at the 1985 International Clay Conference, July, Denver, Colorado.

Bennett, R. H., J. T. Burns, T. L. Clarke, J. R. Faris, E. B. Forde, and A. F. Richards. 1982. Piezometer probes for assessing effective stress and stability in submarine sediments. In *Marine slides and other mass movements*, ed. S. Saxov and J. K. Nieuwenhuis. New York: Plenum.

Bennett, R. H., J. T. Burns, J. Lipkin, and C. M. Percival. 1983. Piezometer probe technology for geotechnical investigations in coastal and deep-ocean environments. Presented at Range Commanders Council Twelfth Transducer Workshop, 7–9 June, Melbourne, Florida.

Bennett, R. H., J. T. Burns, H. Li, C. M. Percival, and J. Lipkin. 1987. *Pore-water pressure events during the in situ heat transfer experiment simulation: Piezometer probe technology.* SAND86-7172. Albuquerque: Sandia National Laboratories.

Bennett, R. H., J. T. Burns, F. L. Nastav, J. Lipkin, and C. M. Percival. 1985b. Deep-ocean piezometer probe technology for geotechnical investigations. *IEEE Journal of Oceanic Engineering* 10:17–22.

Bennett, R. H., H. Li, J. T. Burns, C. M. Percival, and J. Lipkin. 1989. Application of piezometer probes to determine engineering properties and geological processes in marine sediments. *Applied Clay Science* 4:337–55.

Bennett, R. H., H. Li, P. J. Valent, J. T. Burns, D. J. Walter, F. L. Nastav, C. M. Percival, and J. Lipkin. 1986a. *Deep-ocean piezometer probes in support of the in situ heat transfer experiment (ISHTE): Pore pressure experiments (1981–1985).* NORDA Technical Note no. 275.

Bennett, R. H., H. Li, P. J. Valent, J. Lipkin, and M. I. Esrig. 1986b. *In situ undrained shear strengths and permeabilities derived from piezometer measurements.* ASTM Special Technical Testing Publ. no. 883. Philadelphia: American Society for Testing and Materials.

Bennett, R. H., H. Li, D. Walter, P. J. Valent, C. M. Percival, and J. Lipkin. In press. Subseabed Disposal Project experiment: Piezometer probe measurement technology. In *Geotechnical aspects of ocean waste disposal*, ed. R. Chaney and K. Demars. ASTM STP 1087. Philadelphia: American Society for Testing and Materials.

Birch, F., and H. Clark. 1940. The thermal conductivity of rocks and its dependence upon temperature and composition. *American Journal of Science* 238:37.

Bishop, W. P., and C. D. Hollister. 1974. Seabed disposal—Where to look. *Nuclear Technology* 24.

Briefing Book. 1985. *The subseabed disposal project.* Austin, TX: J. K. Associates, 51 p.

Bryant, W. R., and R. H. Bennett. 1988. Origin, physical, and mineralogical nature of red clays: The Pacific Ocean Basin as a model. *Geo-Marine Letters* 4:189–249.

Burkett, P. J., R. H. Bennett, and W. R. Bryant. In press. The role of the microstructure of Pacific red clays to radioactive waste disposal. In *The microstructure of fine-grained sediments: From mud to shale*, ed. R. H. Bennett, W. R. Bryant, and M. H. Hulbert. New York: Springer-Verlag.

Burkett, P. J., R. H. Bennett, H. Li, F. L. Nastav, W. R. Bryant, L. E. Shephard, and W.-A.

Chiou. 1987. Microstructure of red clay from the Central Pacific Deep-Sea Basin: Significance to subseabed nuclear waste disposal. SAND86-2492. Albuquerque: Sandia National Laboratories, July.

Erickson, K. L. 1979. Radionuclide sorption studies on abyssal red clays. In *Radioactive waste in geologic storage*, ed. S. Fried. Washington, D.C.: American Chemical Society.

Fried, S., A. M. Friedman, and J. C. Sullivan. 1980. The radiolytic oxidation and reduction of plutonium. In *Scientific basis for nuclear waste management*, vol. II, ed. C. J. Northrup. New York: Plenum.

Fried, S., A. M. Friedman, J. Hines, R. Sjoblum, G. Schmitz, and F. Schreiner. 1980. Measurement of penetration depths of plutonium and americium in sediment from the ocean floor. In *Scientific basis for nuclear waste management*, vol. II, ed. C. J. Northrup. New York: Plenum.

Gartling, D. K. 1982. *COYOTE—A finite element computer program for nonlinear heat conduction problems.* SAND77-1332. Albuquerque: Sandia National Laboratories.

Gartling, D. K., and C. E. Hickox. 1982a. *MARIAH—A finite element computer program for incompressible porous flow problems: Theoretical background.* SAND79-1622. Albuquerque: Sandia National Laboratories.

Gartling, D. K., and C. E. Hickox. 1982b. *MARIAH—A finite element computer program for incompressible porous flow problems: Users manual.* SAND79-1623. Albuquerque: Sandia National Laboratories.

General Electric. 1977. *Multi-hundred watt radioisotope thermoelectric generator program: Final safety analysis report for the MJS-77 mission.* Document no. 77SDS4206. Fairfield, CT: General Electric Space Division.

Hadley, G. R., D. F. McVey, and R. Morin. 1980. Thermo-physical properties of deep ocean sediments. Presented at the 16th Annual Conference of the Marine Technology Society, October, Washington, D.C.

Heath, G. R., G. Epstein, and R. A. Prince. 1977. *Seabed Disposal Program: Geomechanical and sedimentological studies of North Pacific sediments: Subseabed Disposal Program annual report, January–December 1976, vol. II.* SAND77-1270. Albuquerque: Sandia National Laboratories.

Heath, G. R., et al. 1980. Characterization of pelagic sedimentation in the North Pacific. Presented at Marine Technology '80, 16th Annual Conference of the Marine Technology Society, October, Washington, D.C.

Hickox, C. E. 1984a. Analysis of heat and mass transfer in subseabed disposal of nuclear waste. *Marine Geotechnology* 5:335–60.

Hickox, C. E. 1984b. Memorandum to distribution: Consideration of thermal convection in the ISHTE simulation. Albuquerque: Sandia National Laboratories, 7 February.

Hickox, C. E. 1984c. Memorandum to distribution: Numerical simulation of a calibration test of the electric heat source for the trial deployment of ISHTE. Albuquerque: Sandia National Laboratories, 13 July.

Hickox, C. E. 1984d. Memorandum to distribution: Permeability measurement for reconsolidated illite seabed sediment. Albuquerque: Sandia National Laboratories, 20 March.

Hickox, C. E. 1984e. Memorandum to distribution: Prediction of temperature distribution in the ISHTE simulation. Albuquerque: Sandia National Laboratories, 25 January.

Hickox, C. E. 1984f. Memorandum to distribution: Thermal conductivity measurements for reconsolidated illite seabed sediment. Albuquerque: Sandia National Laboratories, 13 February.

Hickox, C. E. 1984g. Memorandum to distribution: Thermal conductivity of reconsolidated illite seabed sediment used in pore pressure measurements. Albuquerque: Sandia National Laboratories, 16 April.

Hickox, C. E., and R. R. Eaton. 1980. Prediction of induced pore pressure for the ISHTE using SHAFT 79: Memorandum to C. M. Percival. Albuquerque: Sandia National Laboratories, 12 May.

Hickox, C. E., and H. A. Watts. 1980a. *Numerical solutions for steady thermal convection from a*

concentrated source in a porous medium. SAND79-2214. Albuquerque: Sandia National Laboratories.

Hickox, C. E., and H. A. Watts. 1980b. Steady thermal convection from a concentrated source in a porous medium. *Journal of Heat Transfer* 102:2.

Hickox, C. E., D. K. Gartling, D. F. McVey, A. J. Russo, and H. E. Nuttall. 1980. Analysis of heat and mass transfer in subseabed disposal of nuclear waste. Presented at Marine Technology '80, 16th Annual Conference of the Marine Technology Society, October, Washington, D.C.

Hickox, C. E., D. F. McVey, J. B. Miller, L. O. Olson, and A. J. Silva. 1986. Thermal conductivity measurements of Pacific illite sediment. *International Journal of Thermophysics* 7:755–64.

Hollister, C. D. 1977. The seabed option. *Oceanus* 20:18.

Hollister, C. D., D. R. Anderson, and G. R. Heath. 1981. Subseabed disposal of nuclear wastes. *Science* 213:4514.

Jones, R. E. 1982. *Users manual for QMESH, a self-organizing mesh generation program.* SLA74-0239. Albuquerque: Sandia National Laboratories, July. Reprinted.

Lipkin, J., R. H. Bennett, and D. F. McTigue. 1986. Consolidation under an isotopic total stress increase: Part II, experimental results for marine clay. *Geotechnique* 36:11–25.

McTigue, D. F., and D. K. Gartling. 1986. *Numerical simulation of thermally driven pore pressure rise in the ISHTE simulation experiment.* Albuquerque: Sandia National Laboratories.

McTigue, D. F., J. Lipkin, and R. H. Bennett. 1986. Consolidation under an isotopic total stress increase: Part I: Analysis for compressible constituents. *Geotechnique* 36:1–9.

McVey, D. F., K. L. Erickson, and W. E. Seyfried. 1983. Thermal, chemical, and mass transport processes induced in abyssal sediments by the emplacement of nuclear waste. In *Radioactive wastes and the ocean,* ed. I. W. Duedall. New York: Wiley.

Miller, J. B., V. W. Miller, and L. O. Olson. 1982. ISHTE simulation APL-UW engineering report. Prepared for Sandia National Laboratories by the Applied Physics Laboratory at the University of Washington in Seattle, April.

Miller, V. W., J. B. Miller, and L. O. Olson. 1986. Final report under contract 52-5769. Prepared for Sandia National Laboratories by the Applied Physics Laboratory at the University of Washington in Seattle, December.

Mondy, L. A. 1985a. Memorandum to distribution: Prediction of steady state temperatures during the ISHTE using an isotopic heat source of 475 watts. Albuquerque: Sandia National Laboratories, 16 September.

_____. 1985b. Memorandum to distribution: Prediction of steady state temperatures in the sediment around the isotopic heat source during the in situ heat transfer experiment. Albuquerque: Sandia National Laboratories, 2 August.

Nuttall, H. E., A. K. Ray, E. J. Davis. 1981. An analysis of diffusional ion transport in ocean sediments: Subseafloor disposal of radioactive waste. *Nuclear Technology* 00:52.

Olson, L. O. 1981. Acoustic and thermal sensor systems for the in situ heat transfer experiment. Prepared for Sandia National Laboratories by the Applied Physics Laboratory at the University of Washington in Seattle, July.

Olson, L. O. 1984. *Cruise report.* Seattle: University of Washington Applied Physics Laboratory.

Olson, L. O., and J. G. Harrison. 1979. Sea floor systems for an in situ heat transfer experiment. *Oceans 1979.*

Olson, L. O., and J. G. Harrison. 1982. *ISHTE deep ocean corers and heater implant system.* Contractor report 62-1476. SAND82-7048. Albuquerque: Sandia National Laboratories, October.

Olson, L. O., and J. B. Miller. 1985. ISHTE component test cruise at MPG-I, September 1984 cruise report. Prepared for Sandia National Laboratories by the Applied Physics Laboratory at the University of Washington in Seattle, March.

Olson, L. O., and V. W. Miller. 1986. ISHTE hydrostatic piston corers. Prepared for Sandia National Laboratories under contract 64-0507 by the Applied Physics Laboratory at the University of Washington in Seattle, September.

Olson, L. O., and J. B. Miller. 1986*. ISHTE ocean test cruise at MPG-I, September 1985 cruise

report. Prepared for Sandia National Laboratories by the Applied Physics Laboratory at the University of Washington in Seattle, February.

Olson, L. O., and J. L. Roberts-Backes. 1980. ISHTE system tests at MPG-I, July 1980: Cruise report, APL-TN 12-80. Prepared for Sandia National Laboratories by the Applied Physics Laboratory at the University of Washington in Seattle, October.

Olson, L. O., J. L. Backes, and J. B. Miller. 1985. Communication, control, and data acquisition systems on the ISHTE lander. *IEEE Journal of Oceanic Engineering* 10:1.

Percival, C. M. 1982. Laboratory simulation of a deep ocean in situ heat transfer experiment. In *Oceans 1981.*

Percival, C. M. 1983. *The Subseabed Disposal Program in situ heat transfer experiment (ISHTE).* SAND80-0202. Albuquerque: Sandia National Laboratories, May.

Percival, C. M. 1984. *Subseabed Disposal Project annual report: Thermal response studies October 1981–September 1982.* SAND82-2717. Albuquerque: Sandia National Laboratories, April.

_____. 1985a. *ISHTE component test cruise report.* SAND85-1759. Albuquerque: Sandia National Laboratories.

_____. 1985b. *1983 Subseabed Disposal Project annual report: Thermal response studies October 1982–September 1983.* SAND85-1445. Albuquerque: Sandia National Laboratories, November.

_____. 1986a. *In situ heat transfer experiment (ISHTE): Ocean test cruise report (Alcyone cruise, leg IV), September 1985.* SAND86-0829. Albuquerque: Sandia National Laboratories, August.

_____. 1986b. *1984 Subseabed Disposal Project annual report: Thermal response studies October 1983–September 1984.* SAND86-0830. Albuquerque: Sandia National Laboratories, July.

_____. 1987. *Subseabed Disposal Project thermal response studies, 1985 and 1986 annual reports, October 1984 through September 1986.* SAND87-0241. Albuquerque: Sandia National Laboratories, February.

Percival, C. M., D. F. McVey, L. O. Olson, and A. J. Silva. 1980. In situ heat transfer experiment (ISHTE). In *Marine technology '80—Proceedings: The decade of the oceans.*

_____. *1984. In situ heat transfer experiment. Geotechnology* 5:361–77.

Percival, C. M., L. O. Olson, R. H. Bennett, F. L., Sayles, and A. J. Silva. 1987. *The Subseabed Disposal Program in situ heat transfer experiment (ISHTE) final design report.* SAND86-2008. Albuquerque: Sandia National Laboratories, April.

Pruess, K., and R. C. Schroeder. 1980. *SHAFT 79, User's Manual.* LBL-10861, UC-669. Berkeley: Lawrence Berkeley Laboratory.

Riggins, M., 1985. *Pore pressure response to probe insertion and thermal gradient: ISIMIU-II.* NORDA Technical Note no. 259.

Riley, J. P., and G. Skirrow, eds. 1975. *Chemical Oceanography,* vol. 1, 3d ed. New York: Academic Press.

Roberts-Backes, J. L., B. M. Bell, W. E. Nodland, and L. O. Olson. 1980. A deep-ocean acoustic tracking and telemetry system: APL-UW report 8015. Prepared for Sandia National Laboratories by the Applied Physics Laboratory at the University of Washington in Seattle, December.

Russo, A. J. 1980. *Prediction of the migration of several radionuclides in ocean sediment with the computer code IONMIG, a preliminary report.* SAND79-1666. Albuquerque: Sandia National Laboratories, May.

Savvidon, C. 1988. Modeling of the coupled heat flow and consolidation around hot cylinders buried in clay. Presented at conference, Radioactive Waste Disposal in Seabed Sediments, September, Oxford, England.

Schultheiss, P. J., and S. D. McPhail. 1986. Direct indication of pore water advection from pored pressure measurements in Madeira Abyssal Plain. *Nature (London)* 320:348–350.

Seyfried, W. E. Jr., and E. C. Thornton. 1982. *Experimental and theoretical modeling of hydrothermal processes in the near field environment: Subseabed Disposal Program annual report, January–September 1981, vol. II, part 1 of 2.* SAND82-0664/II. Albuquerque: Sandia National Laboratories.

Silva, A. J. 1980. Geotechnical properties of sediments from North Pacific and North Bermuda Rise. Presented at Marine Technology '80, 16th Annual Conference of the Marine Technology Society, October Washington, D.C.

_____. 1985. Comparison of in situ and ship board vane measurements on a deep sea clay. In *Advances in underwater technology and offshore engineering*, vol. 3.

Silva, A. J., and D. I. Calnan. 1981. *Geotechnical aspects of sub-surface seabed disposal of high level radioactive wastes: Subseabed Disposal Program annual report, January-December 1979, vol. II, part 1 of 2.* SAND80-2577/II. Albuquerque: Sandia National Laboratories.

Silva, A. J., S. A. Jordan, and W. L. Levy. 1982. Geotechnical studies for subseabed disposal of high level radioactive wastes: Progress report. Prepared for Sandia National Laboratories by the Applied Physics Laboratory at the University of Rhode Island.

Silva, A. J., J. D. Babb, J. Lipkin, P. Pietryka, and D. Butler. 1985. In situ vane system for seafloor strength investigations. *IEEE Journal of Oceanic Engineering* 10:29–31.

Silva, A. J., S. J. Criscenzo, S. A. Jordan, J. D. Babb, and W. L. Levy. 1982. URI Geotechnical program of the in situ heat transfer experiment: Progress report. Prepared for Sandia National Laboratories by the Applied Physics Laboratory at the Universty of Rhode Island.

Soderberg, L. O. 1962. Consolidation theory applied to foundation pile time effects. *Geotechnique* 12:217–25.

Thornton, E. C. 1983. Experimental and theoretical modeling of sediment seawater hydrothermal interaction at constant temperature and in a thermal gradient. Implications for the diagenesis and metamorphism of marine clay and the subseabed disposal of nuclear waste. PhD. diss., University of Minnesota.

Valent, P. J., R. H. Bennett, H. Li, and J. T. Burns. 1985. *NORDA contribution to the in-situ heat transfer experiment: FY84 annual report.* NORDA Technical Note no. 263.

Von Herzen, R., and A. E. Maxwell. 1959. The measurement of thermal conductivity of deep sea sediments by a needle probe method. *Journal of Geophysical Research* 64:10.

Walter, D. J., J. T. Burns, and P. J. Valent. 1986. *Cruise report on in situ heat transfer experiment (ISHTE): Ocean test cruise report (Alcyone cruise, leg IV), September 1985.* SAND86-0829. Albuquerque: Sandia National Laboratories.

Wroth, C. P., J. P. Carter, and M. F. Randolph. 1979. Stress changes around a pile driven into cohesive soil. In *Recent developments in the design and construction of piles*, Savoy Place, England: Institution of Electrical Engineers.

VOLUME 8 • 1989

MARINE GEOTECHNOLOGY

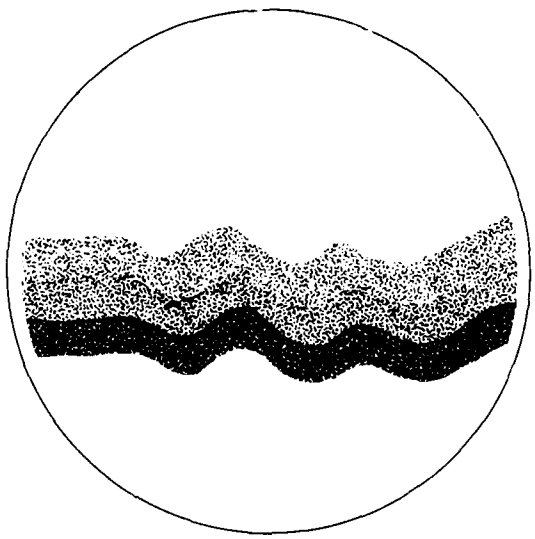

AN INTERNATIONAL
JOURNAL OF SEA-FLOOR SCIENCE
AND ENGINEERING

RONALD C. CHANEY
EDITOR-IN-CHIEF

TAYLOR & FRANCIS
NEW YORK • BRISTOL, PA • WASHINGTON, DC • LONDON

MARINE GEOTECHNOLOGY

EDITOR-IN-CHIEF
Ronald C. Chaney,
Telonicher Marine Laboratory, Humboldt State University

ASSOCIATE EDITOR FOR EUROPE
Adrian F. Richards, Consultant, The Netherlands

ASSOCIATE EDITOR FOR THE FAR EAST
Shigeyasu Okusa, (deceased), Niigata University, Japan

EDITORIAL BOARD

Gideon Almagor, Geological Survey of Israel; **Richard H. Bennett,** NORDA, NSTL Station, Mississippi; **James S. Booth,** U.S. Geological Survey, Massachusetts; **Bengt B. Broms,** Nanyang Technological Institute, Singapore; **William R. Bryant,** Texas A & M University; **R. G. Campanella,** The University of British Columbia, Vancouver, Canada; **Kenneth R. Demars,** University of Connecticut; **Jaap De Ruiter,** Fugro Consultants International, Holland; **Earl Doyle,** Shell Development Company, Texas; **Ben C. Gerwick, Jr.,** University of California; **S. K. Gulhati,** Indian Institute of Technology, New Delhi, India; **Terence J. Hirst,** Vancouver, Canada; **Kaare Hoeg.** Norwegian Geotechnical Institute; **George H. Keller,** Oregon University; **Homa Lee,** U.S. *Geological Survey, California*; **Bramlette McClelland,** McClelland Engineers, Inc., Texas; **Iraj Noorany,** San Diego State University; **Shigeyasu Okusa,** Tokai University; **Harold W. Olsen,** U.S. Dept. of Interior; **Sibel Pamukcu,** Fritz Laboratory, Pennsylvania; **H. G. Poulos,** The University of Sydney; **V. Savelyev,** VNII Okeangeologia, U.S.S.R.; **Armand J. Silva,** University of Rhode Island; **Tokuo Yaminoto,** University of Miami; **Liang Yuanbo,** South China Sea Institute of Oceanology, Academia Sinica, P.R.C.

Abstracted and/or Indexed in: Aquatic Sciences and Fisheries Abstracts; Articles in Civil Engineering; Bibliography and Index of Geology; Bibliography and Index of Micropaleontology; Biological Abstracts; Cambridge Abstracting Services; Current Contents/Engineering, Technology and Applied Sciences; Engineering Index; Engineering Information, Geo Abstracts; Geotechnical Abstracts; IMM Abstracts; Marine Science Contents Tables; Oceanic Abstracts; Offshore Abstracts; Petroleum Abstracts.

Editorial Office: Ronald C. Chaney, Telonicher Marine Lab., Humboldt State University, P.O. Box AE, Trinidad, CA 95570

Publishing, Advertising, and Subscription Offices: Taylor & Francis Inc., 1900 Frost Road, Suite 101, Bristol, PA 19007, USA; or Taylor & Francis Ltd., Rankine Road, Basingstoke, *Hampshire* RG24 0PR, England.

Marine Geotechnology (ISSN 0360-8867) is published quarterly by Taylor & Francis Ltd., 4 John Street, London, WC1N 2ET. Annual 1989 institutional subscription £50, US $90. Personal subscription rate available to home address only US £29, U.S. $50.

Application to mail at second-class postage rates is pending at New York, NY, and additional mailing offices. **POSTMASTER:** Send address changes to MARINE GEOTECHNOLOGY, Publications Expediting, Inc., 200 Meacham Avenue, Elmont, New York 11003, U.S.A.

Dollar rates apply to subscribers in all countries except the UK and the Republic of Ireland, where the sterling price applies. All subscriptions are payable in advance and all rates include postage. Subscriptions are entered on an annual basis, i.e., January to December. Payment may be made by sterling check, dollar check, international money order, National Giro, or credit card (AMEX, VISA, Mastercard/Access).

Orders originating in the following territories should be sent directly to: **Australia**—R. Hill & Son, Ltd., 117 Wellington Street, Windsor, Victoria 3181. **India**—Universal Subscription Agency Pvt. Ltd., 101-102 Community Centre, Malviya Nagar Extn., Post Bag No. 8, Saket, New Delhi. **Japan**—*Kinokuniya* Company Ltd., Journal Department, P.O. Box 55, Chitose, *Tokyo* 156. **New Zealand**—R. Hill & Son, Ltd., Private Bag, Newmarket, Auckland 1. **USA, Canada, and Mexico**—Taylor & Francis, Inc., 1900 Frost Road, Suite 101, Bristol, PA 19007, USA. **UK and all other territories**—Taylor & Francis Ltd., Rankine Road, Basingstoke, Hampshire RG24 0PR, England.

Copyright:
The appearance of the code at the top of the first page of each article in this journal indicates the copyright owner's consent that a single copy of the article may be made for personal use. This consent is given on the condition that for multiple copies of the article the copier pay a fee of $3.00 per copy through the Copyright Clearance Center, Inc., 27 Congress Street, Salem, MA 01970. This consent does not extend to other kinds of copying, such as copying for general distribution, for advertising or promotional purposes, for creating new collective works or for resale. No part of this publication may be stored on an electronic retrieval system or transmitted electronically without the prior written permission of the publisher.
Copyright © 1989 Taylor & Francis. Printed by Burgess Science Press, Basingstoke, England.

The publisher assumes no responsibility for any statements of fact or opinion expressed in the published papers or in the advertisements. **Marine Geotechnology** is owned by Taylor & Francis Inc.

MARINE GEOTECHNOLOGY

Volume 8, Number 1
1989

Contents

Abstracted and/or indexed in: Aquatic Sciences and Fisheries Abstracts; Articles in Civil Engineering; Bibliography and Index of Geology; Bibliography and Index of Micropaleontology; Biological Abstracts; Current Contents/Engineering, Technology and Applied Sciences; Engineering Index; Geo Abstracts; Geotechnical Abstracts; IMM Abstract; Marine Science Contents Tables; Oceanic Abstracts; Offshore Abstracts; Petroleum Abstracts.

Taylor & Francis
New York • Bristol, PA • Washington, DC • London

MARINE GEOTECHNOLOGY

Volume 8, Number 2
1989

Contents

Abstracted and/or indexed in: Aquatic Sciences and Fisheries Abstracts; Articles in Civil Engineering; Bibliography and Index of Geology; Bibliography and Index of Micropaleontology; Biological Abstracts; Current Contents/Engineering, Technology and Applied Sciences; Engineering Index; Geo Abstracts; Geotechnical Abstracts; IMM Abstract; Marine Science Contents Tables; Oceanic Abstracts; Offshore Abstracts; Petroleum Abstracts.

MARINE GEOTECHNOLOGY

Volume 8, Number 3
1989

Contents

Abstracted and/or indexed in: Aquatic Sciences and Fisheries Abstracts; Articles in Civil Engineering; *Bibliography and Index of Geology*; *Bibliography and Index of Micropaleontology*; Biological Abstracts; Current Contents/Engineering, Technology and Applied Sciences; Engineering Index; Geo Abstracts; Geotechnical Abstracts; IMM Abstract; Marine Science Contents Tables; Oceanic Abstracts; Offshore Abstracts; Petroleum Abstracts.

Taylor & Francis
New York • Bristol, PA • Washington, DC • London

MARINE GEOTECHNOLOGY

Volume 8, Number 4
1989

Contents

Abstracted and/or indexed in: Aquatic Sciences and Fisheries Abstracts; Articles in Civil Engineering; Bibliography and Index of Geology; Bibliography and Index of Micropaleontology; Biological Abstracts; Current Contents/Engineering, Technology and Applied Sciences; Engineering Index; Geo Abstracts; Geotechnical Abstracts; IMM Abstract; Marine Science Contents Tables, Oceanic Abstracts; Offshore Abstracts; Petroleum Abstracts.

Taylor & Francis
New York ● Bristol, PA ● Washington, DC ● London

MARINE GEOTECHNOLOGY

Instructions to Authors

MARINE GEOTECHNOLOGY publishes research devoted to all scientific and engineering aspects of seafloor sediments and rocks. With the goal of solving marine problems in civil engineering and the earth sciences, MARINE GEOTECHNOLOGY includes the study of the acoustical, biological, chemical, mechanical, and physical properties affecting the electrolyte-gas-solid sedimentary system to applied static and dynamic loads is also included. Other topics covered in MARINE GEOTECHNOLOGY include anchoring and mooring systems, bottom installations, cables, coastal engineering structures, islands, mining, pipelines, platforms, and transporation, as well as case studies

Manuscripts should be submitted in triplicate to either Ronald C. Chaney, Director, Telonicher Marine Laboratory, Humboldt State University, PO Box AE, Trinidad, CA 95570; or to the Associate Editor of the Far East, Dr. Shigeyasu Okusa, Department of Civil Engineering, Marine Science and Technology, Tokai University, 3-20-1 Orido, Shimizu, Japan 424; or to the Associate Editor for Europe, Adrian F. Richards, Uiterweg 309, 1431 AJ Aalsmeer, The Netherlands.

Manuscript. Manuscripts will be accepted with the understanding that their content is unpublished and is not being submitted for publication elsewhere. All parts of the manuscript, including the title page, abstract, tables, and legends, should be type-written, double-spaced on one side of white bond in English. Allow margins of at least one inch (3 cm). on all sides of the typed pages. Number manuscript pages consecutively throughout the paper. Translations of papers previously published in languages other than English can be considered, but this information must be provided by the author at the time of submission.

Title. All titles should be as brief as possible, 6 to 12 words. Authors should also supply a shortened version of the title suitable for the running head, not exceeding 50 character spaces.

Affiliation. On the title page include full names of authors, academic and/or other professional affiliations, and the complete mailing address of the author to whom proofs and correspondence should be sent.

Abstract. Each paper should be summarized in an abstract of not more than 250 words. Avoid abbreviations, diagrams, and reference to the text.

Keywords. Authors must give from three to ten key words or phrases which identify the most important subjects covered by the paper

References. Within text citations should be cited by author(s) and date in parentheses. Full citations are required and should be arranged alphabetically. For further information, consult the *Chicago Manual of Style, 13th ed.*

Journal article:

Hulbert, M. and A. F. Richards. 1980. Investigation of geotechnical and geochemical relationships by parameter cross-correlation methods, Oslofjorden and Dramafjorden, Norway. *Marine Geotechnology* 4(2):163–180.

Book:

Bowles, J. E. 1978. *Engineering Properties of Soils and Their Measurement*. 2nd ed. New York: McGraw-Hill Book Co.

Figures. All figures must be submitted in camera-ready form. Xerox copies are not acceptable. figures must be submitted either as black & white glossy photographs or photostats (bromides). Label each figure with article title, author's name, and figure number by attaching a separate sheet of white paper to the back of each figure. Do not write on the camera-ready art. Each figure should be provided with a brief, descriptive legend. All legends should be typed on a separate page at the end of the manuscript.

Tables. All tables must be discussed or mentioned in the text and numbered in order of mention. Each table should have a brief descriptive title. Do not include explanatory material in the title; use footnotes, keyed to the table with superior lower-case letters. Place all footnotes to a table at the end of the table. Define all data in the column heads. Every table should be fully understandable even without reference to the text. Type all tables on separate sheets; do not include them within the text.

Permission to Reprint. If any figure, table, or more than a few lines of text from previously published material are included in a manuscript the author must obtain written permission for republication from the copyright holder and forward a copy to the publisher.

Transfer of Copyright. Under the copyright law, the transfer of copyright from author to publisher must now be explicitly stated to enable the publisher to ensure maximum dissemination of the author's work. The completed form must be returned to the publisher before any manuscript can be assigned an issue for publication.

Page Proofs. All proofs must be corrected and returned to the publisher within 48 hours of receipt. If the manuscript is not returned within the allotted time, the editor will proofread the article, and it will be printed according to his instruction. Only correction of typographical errors is permitted. The author will be charged for additional alterations to text at the proof stage.

Offprints. A total of fifty (50) offprints of each paper will be supplied free of charge to the first named author unless otherwise specified. Additional copies may be ordered at charges shown on the offprint price scale, which will be sent to the author with the proofs. Offprints are not available after publication of the issue.